ΠΑΝΕΠΙΣΤΗΜΙΟ ΚΡΗΤΗΣ

ΣΧΟΛΗ ΕΠΙΣΤΗΜΩΝ ΥΓΕΙΑΣ

ΤΜΗΜΑ ΙΑΤΡΙΚΗΣ

ΤΟΜΕΑΣ ΒΑΣΙΚΩΝ ΕΠΙΣΤΗΜΩΝ

ΕΡΓΑΣΤΗΡΙΟ ΛΕΙΤΟΥΡΓΙΚΗΣ ΑΠΕΙΚΟΝΙΣΗΣ ΤΟΥ ΕΓΚΕΦΑΛΟΥ

Χαρτογράφηση των βρεγματο-μετωπιαίων νευρωνικών κυκλωμάτων εγκεφάλου πιθήκου, τα οποία εμπλέκονται στην οπτικά και σωματαισθητικά καθοδηγούμενη κίνηση του άνω άκρου.

Μελέτη με τη χρήση της ποσοτικής αυτοραδιογραφικής μεθόδου της $[^{14}C]$-2-δεοξυγλυκόζης

ΓΕΩΡΓΙΑ Γ. ΓΡΗΓΟΡΙΟΥ

ΔΙΔΑΚΤΟΡΙΚΗ ΔΙΑΤΡΙΒΗ

ΗΡΑΚΛΕΙΟ 2001

UNIVERSITY OF CRETE

SCHOOL OF HEALTH SCIENCES

FACULTY OF MEDICINE

DEPARTMENT OF BASIC SCIENCES

LABORATORY OF FUNCTIONAL BRAIN IMAGING

Functional mapping of the monkey parieto-frontal circuits involved in the visual and somatosensory guidance of reaching movements.

A quantitative autoradiographic study using the [^{14}C]-2-deoxyglucose method

GEORGIA G. GREGORIOU

PH.D THESIS

HERAKLION 2001

Στους γονείς μου και
στους δασκάλους μου

TABLE OF CONTENTS

LIST OF ABBREVIATIONS

$[^{14}C]DG$ 2-deoxy-D-1-$[^{14}C]$glucose
2-δεοξυ-D-1-$[^{14}C]$γλυκόζη

2-DG   2-deoxy-D-glucose
2-δεοξυ-D-γλυκόζη

5DIP   dorsal intraparietal area 5
ραχιαία ενδοβρεγματική περιοχή 5

5VIP   ventral intraparietal area 5
κοιλιακή ενδοβρεγματική περιοχή 5

7DIP   dorsal intraparietal area 7
ραχιαία ενδοβρεγματική περιοχή 7

7IP   intraparietal area 7
ενδοβρεγματική περιοχή 7

7VIP   ventral intraparietal area 7
κοιλιακή ενδοβρεγματική περιοχή 7

AG   annectant gyrus

AI   inferior limb of the arcuate sulcus
κάτω σκέλος της τοξοειδούς αύλακας

AIP   anterior intraparietal area
πρόσθια ενδοβρεγματική περιοχή

AS   superior limb of the arcuate sulcus
άνω σκέλος της τοξοειδούς αύλακας

As   arcuate sulcus
τοξοειδής αύλακα

C   untrained control monkey
ανεκπαίδευτος πίθηκος ελέγχου

Cas   calcarine sulcus
πληκτραία αύλακα

Cgs   cingulate sulcus
αύλακα του προσαγωγίου

Cs   central sulcus
κεντρική αύλακα

DG-6-P   2-deoxyglucose-6-phosphate
2-δεοξυγλυκόζη-6-φωσφορική

F   fixating monkey
πίθηκος που πραγματοποιούσε εστίαση του βλέμματος

F1   primary motor area
πρωτοταγής κινητική περιοχή

F2   caudal dorsal premotor area
πίσω ραχιαία προκινητική περιοχή

F2AS   periarcuate part of F2
τμήμα της F2 περί την τοξοειδή αύλακα

F3   caudal mesial premotor area
πίσω έσω προκινητική περιοχή

F4   caudal ventral premotor area
πίσω κοιλιακή προκινητική περιοχή

F5   rostral ventral premotor area
πρόσθια κοιλιακή προκινητική περιοχή

F6   rostral mesial premotor area
πρόσθια έσω προκινητική περιοχή

F7   rostral dorsal premotor area
πρόσθια ραχιαία προκινητική περιοχή

FEF   frontal eye fields
πρόσθια οφθαλμικά πεδία

FST   fundal superior temporal area
επί του πυθμένα της άνω κροταφικής αύλακας περιοχή

G-6-P   glucose-6-phosphate
γλυκόζη-6-φωσφορική

IOs   inferior occipital sulcus
κάτω ινιακή αύλακα

IPd   inferior precentral dimple
κάτω προκεντρική αύλακα

IPL   inferior parietal lobule
κάτω βρεγματικό λόβιο

IPs   intraparietal sulcus
ενδοβρεγματική αύλακα

Laf   lateral fissure
πλάγια σχισμή

LCGU   local cerebral glucose utilization
τοπική εγκεφαλική κατανάλωση γλυκόζης

LIP   lateral intraparietal area
έξω ενδοβρεγματική περιοχή

Ls   lunate sulcus
μηνοειδής αύλακα

MIP   medial intraparietal area
έσω ενδοβρεγματική περιοχή

MST   middle superior temporal area
έσω άνω κροταφική περιοχή

MT   middle temporal area
έσω κροταφική περιοχή

OTs   occipitotemporal sulcus
ινιακοκροταφική αύλακα

OFO   orbitofrontal operculum
κογχομετωπιαία καλύπτρα

PE   architectonic subdivision of area 5 in the rostral superior parietal lobule

αρχιτεκτονική υποδιαίρεση της περιοχής 5 στο πρόσθιο τμήμα του άνω βρεγματικού λοβίου

PEc   architectonic subdivision of area 5 in the caudal superior parietal lobule

αρχιτεκτονική υποδιαίρεση της περιοχής 5 στο πίσω τμήμα του άνω βρεγματικού λοβίου

PEip   architectonic subdivision of intraparietal area 5
αρχιτεκτονική υποδιαίρεση της ενδοβρεγματικής περιοχής 5

PF   architectonic subdivision of area 7 in the inferior parietal lobule
αρχιτεκτονική υποδιαίρεση της περιοχής 7 στο πρόσθιο τμήμα του κάτω βρεγματικού λοβίου

PFG   architectonic subdivision of area 7 in the inferior parietal lobule
αρχιτεκτονική υποδιαίρεση της περιοχής 7 στο πρόσθιο τμήμα του κάτω βρεγματικού λοβίου

PFR   parietal fixation region
βρεγματική περιοχή σχετιζόμενη με εστίαση του βλέμματος

PMd   dorsal premotor cortex
ραχιαίος προκινητικός φλοιός

PMv   ventral premotor cortex
κοιλιακός προκινητικός φλοιός

PG   architectonic subdivision of area 7in the
inferior parietal lobule
αρχιτεκτονική υποδιαίρεση της περιοχής 7 στο πίσω τμήμα του κάτω βρεγματικού λοβίου

PO   parieto-occipital area
βρεγματο-ινιακή περιοχή

POs   parieto-occipital sulcus
βρεγματο-ινιακή αύλακα

PPC   posterior parietal cortex
πίσω βρεγματικός φλοιός

Prco   precentral operculum
προκεντρική καλύπτρα

pre-SMA   pre-supplementary motor area
προ-συμπληρωματική κινητική περιοχή

Ps   principal sulcus
κύρια αύλακα

PSR   parietal saccade region
βρεγματική περιοχή που σχετίζεται με σακκαδικές κινήσεις

RD   reaching in the dark monkey
πίθηκος που εκτελούσε κίνηση του άκρου στο σκοτάδι

RL   reaching in the light monkey
πίθηκος που εκτελούσε κίνηση του άνω άκρου στο φώς

RLf — reaching in the light during fixation monkey
πίθηκος που εκτελούσε κίνηση του άνω άκρου υπό εστίαση του βλέμματος

SC — superior colliculus
άνω διδύμιο

SEF — supplementary eye fields
συμπληρωματικά οφθαλμικά πεδία

Sh — monkey executing horizontal saccades
πίθηκος που εκτελούσε οριζόντιες σακκαδικές κινήσεις

SI — primary somatosensory cortex
πρωτοταγής σωματαισθητικός φλοιός

SII — secondary somatosensory cortex

δευτεροταγής σωματαισθητικός φλοιός

So — monkey executing oblique saccades
πίθηκος που εκτελούσε πλάγιες σακκαδικές κινήσεις

SMA — supplementary motor area
συμπληρωματική κινητική περιοχή

SPd — superior precentral dimple
άνω προκεντρική αύλακα

SPL — superior parietal lobule
άνω βρεγματικό λόβιο

STs — superior temporal sulcus
άνω κροταφική αύλακα

VIP — ventral intraparietal area
κοιλιακή ενδοβρεγματική περιοχή

1. INTRODUCTION

Perception of the space surrounding us, in terms of the location and nature of the objects we act upon, constitutes the foundation of voluntary movements. Accurate reaching towards objects of interest requires a precise neural representation of target location relative to the body. The construction of such a representation and the engagement of the appropriate executive systems which output the desired movement is mediated by multiple brain areas which are involved in the:

(a) engagement of attention in terms of orienting to locations of present or expected visual stimuli

(b) perception of the visual stimulus location in the extrapersonal space based on head position, gaze direction and retinal position of the target

(c) transformation of signals about the extrapersonal location of the stimulus into an intrinsic coordinate system of central representation

(d) selection of the oculomotor schema

(e) execution of the eye movement to foveate the visual target

(f) selection of the skeletomotor schema

(g) execution of the arm movement toward the visual target

(h) constant interactions between visual input (concerning the target and forelimb positions), proprioceptive somatosensory input (concerning the forelimb position and configuration), and motor outflow during performance of the behavior.

To study visually guided reaching, one, therefore, needs to take into account each one of these parameters separately as well as in conjunction in order to construct simpler tasks-behaviors, which may help to reveal the neuronal machinery underlying visually guided forelimb reaching. Although much is known about the way sensory information is being processed in the cortical areas, which stand lower in the hierarchy of sensory processing, there are still questions about the way sensory information of different modalities converges onto higher order areas and is used in order to accurately guide forelimb reaching. Recent functional and anatomical studies have established the existence of highly specific parieto-frontal networks, which mediate different aspects of voluntary movements central to the construction of spatial representation and action.

1.1 POSTERIOR PARIETAL CORTEX

Anatomically the posterior parietal cortex (PPC) is formed by two lobules, the superior parietal lobule (SPL) and the inferior parietal lobule (IPL). Traditionally, PPC in the macaque monkey is composed of two major cytoarchitectonic areas, Brodmann's area 5 in the SPL and Brodmann's area 7 in the IPL with their border considered as the fundus of the intraparietal sulcus (IPs) (Peele, 1942). The areas forming the posterior parietal cortex are shown in Figure 1.

The central role of the posterior parietal cortex in space perception and action has been supported by functional, anatomical and lesion studies. Patients with lesions of the parietal lobe exhibit a variety of spatial deficits. From the beginning of the 20th century, lesions of the PPC were reported to induce a variety of symptoms including psychic paralysis of gaze, optic ataxia, visuospatial and visuomotor disorders which became collectively known as Balint's syndrome (Balint, 1909; Holmes, 1918). The most striking of these is neglect, the tendency to ignore objects in the half of space opposite to the side of the lesion. A patient with a right parietal lobe lesion may fail to notice or respond to objects on the left. Visuospatial deficits, which are basically sensory in nature, can be dissociated from visuomotor deficits, which are expressed as an inability to respond to objects in the contralesional field. The pattern of impairments is rather diverse, displays effector specificity and can be expressed relative to any of several spatial reference systems (Riddoch, 1935; Ratcliff and Davies-Jones, 1972; Duhamel and Brouchon, 1990; Farah et al., 1990; Karnath et al., 1991; Moscovitch and Behrman, 1994).

The variety of deficits observed following parietal lobe damage suggests that parietal cortex contains more that one kind of spatial representation. To understand more precisely how parietal cortex contributes to spatial perception and action, recording experiments from single neurons have been carried out in alert monkeys trained to perform spatial tasks. The sensory and motor conditions under which parietal neurons are activated have been explored using tasks that typically require an arm or an eye movement toward a visual target. The results of these studies have shown the existence of multiple distinct functional areas (Fig. 1) within Brodmann's areas 5 and 7.
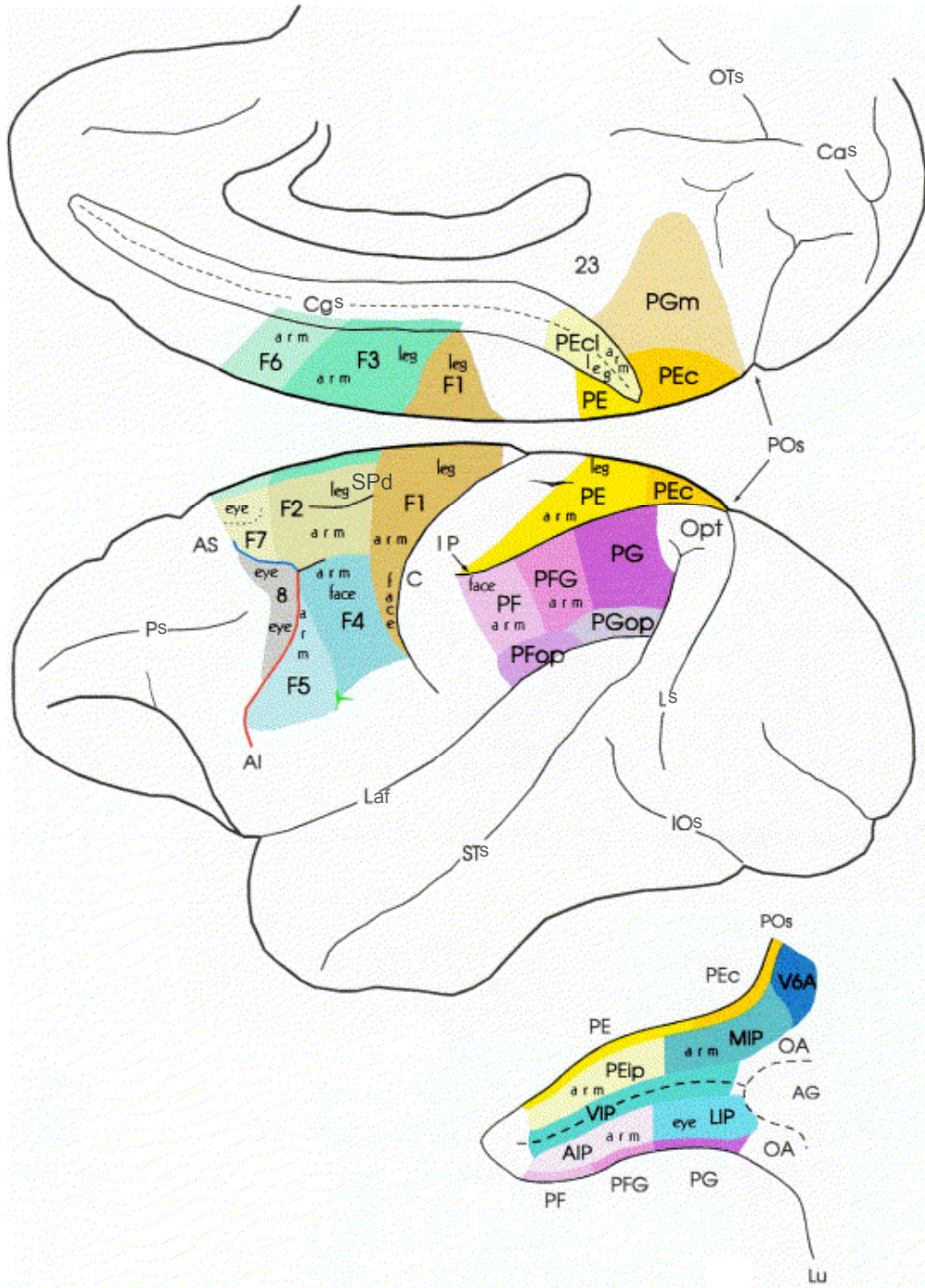
Figure 1. Mesial and lateral views of the macaque brain showing the cytoarchitectonic parcellation of the agranular frontal cortex and of the posterior parietal cortex. Motor areas are defined according to Matelli

and colleagues (Matelli et al., 1985; Matelli et al., 1991)]. All parietal areas with the exception of those buried within the intraparietal sulcus are defined according to Pandya and colleagues (Pandya and Seltzer, 1982). The areas within the intraparietal sulcus are defined according to physiological data and are shown in an unfolded view of the sulcus, in the lowest part of the figure. The various body parts representations are also illustrated (Adapted from Rizzolatti et al., 1998).

1.1.1 Parietal cortical area 5

For many years area 5 was regarded as a higher order somatic sensory association area that generated a complex representation of body postures and movements (Hyvärinen, 1982). Anatomical studies showed that area 5 received a strong input from the primary somatosensory cortex, SI (Jones and Powell, 1970; Jones et al., 1978). These projections were highly convergent (Pearson and Powell, 1985) so that the somatotopic map was not as fine grained in area 5 as in SI. Single-unit experiments also confirmed that area 5 cells had more complex passive somatic receptive fields with greater degrees of topographic and mechanoreceptor modality convergence than that found in SI (Duffy and Burchfiel, 1971; Sakata et al., 1973). Many area 5 cells were optimally activated by the combination of tactile and proprioceptive input that arose during characteristic postures and motor acts of monkeys, including reaching, manual exploration, and grooming (Sakata et al., 1973).

This "sensory" hypothesis was challenged by pioneering single-cell studies in behaving monkeys (Hyvärinen and Poranen, 1974; Mountcastle et al., 1975) which showed that some cells in parietal areas 5 and 7 had no peripheral receptive field, yet discharged during reaching movements of the limb. These results were taken to suggest that whereas some area 5 cells generate a somatic sensory representation of the body, other cells are rather implicated in the planning of visually guided motor behavior. It became therefore obvious that a strict sensory versus motor dichotomy is too simplistic to apply to parietal function (Mountcastle, 1995).

Since these first studies of area 5 function, physiologists have employed more sophisticated experimental paradigms to explore the role of the superior parietal cortex in reaching. The anatomical and functional data that will be described below suggest that area 5 is implicated in the sensorimotor guidance of motor behavior, by contributing to the somatic sensory analyses and sensorimotor coordinate transformations necessary to guide movements.

An area which is implicated in the sensorimotor guidance of movement should project to the precentral motor areas of the frontal lobe. Indeed, projections of area 5 to the primary motor cortex, premotor cortex, and supplementary motor cortex were demonstrated by anatomical methods (Jones and Powell, 1970; Jones et al., 1978; Petrides and Pandya, 1984). Johnson and co-workers (Johnson et al., 1993; Johnson et al., 1996) found a continuous topographic gradient of projections from different parts of area 5 to different regions of the precentral gyrus, by using injections of three fluorescent retrograde tracers into the precentral gyrus of monkeys. The most anterior part of area 5 projects most heavily to the primary motor cortex, while more posterior parts of area 5, in the medial bank of IPs project to the border between primary motor and premotor cortex around the superior precentral dimple. Matelli and co-workers (Matelli et al., 1998) have also shown that within the medial bank of IPs, its rostral and dorsal part, characterized as area PEip, projects to the region of the superior precentral dimple, while the more posterior part of the medial bank of IPs, the medial intraparietal area (MIP), projects more anteriorly within the premotor cortex in the ventral and rostral part of premotor area F2. Area PEip is the source of a dense corticospinal projection, whereas area MIP does not send projections to the spinal cord (Matelli et al., 1998).

Area MIP

Neurons in area MIP are specialized for responding to stimuli within reaching distance and exhibit a range of response properties from purely somatosensory, to bimodal, to purely visual (Colby and Duhamel, 1991). These different response types are encountered sequentially as the electrode is moved down the medial bank of the sulcus towards the fundus. Purely somatosensory neurons, encountered dorsally, usually have receptive fields on the contralateral limbs, most often on the arm. Bimodal neurons in area MIP respond to both the onset of a visual stimulus and to passive touch. These bimodal neurons are strongly activated when the monkey reaches for a visual target and can be specific both for the location of the target and the arm used to reach toward it. Below these bimodal

neurons is a purely visual region. Within this region some neurons give visual responses that become stronger when the target is moving within reaching distance. These "near" cells presumably signal the presence of a target that can be acquired by reaching with the arm. The visual responsiveness of neurons in area MIP is in accordance with the anatomically demonstrated connections of this area with the visual parieto-occipital area (PO) (Colby et al., 1988).

The progression in sensory receptive field properties from somatosensory to visual, through the depth of MIP is also reflected in the response properties observed in a directional reaching task. For more dorsal neurons selectivity for movement direction was prominent around the time of the movement, while more ventral movements showed direction selectivity around the time of stimulus onset (Johnson et al., 1996).

Finally, receptive fields in area MIP are dynamic, reflecting the fact that reaching-related representations must be plastic enough to accommodate expansions of reach space. A tennis player experiences the racquet as an extension of his arm. Recent experiments have shown that bimodal neurons of area MIP extend likewise their visual receptive fields when the monkey uses a tool (Iriki et al., 1996). In these experiments monkeys were trained to use a rake to retrieve distant objects and visual receptive fields were mapped before and immediately after tool use. While the somatosensory receptive fields were unchanged the visual receptive fields were expanded when the monkey used the rake as an extension of its hand. This was interpreted as a change in the body image.

Area VIP

More ventrally located within the medial bank of IPs area VIP (ventral intraparietal), which covers also the ventral part of the lateral bank of IPs (Maunsell and Van Essen, 1983) has strongly visually responsive cells most of which can also be excited by tactile stimuli (Colby et al., 1993; Duhamel et al., 1998). The tactile receptive fields are generally restricted to the head and face and the visual and tactile receptive fields match in size and location. In a monkey fixating a central point a neuron that responds to a visual stimulus in the upper left quadrant also responds to a tactile stimulus applied to the upper left portion of the face. The fovea of the visual representation corresponds to the mouth of the tactile representation. Neurons with visual fields close to the fovea have tactile receptive fields close to the mouth. Cells in this area display directional selectivity with tactile and visual receptive fields also matching with respect to direction preference: a neuron which responds preferentially to a visual stimulus moving in one direction relative to the fovea also responds preferentially to a stimulus moving across the tactile receptive field in the same direction relative to the mouth.

Visual receptive fields in area VIP range from purely retinocentric to purely head-centered when studied in head-fixed monkeys (Duhamel et al., 1997). A head-centered representation may specify goals for movements of the head, lips and tongue and facilitate reaching with the mouth. Further evidence for this view comes form the responses of a certain class of VIP neurons, which respond only to visual stimuli presented at very close range, within 5 cm of the face (Colby et al., 1993). These "ultranear" neurons in VIP, therefore, could specify a target for a mouth movement. Moreover, microstimulation of this area can evoke rapid eye movements from a restricted zone, in head-centered space, independent of the starting position of the eye (Thier and Andersen, 1996). In other words, the stimulation of these cortical sites produces saccades, which tend to end at the same point in space, independent of the initial position of the eye when the head is fixed. The coexistence of neurons with retinocentric and head-centered receptive fields suggests that neurons in a single cortical area may contribute to multiple representations of space and the guidance of multiple kinds of actions.

A somatosensory to visual gradient within the medial bank of IPs similar to that found in the electrophysiological studies described above was also established with the [^{14}C]-deoxyglucose quantitative autoradiographic method (Savaki et al., 1993). The metabolic activity in the brain of intact

monkeys and monkeys with one hemisphere deprived of all known visual input by optic chiasm section and commissurotomy was mapped during the performance of a visually cued reaching task. Visually guided reaching with one forelimb induced activations in the entire medial bank of the contralateral IPs. When that hemisphere was surgically deprived of visual input, the monkeys could still reach to visual targets with their contralateral arm, and the dorsal part of intraparietal area 5 remained active. In contrast its ventral part 5 was metabolically depressed indicating that its activation during visually guided reaching was strongly dependent on visual input.

In other studies when the relationship between the discharge of area 5 neurons and certain parameters of limb movement was examined it was found that this covaries with movement velocity (Ashe and Georgopoulos, 1994), movement direction, and with static arm position over the targets during reaching movements, approximately as a function of the cosine of movement direction or target location (Kalaska et al., 1983; Georgopoulos et al., 1984; Kalaska et al., 1990).

In summary, the response properties of area 5 neurons together with the well established connections of the different subdivisions of this area with the primary somatosensory cortex and the motor areas of the frontal lobe have suggested a role of area 5 in the sensorimotor guidance of movement (for a review see Kalaska, 1996). During reaching area 5 could transmit to precentral motor areas proprioceptive signals about the posture and movement of the limb for the somesthetic guidance of movement. This could be achieved by operating in a feedback mode relaying kinesthetic signals about current hand-limb position and movement, derived from reafferent volleys from the periphery, to other populations for the ongoing monitoring and correction of movement (Kalaska, 1988). Alternatively, its function could be predominantly feedforward providing kinesthetic information about the limb prior to the initiation of a response to visual targets. Information about starting arm position, which is necessary to plan the movement of the limb toward a target (Flanders et al., 1992), could be embedded in the activity of area 5 neurons during static condition when the current posture of the limb is encoded (Kalaska et al., 1983; Georgopoulos et al., 1984; Kalaska et al., 1990).

1.1.2 Parietal cortical area 7

The parietal cortical area 7 has been extensively studied in relation to its contribution in the planning and execution of rapid eye movements, called saccades, which are used to explore the world. Since the early days of neurophysiological studies of the posterior parietal cortex there was a debate about whether this area should be considered a sensory or a motor area. The initial single-unit studies demonstrated that parietal neurons discharge in association with visually guided saccades suggesting a motor command function for this area (Hyvärinen and Poranen, 1974; Mountcastle et al., 1975; Lynch et al., 1977). A different group of investigators found, however, that parietal neurons were also active during fixation when a visual stimulus appeared in the neuron's receptive field indicating a sensory role for these neurons (Robinson et al., 1978). These visual responses were enhanced when the stimulus was made behaviorally relevant suggesting a specific attentional role for the parietal cortex.

Area LIP

These first studies did not subdivide area 7 into specific subdivisions. More recent anatomical studies have delimited a number of subregions within architectonic area 7 with distinct anatomical connections (Pandya and Seltzer, 1982; Andersen et al., 1985; Colby et al., 1988; Cavada and Goldman-Rakic, 1989). One of these, the lateral intraparietal area (LIP) is ideally positioned to participate in the guidance of saccadic eye movements because of its connections with the frontal eye fields (FEF), and the superior colliculus (SC) (Andersen et al., 1985; Lynch et al., 1985; Andersen et al., 1990). Furthermore, microstimulation of this area evokes saccades but at higher thresholds than the ones used in the FEF and the SC (Shibutani et al., 1984; Thier and Andersen, 1996).

Although the debate on the nature of the signals that area LIP neurons carry still holds, to date data suggest that single neurons carry multiple signals. Visual, presaccadic, attentional and memory signals modulate the discharge of single neurons in LIP (Gnadt and Andersen, 1988; Barash et al., 1991; Colby et al., 1996). Visual responses have been found from different investigators and visual receptive field mapping in area LIP has demonstrated that receptive fields in this area are small and mainly confined to the contralateral visual field. The visual receptive field organization yielded only a rough topography with the central visual field represented more dorsally and the peripheral visual field more ventrally within the IPs. The lower visual field was represented more anteriorly and the upper visual field more posteriorly (Blatt et al., 1990).

Responses to visual stimuli within the neuron's receptive field increase when the stimulus is used to elicit a specific behavior (Robinson et al., 1978; Colby et al., 1996). This enhanced response is independent of the monkey's action; the amount of enhancement is similar when the monkey has either to execute a saccade to the target or release a bar when it detects dimming of the peripherally attended target. This is quite different from the saccade specific enhancement of the visual response observed in the FEF (Goldberg and Bushnel, 1981) and the SC (Wurtz and Mohler, 1976) which are together responsible for the generation of saccades. This difference has suggested that enhancement in LIP reflects visuospatial attention (Goldberg et al., 1990; Colby et al., 1996). Attentional activity has also been suggested to be responsible for the vigorous on-response of many LIP neurons to the abrupt onset of a visual stimulus which falls into the neuron's field (Gottlieb et al., 1998). The salience of the stimulus therefore modulates the sensory responses of LIP neurons. It is interesting here to add that LIP neurons also respond to attended auditory signals which are used as targets for saccades while pure auditory responses are not recorded in this area (Mazzoni et al., 1996; Grunewald et al., 1999; Linden et al., 1999). The above data have suggested that LIP may hold a representation of space that we explore best with our eyes and is beyond our immediate grasp with the arms or the mouth. This representation could be limited to attended objects and their locations (Colby and Goldberg, 1999).

The delayed saccade task can distinguish between a visual and a motor response because a delay period intervenes between the saccade's target onset and the initiation of the saccade. LIP neurons typically discharge both in response to the onset of the visual stimulus and also before the initiation of the saccade (Andersen et al., 1987; Gnadt and Andersen, 1988; Barash et al., 1991; Colby et al., 1996). The presaccadic activity is similar in the learned saccade task, in which a saccade occurs without any target appearing during the trial, confirming that the presaccadic discharge is motor in nature and is not due to a reactivation of the visual response (Colby et al., 1996). LIP neurons are thus activated by both visual and motor events. It is interesting however that the presaccadic burst is weak compared to the more robust visual signal (Colby et al., 1996).

The way the above mentioned signals are used from area LIP neurons, which have retinotopic receptive fields, in order to construct a stable representation of the world as we move our eyes has been a matter of considerable debate. This is typically tested with the double step saccade task (Mays and Sparks, 1980) where two targets are presented sequentially very briefly and the subject has to look at the targets in order. The targets are no longer present at the time when the saccades are performed. Thus, the first saccade is easily programmed, because its size and direction exactly match the retinal position of the first target. The second saccade, however, starts from one location (from the endpoint of the first saccade) but its target was seen from another location. Two different views have been proposed to explain how this is accomplished. According to the first one the system uses eye-position signals to encode the position of the target in head-centered coordinates (Mays and Sparks, 1980; Andersen et al., 1985; Zipser and Andersen, 1988). However an explicit head-centered signal has not been observed in the oculomotor system, in general, and in area LIP in particular. According to the other view in order to program the second saccade the system takes into account the amplitude and direction (the vector) of the first saccade ("eye displacement" signal) and the vector corresponding to the spatial location of the second target ("retinal error" signal) coded in the initial gaze position, in

order to compute the new saccade vector, the "desired eye displacement" (Moschovakis et al., 1988; Goldberg et al., 1990).

In summary, area LIP seems to maintain a spatial representation of the world and its salient features in eye-centered coordinates suitable for the guidance of eye movements. It has projections to and from the FEF and the intermediate layers of the superior colliculus (Andersen et al., 1985; Lynch et al., 1985; Stanton et al., 1995). These connections are appropriate for transmitting spatial information to the oculomotor system.

Area AIP

Neurons in the rostral part of the lateral bank of IPs, (area AIP) respond to visual stimuli that the monkey can manipulate. Visual neurons in this area are sensitive to the shape and orientation of objects (Sakata et al., 1995; Murata et al., 2000). Motor neurons in AIP are activated in relation to specific hand movements. Reversible inactivation of area AIP affects the monkey's ability to shape its hand appropriately for grasping an object, but does not produce a deficit in reaching (Gallese et al., 1994). AIP holds a spatial representation related to the action (grasping movement) that the object can elicit. In other words, AIP provides multiple descriptions of a 3D object thus proposing several grasping possibilities to its projection target, area F5 in the ventral premotor cortex, which is responsible for grasping movements (Rizzolatti et al., 1997).

Area 7a

The part of Brodmann's area 7 which lies on the convexity has been subdivided into subregions 7a and 7b which correspond to cytoarchitectonic areas PG, PFG and PF (Pandya and Seltzer, 1982). Area 7a appears to play a role in spatial analysis through the integration of eye position signals and retinotopic visual information. The majority of the cells in this area have large, often bilateral visual receptive fields (Hyvärinen, 1981; Andersen et al., 1987; Andersen et al., 1990). Some cells display saccade-related activity although the neuronal activity in area 7a is mainly postsaccadic with fewer saccade-related neurons than LIP (Andersen et al., 1987). Unlike area LIP, area 7a is only weakly connected to the FEF and has no projections to the superior colliculus (Barbas and Mesulam, 1981; Andersen et al., 1990).

Area 7b

The majority of the cells in area 7b respond to somatosensory stimuli (Robinson and Burton, 1980; Hyvärinen, 1981). There is only a crude topographic arrangement of the body represented in area 7b with large somatosensory receptive fields. Cells in this area have also been reported to respond to reaching and hand manipulation (Mountcastle et al., 1975). As would be expected from an area with such response properties, area 7b shares corticocortical connections with other areas involved in somatosensory processing including area 5 and the insular cortex as well as areas involved in motor programming such as the ventral premotor cortex and the supplementary motor area (Cavada and Goldman-Rakic, 1989; Andersen et al., 1990).

1.2 AGRANULAR MOTOR CORTEX

The agranular frontal cortex of human and non-human primates has been subdivided into two regions: areas 4 and 6 (Brodmann, 1909). Area 4 is characterized by large pyramidal or Betz cells in layer V, cells that are not present in area 6. This early almost simplistic cytoarchitectonic map corresponded to an equally simple view of functional organization including two complete representations of body movements in the motor cortex (Penfield and Welch, 1951; Woolsey et al., 1952). The first representation, located on the lateral cortical convexity, is large and detailed and includes the entire area 4 of Brodmann as well as most of the lateral Brodmann's area 6. At that time the region including this first body representation was considered to be the primary motor cortex or M1. The second region, on the mesial cortical surface, is smaller than the former one, includes a less precise representation and is involved in proximo-axial movements. This region was called supplementary motor area, SMA.

Since these early studies, and over the recent years, the view on the organization of the motor cortex in the monkey has changed radically. The use of powerful anatomical and functional techniques has shown that the primate isocortical motor system is made up of at least 7 structural and functional fields each of which processes different aspects of motor behavior (for reviews (Rizzolatti et al., 1998; Geyer et al., 2000). These areas, through their reciprocal connections with the parietal areas described above, form a series of specialized circuits which work in parallel to transform sensory information into action. Each of the motor areas and the possible role of the corresponding parieto-frontal circuit will be discussed below.

1.2.1 Primary motor cortex (area F1)

Area F1 is organized somatotopically. On the cortical convexity the face is represented laterally close to the Sylvian fissure, the leg medially close to the midline extending also on the mesial wall of the hemisphere, and the arm in between (Fig. 1). Proximal parts of the limbs and axial body parts are primarily represented on the exposed cortical surface, whereas distal parts of the limbs and parts of the face, such as the lips and the tongue, are mainly represented in the rostral bank of the central sulcus (Woolsey et al., 1952). The body parts which are used for fine movements (fingers, lips, tongue) are represented over a larger cortical surface than body parts that are used in coarser movements (trunk, proximal extremities). This topography was described by the "motor homunculus" of Penfield in the human brain (Penfield and Rasmussen, 1952), and by the equivalent "motor simiusculus" of Woolsey in the monkey brain (Woolsey et al., 1952).

The role of F1 in motor control has been studied since the '60s in the experiments of Evarts. Evarts recorded from pyramidal tract neurons, which output the motor command from the cortex to the spinal cord, in monkeys trained to raise and lower weights with flexion and extension movements of the wrist (Evarts, 1968). Neurons showed specificity for either flexion or extension. A typical flexion-related neuron discharged several hundreds of milliseconds before the onset of flexion, increased its firing rate as the onset of movement approached and fired with maximal intensity during flexion. During extension the same neuron fired with considerably lower frequency or remained silent. An extension-related neuron showed the opposite behavior. In subsequent experiments, it was shown that the discharge frequency of pyramidal tract neurons was related to various mechanical parameters of the movement, such as the force that the monkey had to exert, the rate of change of the force, the joint position, or the velocity of the movement. Single neurons' activity was modulated by several of these parameters. Thus, it was shown that area F1 neurons control kinematic and dynamic parameters of movement.

The relation of neuronal activity in this area with other kinematic parameters of movement, such as the movement direction, was examined by Georgopoulos and colleagues (Georgopoulos et al., 1982). Each neuron discharged maximally for movements in one direction (the so-called "preferred

direction") and less during movements that deviated from the preferred direction. The directional tuning curve of each neuron had the shape of a Gaussian distribution curve with the curve's peak representing the preferred direction. The broad tuning at the single neuron level cannot account for the accuracy in the execution of specific movements. To explain that, many neurons were recorded during the movement in one direction and each neuron's contribution to the movement was represented as a vector. The vector's direction was that of the neuron's preferred direction, whereas the vector's amplitude reflected the discharge frequency of the neuron. At the population level, the population vector, which was calculated as the sum of the individual vectors of the recorded neurons, was in agreement with the direction of the actual movement.

Area F1 receives strong projections from area PE, the anterior part of area 5 lying on the convexity of the superior parietal lobule. Because of the involvement of this part of area 5 in somatosensory processing, it was suggested that the main role of the PE-F1 circuit could be the transfer of information (concerning the location of body parts) from the parietal cortex to the primary motor cortex in order to control the movement of the different body parts (Rizzolatti et al., 1998).

1.2.2 Ventral premotor cortex

The ventral sector of Brodmann's area 6 (PMv) is constituted by two distinct areas, F4 and F5 (Fig. 1) (Matelli et al., 1985). Area F4 has a low cellular density with scattered large pyramidal cells in its caudal and dorsomedial part. Area F5 is clearly laminated with a prominent layer V and a higher cell density than F4 (Geyer et al., 2000). The spur and the inferior arcuate sulcus separate F4 and F5 from the dorsal premotor cortex and the prefrontal cortex. Area F4 lies rostral to F1 extending dorsomedially to the arcuate spur and ventrolaterally to the rostralmost extension of the primary somatosensory cortex at the level of the inferior precentral dimple. Area F5 occupies the rostral part of the PMv and borders the prefrontal cortex at the fundus of the inferior arcuate sulcus. Recent cytoarchitectonic and immunohistochemical findings have shown that area F5 is not homogeneous but is formed by two major sectors, one located in the posterior bank of the inferior limb of the arcuate sulcus, and the other located on the cortical convexity adjacent to the arcuate sulcus (Matelli et al., 1996). Therefore, there are three different subdivisions within the ventral premotor cortex participating in three different parietofrontal circuits.

Area F4

Area F4 is electrically excitable and is organized in a somatotopic fashion; arm movements are represented dorsally and orofacial movements ventrally (Fig. 1). Microstimulation studies have shown that thresholds for eliciting movements are higher in F4 than in F1, and the evoked movements are complex in that they usually involve more than two articulations. Arm, neck, face and mouth movements are represented. From the arm field of F4 mainly proximal movements are elicited (Gentilucci et al., 1988; Godshalk et al., 1995). Single neuron recordings have also confirmed the results of the microstimulation studies and showed, furthermore, that many neurons fire during reaching movements directed toward the body or away from it (Gentilucci et al., 1988).

The majority of neurons in area F4 are bimodal responding to both visual and tactile stimuli (Fogassi et al., 1996; Graziano et al., 1997). These cells resemble the bimodal neurons in area VIP. However, in contrast to VIP where unimodal neurons are visual, unimodal neurons in F4 are typically tactile, and purely visual neurons are very rare. Tactile receptive fields are predominantly located on the face, arm and the upper part of the body. The visual receptive fields are located in the peripersonal space and are in register with the tactile fields. In most cases the visually responsive neurons respond preferentially to stimuli directed toward the tactile receptive field. Some cells respond only if the stimulus is within a few cm of the tactile receptive field, whereas others respond to stimuli as far away

as 1 m; all cells respond better to closer stimuli. Of interest is that in the majority of these neurons the visual receptive field remains anchored to the tactile receptive field when the body part, where the tactile receptive field is located, is moved. In other words a visual receptive field located on the arm does not move when the monkey moves its eyes but it does move when the monkey moves its arm (Graziano et al., 1997; Graziano and Gross, 1998). The fact that arm position influences the visual receptive field location even when the arm is not visible to the monkey indicates that this effect is at least partly mediated by proprioception. These properties indicate that, within F4, space is encoded in body-parts-centered coordinates (Graziano et al., 1994; Fogassi et al., 1996).

Moreover, it was shown that the effect of arm position on the visual responses of F4 neurons is both visual and proprioceptive. The two influences converge on single neurons. These neurons responded to the felt position of the arm when the arm was covered from view and they also responded in a similar fashion to the seen position of a fake arm (Graziano, 1999). However, removing the sight of the arm caused a reduction in the effect of arm position on the response of the neuron, indicating that the sight of the arm also contributed to the neuron's information about arm position.

Many F4 neurons fire upon reaching movements i.e. movements of the proximal arm, but not upon movements of the distal arm. A correlation is often found between the positions of the somatosensory and visual receptive fields and the direction of the effective movement, e.g. a neuron with a tactile and visual receptive field in the face region also fires during a movement towards the upper space (Gentilucci et al., 1988).

Anatomically, area F4 receives its "predominant" parietal input from area VIP (Luppino et al., 1999). It also receives additional connections, though weaker ones, from the parietal areas PF and PEip. The VIP-F4 circuit has been suggested to play a role in encoding the peripersonal space and in transforming object location into appropriate movement toward it (Rizzolatti et al., 1998). Furthermore area F4 is directly connected with area F1 and projects mainly to the upper cervical segments of the spinal cord (Matelli et al., 1986; He et al., 1993). Finally, area F4 has strong connections with the mesial premotor area F3 (SMA proper) and sends weaker projections to mesial premotor area F6 (pre-SMA) (Luppino et al., 1993).

Area F5

Area F5 is much less excitable than area F4. Movements can be elicited almost exclusively from the part of area F5 lying in the caudal bank of the inferior limb of the arcuate sulcus. Area F5 is organized somatotopically. Arm movements are represented dorsally and orofacial movements are represented ventrally. In contrast to F4, it is the distal arm that is mainly represented in F5 (Kurata and Tanji, 1986; Gentilucci et al., 1988). F5 neurons discharge during specific goal-directed actions performed with the hand, the mouth or both. The actions which are mostly represented are grasping, holding, tearing and manipulating (Rizzolatti et al., 1988). Most grasping neurons code specific types of hand configuration such as precision grip, whole-hand prehension, finger prehension. When objects with different geometric properties are grasped in a similar way, similar neuronal responses are obtained. Some of these neurons respond to somatosensory stimuli also, with a good correlation between the neuron's preferred type of grip and the location of the somatosensory receptive field (Rizzolatti et al., 1988). Some neurons also respond to the presentation of 3D objects (similar to neurons in AIP) even when no action upon the object is allowed (Murata et al., 1997).

Reversible inactivation of F5 results in disturbances of hand preshaping and object grip but no deficit in reaching. These results are similar to those obtained from area AIP. There are also signs of peripersonal neglect in the hemispace contralateral to the inactivation site following inactivation of F5 (Schieber, 2000; Fogassi et al., 2001). This result could indicate that F5 may also play a role in coding space.

A small part of area F5 in the caudal bank of the arcuate sulcus projects to F1. In contrast to F4, area F5 is strongly connected with the mesial premotor area F6 rather than with the mesial area F3

(Matelli et al., 1986; Luppino et al., 1993). The part of F5 lying in the caudal bank of the inferior arcuate receives its predominant connections from area AIP (Luppino et al., 1999), as it would be expected on the basis of the similarity of responses obtained from these two areas. The AIP-F5 circuit has been suggested to play a crucial role in transforming the intrinsic properties of the object into the appropriate hand movements (Jeannerod et al., 1995). The description of objects, in terms of their 3D shape, is carried out in AIP and then is transmitted to F5 where different types of grips are encoded. This way, the object characteristics are matched to a specific grip appropriate for grasping this object. Further support for such a role in the AIP-F5 circuit comes from the results of the inactivation studies in both F5 and AIP. Although preshaping is disrupted, grasping movements are still possible through a series of corrections based on tactile exploration of the object to be grasped. These results show that inactivation of both F5 and AIP disrupts only the capacity to transform the 3D properties of objects into appropriate hand movements.

Neurons located in the part of F5 lying on the cortical convexity have the same motor properties as the F5 neurons described above. The visual properties of the neurons in the two sectors of F5, however, are markedly different. The main characteristic of F5 convexity neurons is that they fire when the monkey observes another individual performing an action similar to that encoded by the neuron e.g. a grasping movement using a precision grip. The object presentation itself is not sufficient to activate them. The movement of the hand is also not sufficient to activate the neurons when no interaction with the object is established, or when the object is grasped with a tool. These neurons were called "mirror neurons" (Gallese et al., 1996; Rizzolatti et al., 1996). The F5 convexity sector seems to participate in a circuit which also involves area PF from which it receives its predominant connections (Pandya and Seltzer, 1982). The role of this circuit has been suggested to be the internal representation of actions and the understanding of the biological meaning of actions (Rizzolatti et al., 1998).

1.2.3 Dorsolateral premotor cortex

The dorsal premotor cortex (PMd) or superior area 6 is constituted by two areas, F2 caudally and F7 rostrally (Fig.1). The subdivision of PMd in a rostral and a caudal area has long been accepted although the border between the two areas is highly variable (Vogt and Vogt, 1919; Bonin and Bailey, 1947; Barbas and Pandya, 1987). The parcellation of PMd into areas F2 and F7 is supported by converging results from histochemical (Matelli et al., 1985), cytoarchitectonic (Matelli et al., 1991), and immunohistochemical data (Geyer et al., 2000). In Nissl-stained sections, area F2 shows poor lamination and the transition from F1 to F2 is characterized by an increase in cellular density in layers III and V. Area F7 on the contrary is well laminated and is characterized by a prominent layer V. The spur and the superior arcuate sulcus separate areas F2 and F7 from the PMv and the prefrontal cortex. Area F2 extends from 2 to 3 mm lateral to the midline, to the fundus of the arcuate spur and the fundus of the caudal part of the superior arcuate sulcus. The border between F2 and F7 lies slightly anterior to the genu of the arcuate sulcus. Area F7 extends from 2 to 3 mm lateral to the midline, to the fundus of the rostral part of the superior arcuate sulcus (Matelli et al., 1991).

Area F2

Area F2 is electrically excitable and has a rough somatotopic organization. The leg is represented dorsal to the superior precentral dimple while the arm ventral to the same dimple (Kurata, 1989; Dum and Strick, 1991; He et al., 1993; Godshalk et al., 1995; Fogassi et al., 1999). Functional studies involving single-unit recording have shown that some F2 neurons discharge in association with movement onset while others become active long in advance of it. Neurons showing this anticipatory response may play a role in motor preparation (Wise et al., 1997). Some neurons respond to the presentation of visual stimuli, instructing the monkey on the movement that they have to perform.

These "signal-related" neurons are more numerous in the rostral part of F2 than in its caudal part (which surrounds the dimple). Neurons with "set-related" activity, discharging in the delay period between the instruction and the trigger signal, are found in the central part of F2 while "movement-related" neurons, firing between the trigger signal and the movement onset, are found in the caudal part of F2, close to area F1 (Caminiti et al., 1996; Johnson et al., 1996).

In the forelimb representation, distal and proximal movements are equally represented, with distal movements located more laterally. Proprioceptive responses were recorded from 70% of the neurons while tactile responses were recorded from less than 20% (Fogassi et al., 1999). In the same study purely visual neurons were found in the rostrolateral sector of the forelimb representation of F2, which discharged when the monkey observed 3D objects regardless of the object's spatial location and its distance from the monkey. Bimodal neurons responded to both tactile and visual stimulation, with their receptive fields mostly located on the forelimb or the upper trunk. Finally, "peripersonal" neurons and "extrapersonal" neurons responded to visual stimuli moving within the monkey's peripersonal and extrapersonal space, respectively.

The finding that proprioceptive responses are predominant in the dimple region in the caudal F2 while visual responses are present in the rostrolateral sector of F2 parallels the anatomical data which have shown that visual input from the parietal areas MIP and V6A is fed to the arm field of F2 while somatosensory input from parietal areas PEc and PEip is transmitted to the F2 dimple region (Matelli et al., 1998). On the basis of these data it has been suggested that the PEip/PEc-F2 dimple circuit is involved in the planning and controlling of movements on the basis of somatosensory information. In contrast, the MIP/V6A-F2 ventrorostral circuit uses visual information for the same purpose.

Furthermore, area F2 is directly connected to F1 and not with the prefrontal cortex (Barbas and Pandya, 1987; Luppino et al., 1990). It also has direct connections with the spinal cord as well as with the brainstem (Keizer and Kuyepers, 1989; He et al., 1993). The pattern of connections with the spinal cord matches the topography observed in area F2 with largely separate regions projecting to the upper cervical, lower cervical, and lower lumbosacral segments of the spinal cord (He et al., 1993).

Area F7

Electrophysiological evidence has shown that in the dorsolateral part of area F7, low-threshold eye and/or neck movements can be evoked by intracortical microstimulation. This part of F7 is generally referred to as the supplementary eye field (SEF) and its neurons fire before a saccade is initiated (Schlag and Schlag-Rey, 1985; Schlag and Schlag-Rey, 1987). Interestingly it has been suggested that many SEF neurons encode the direction of an impending saccade relative to an object-centered frame of reference (Olson et al., 1996).

The remaining part of F7 is scarcely excitable with electrical stimulation although eye movements were sometimes evoked from it by applying high current intensities (Godshalk et al., 1995). Although the physiological properties of neurons in this part of F7 remain largely unknown, recording experiments have shown that these neurons respond to arm movements or visual stimuli. Visually responsive F7 neurons do not require a subsequent stimulus related movement to become active (di Pellegrino and Wise, 1991). In conditional stimulus-response association tasks area F7 plays a crucial role with the contribution of area F2. This result was derived from ablation studies of the postarcuate (Halsband and Passingham, 1982) or periarcuate cortex (Petrides, 1982) in monkeys trained to perform a conditional association motor task. After the lesion the monkeys were unable to perform the task although no obvious motor deficit was present.

The only parietal input to the oculomotor sector of F7 corresponding to the SEF comes from area LIP. The role of the LIP-SEF circuit should therefore be the control of saccadic eye movements. In contrast, the ventral and caudal parts of F7, which have been much less studied, receive their major inputs from the mesial sector of the superior parietal lobule, area PGm, with additional inputs

originating from area V6A (Cavada and Goldman-Rakic, 1989; Matelli et al., 1998). This circuit has been suggested to play a role in the visual localization in space of stimuli used as targets for reaching movements.

Furthermore, area F7 is strongly connected with the prefrontal cortex, Brodmann's areas 8 and 46, but has no direct connections with area F1 (Barbas and Pandya, 1987; Luppino et al., 1990). When fluorescent tracers were injected in the spinal cord at C2 level and in the medial tegmentum of the medulla oblongata in the brainstem, it was found than no corticospinal projections originate from F7 whereas this area has rich connections with the brainstem (Keizer and Kuyepers, 1989).

1.2.4 Mesial motor cortex

The mesial area 6 was classically defined as the supplementary motor area, SMA (Penfield and Welch, 1951; Woolsey et al., 1952). Electrical stimulation of this part of the monkey brain revealed a complete somatotopic map of the body (Woolsey et al., 1952). Over the recent years it has become clear that the SMA corresponds to two different subregions with distinct cytoarchitectonic and functional properties. These two areas are: area F3 or SMA-proper, and area F6 or pre-SMA. The parcellation of the mesial cortex into areas F3 and F6 is based on histochemical (Matelli et al., 1985), cytoarchitectonic (Matelli et al., 1991), and receptor autoradiographic data (Geyer et al., 1998). In Nissl stained sections area F3 is poorly laminated with higher cellular density in the lower layer III and the upper layer V. Area F6, on the contrary, is clearly laminated with a dark layer V well demarcated from layers III and VI. Area F6 borders the prefrontal cortex where a clear recipient granular layer IV is evident. Area F3 lies on the mesial cortical surface immediately anterior to F1 and extends rostrally for 8 to 10 mm (Fig. 1). Area F6 lies anterior to F3 and extends rostrally for 5 to 6 mm up to the prefrontal cortex. Ventrally areas F3 and F6 cover the mesial wall of the hemisphere until approximately the middle of the dorsal bank of the cingulate sulcus.

Area F3

Area F3 is somatotopically organized. Intracortical microstimulation experiments revealed that hindlimb movements are located caudally, forelimb movements centrally and orofacial movements rostrally at the border with area F6 (Mitz and Wise, 1987; Luppino et al., 1991; Matsuzaka et al., 1992). Forelimb movements are also evoked from a small zone located within the hindlimb field near the border of F3 with F1 (Luppino et al., 1991). Both hindlimb and forelimb zones run obliquely in the rostrocaudal dimension, from dorsorostral-to ventrocaudal. The orofacial representation is smaller and lacks the band-like appearance of the other two.

In contrast to F1, where proximal and distal movements are equally represented, the majority of limb movements in F3 involve proximal joints (Woolsey et al., 1952; Luppino et al., 1991). Distal movements are mostly represented in the deepest part of the medial surface and in the upper bank of the cingulate sulcus, although, in contrast to F1, proximal and distal movements are not segregated in area F3. Moreover, in area F3 movements are evoked at higher thresholds compared to the ones required in F1. Another difference between the two areas is that whereas intracortical electrical microstimulation in F1 evokes movements around a single joint, movements involving two or more articulations are also evoked by microstimulation of F3 (Mitz and Wise, 1987; Luppino et al., 1991).

Single neuron recordings have shown that many F3 neurons respond to somatosensory stimuli (Matsuzaka et al., 1992; Rizzolatti et al., 1996). Most F3 neurons discharge in association with active movements. Although the relation between the discharge and the movement may vary greatly from one neuron to another, the discharge onset of F3 neurons is typically time-locked to the movement onset (Alexander and Crutcher, 1990; Matsuzaka et al., 1992). Although several roles have been attributed to the SMA, including its involvement in (a) internally versus externally triggered

movements (Passingham, 1987; Mushiake et al., 1991), (b) in the preparation for movement (Tanji et al., 1980) and (c) in the planning and execution of sequences of movements (Roland et al., 1980; Mushiake et al., 1991; Tanji and Shima, 1994), none of these properties seem to be unique for SMA proper.

Area F3 receives somatotopically organized projections from somatosensory areas SII, PEci, PE and cingulate area 23 (Petrides and Pandya, 1984; Luppino et al., 1993). Cortical afferents to area F3 originate also from areas F2, F4, F5, F6 and F7 (Luppino et al., 1993). Moreover, area F3 is also directly connected to F1, and has descending corticospinal and corticobulbar connections. The caudal part of F3 projects to the thoraco-lumbar segments, whereas the rostral part to the cervico-thoracic segments of the spinal cord (Keizer and Kuyepers, 1989; Luppino et al., 1994; He et al., 1995).

The above described functional properties of area F3, together with its connectivity pattern, have led some investigators to suggest that F3 controls motor activity in a rather global way, and exerts this control based on proximal and axial synergisms (Rizzolatti et al., 1996).

Area F6

Area F6 is poorly excitable with standard electrical intracortical microstimulation. When appropriate activation procedures are applied, its stimulation usually produces slow global movements resembling natural movements (Luppino et al., 1991). A large part of F6 is related to arm movements. Its forelimb representation is separated from that of F3 by the orofacial field of area F3 (Luppino et al., 1991).

Single unit recordings in F6 neurons have shown that unlike F4 and F5 neurons, F6 neurons donnot discharge in association with distal and proximal arm movements but control action in a more global way. Neurons responding to visual stimuli are found more often in area F6 than in area F3 (Matsuzaka et al., 1992). Premovement neuronal activity long before the onset of the movement is present in area F6 (Alexander and Crutcher, 1990; Rizzolatti et al., 1990; Matsuzaka et al., 1992) in contrast to F3, where phasic activity more frequently locked to the movement onset is more common. In F6 there are neurons related to arm movements that show complex properties. The activity of these neurons is influenced by the distance of the object from the monkey, with complex patterns of excitation-inhibition depending on whether the animal can reach and grasp the presented object (Rizzolatti et al., 1990).

Area F6 is mainly connected with areas F5 and F7, the prefrontal cortex, cingulate area 24c, and only weakly with the posterior parietal areas PG and PFG. In contrast to F3 it is not connected with area F1, and has only corticobulbar projections and no corticospinal ones (Keizer and Kuyepers, 1989; Luppino et al., 1993; Luppino et al., 1994).

These data suggest that area F6 is much less linked to movement execution than F3. Its motor function seems to be of "high-level". Area F6 is considered to be a "supramotor" control center which triggers a movement taking into account external contingencies and motivational factors (Rizzolatti et al., 1998).

1.3 AIM OF THE PRESENT STUDY

Goal directed reaching is usually accomplished by an initial saccadic eye movement to foveate the target of interest, followed by a subsequent arm movement towards the same target. In previous experiments, which were performed in our laboratory, the cortical regions activated during reaching to a visual target with one forelimb were revealed (Dalezios et al., 1996; Savaki et al., 1997) by application of the [^{14}C]deoxyglucose ([^{14}C]DG) quantitative autoradiographic method (Sokoloff et al., 1977) in monkeys. The results of these studies demonstrated the functional involvement of several motor, somatosensory, visual, oculomotor and higher order association cortical regions of the monkey brain in the seemingly simple behavior of reaching toward a visual target. One of the aims of the present study was to dissociate the cortical regions, which are involved in the control of eye movements from those involved in the control of forelimb movements. To this end, we mapped the metabolic activity by means of the [^{14}C]DG method in the brain of monkeys performing (i) fixation of a visual target, (ii) saccades to visual targets, and (iii) reaching of a peripheral visual target during fixation of a central visual target.

Another important issue is the dissociation between visual and somatosensory information used to guide reaching movements. The sense of limb position is necessary for the control of movement. We use two types of cues to determine the position of our arm: the felt position (proprioceptive input) and the seen position (visual input). We know very little about the way these signals are combined in the brain. In previous experiments, the [^{14}C]DG method was used to map the local cerebral metabolic activity, during the performance of a visually cued reaching task, in visually intact monkeys and in monkeys with one hemisphere deprived of all known visual input by optic chiasm section and commissurotomy (Savaki et al., 1993). The different activations induced by the performance of the same behavior in the visually intact and in the visually deprived monkeys suggested that the dorsal part of intraparietal area 5 is associated with the proprioceptive guidance of the moving forelimb, whereas the ventral part of the same area is related to the visual guidance of reaching. To test this hypothesis, we performed an additional experiment in the present study, in which the monkey had to reach from a central to a peripheral position, in complete darkness, while its eyes maintained a straight ahead direction. Only proprioceptive-somatosensory information is available to guide the forelimb during reaching in the dark (RD). In contrast, both visual and somatosensory information is available to guide the forelimb during reaching in the light (RL$_f$). Therefore, comparison of the distribution of activity in the IPs of the RD and the RL$_f$ monkeys should allow for dissociation between subregions responsible for the somatosensory and the visual guidance of reaching. According to the earlier proposal (Savaki et al., 1993), we predicted that only the dorsal part of area 5 would be activated in the RD monkey, whereas the ventral intraparietal region would be activated only in the RL$_f$ monkey. In this study we provide evidence to support these predictions and consequently our earlier hypothesis. Furthermore, the distinct parietal and frontal cortical subregions, which are involved in visual fixation, visually guided saccades, reaching in the light, and reaching in the dark are demonstrated.

2. METHODS

2.1 BEHAVIORAL TASKS

2.1.1 Subjects

All experimental procedures were performed according to the EU directive No 86/609 for the care of laboratory animals. The monkeys were purchased from Labor Agra (Budapest, Hungary) and were housed in our animal facility, having free access to standard food pellets (Mucedola, Milan, Italy).

Seven adult female monkeys (five *Macaca mulatta* and two *Macaca nemestrina*) weighing between 3 and 4 kg were used. The first one was an untrained control whereas the other six monkeys were trained to perform five different tasks. All seven monkeys had their heads fixed and a water delivery tube attached close to their mouth. For immobilization of the head, a metal bolt embedded in dental cement was surgically implanted on the head of each monkey with the use of mandibular plates which were secured on the bone by titanium screws (Synthes). All surgical procedures were performed under general anesthesia (ketamine hydrochloride 20 mg/kg, im.) using aseptic techniques. Eye movements in five experimental monkeys were recorded with implanted search coils (Robinson, 1963) sutured on the sclera (modified from Judge et al., 1980). When the monkey was exposed to two alternating magnetic fields (one vertical and one horizontal) eye position could be accurately recorded from the voltage generated in the wire coil, which was sutured on the sclera. Eye position was digitized on-line at a sampling rate of 500 Hz using the Spike2 software (Cambridge Electronics Design, Cambridge, U.K.) and recorded on hard disk for off-line analysis.

2.1.2 Experimental set-up

The monkeys were seated in a primate chair, with their head fixed, at a distance of 25 cm in front of a video monitor where visual stimuli were presented. Visual targets were red, round illuminated spots of 1.5 deg diameter. Monkeys could not move their forelimbs during the fixation and saccade tasks, and had to maintain fixation during the reaching tasks. Successful completion of each trial was rewarded with water. The animals were deprived of water prior to the daily training session. Behavior was controlled through software that was running on an IBM-compatible personal computer (PC), relied on a series of specialized hardware:

(a) a video monitor used to present visual stimuli to the subjects ("subject monitor")

(b) an ISA-based board (Omnicomp Texan video board) used to provide a video signal to the subject monitor

(c) a Microtouch capacitive touchscreen, installed on the subject monitor. It allows the PC to read the position of the subject's finger when touching the screen

(d) a multipurpose data acquisition board (National Instruments AT-MIO-16E-2) used: (i) to control experimental timing, (ii) to acquire analog signals concerning eye position, (iii) to acquire digital signals from the behavioral apparatus, and (iv) to output digital signals to control the reward circuit (Christ Instrument Co., Hagerstown, MD, U.S.A.)

(e) a digital I/O board (National Instruments PC-DIO-96) used to output digital signals, which were used as markers to transfer timing information to a second computer, where the eye position was recorded on line and saved for off-line analysis.

2.1.3 Tasks

In order to use the smallest possible number of monkeys, the five behavioral tasks used in our study were designed so that, controlled behavioral parameters were gradually added. This way, all tasks were complementary to each other, and the major metabolic findings in each monkey per task were verified by those in the monkey of the following, more complex task (see Results section for further explanations).

The first monkey was an *untrained control* (C monkey), seated in front of the nonfunctioning behavioral apparatus and receiving neither visual stimuli nor liquid reward during the [^{14}C]DG experiment.

Fixation task.

The second monkey (F monkey) had to fixate a central visual target located straight ahead (Fig. 2A). The monkey had to maintain fixation during the whole period of illumination of the target (4 s per trial) within a circular window of 2.5 deg diameter and was allowed to move the eyes only during the intertrial intervals (200 -300 ms). On the experimental day, this monkey maintained fixation for 75% of the time.

Saccade tasks.

The third monkey (S$_h$ monkey) was required to perform a sequence of visually guided horizontal saccades of 5, 10, and 15 deg to the left, then two saccades of 30 deg to the right, and finally a saccade of 30 deg to the left, as illustrated in Figure 2B. The monkey had to fixate each illuminated target for 300-600 ms until it disappeared and the next one was illuminated signaling a saccadic movement to the new location. Fixation was maintained within a circular window of 2.5 deg diameter. The minimum latency to move the eyes after onset of each target was set to 100 ms to discourage anticipatory movements. The intertrial intervals ranged randomly between 500 and 800 ms. On the experimental day, this monkey performed 55 leftward saccades of each amplitude (5, 10, 15, and 30 deg) during the critical five first minutes of the [^{14}C]DG measurement.

The fourth monkey (S$_o$ monkey) was required to execute up-left saccades, 20 deg in amplitude and 45 deg in direction as shown in Figure 2C. Each trial was initiated with the appearance of a central fixation target. The monkey had to fixate it for 500 - 1000 ms until it disappeared and the peripheral target was illuminated signaling that a saccade to it should be executed within 1000 ms. The monkey was required to fixate the peripheral target for 500 - 1000 ms until it too disappeared. The animal was free to move its eyes spontaneously during the inter-trial interval (1000 - 1800 ms). The other task parameters were similar to the previous case. During the critical five first minutes of the experiment, this monkey performed 60 saccades to the visual target.

Reaching in the light tasks

The fifth monkey (RL$_f$ monkey) performed reaching movements in the light with the left forelimb, from a central to a peripheral visual target, during central fixation (Fig. 2D). The central target was located in the median sagittal plane at shoulder height, whereas the peripheral one was located 20 deg away from straight ahead in an oblique direction 45 deg up and to the left. The monkey was required to look at the illuminated central target and touch it with the index of its left forelimb for 800-1500 ms, until the peripheral target was illuminated. Then, the monkey had to reach and touch the peripheral target and hold it for 500-1000 ms while maintaining fixation of the central target. The minimum latency to move the forelimb was set to 250 ms to discourage anticipatory movements. The maximum latency to reach the target was set to 1500 ms, although the movement was usually completed in 500-600 ms. The intertrial intervals ranged between 1000 and 1800 ms. The monkey was required to hold eye and finger position within circular windows of 2.5 deg and 1.5 cm diameter, respectively. On the experimental day, this monkey performed 50 reaching movements during the critical five first minutes of the [^{14}C]DG measurement.

The sixth monkey (RL monkey) performed reaching movements in the light with the left forelimb, from the central to the peripheral visual target without any fixation requirements. The

monkey was free to move its eyes throughout the trial period and used its palm to press illuminated pushbuttons (instead of the index finger of the previous case). All other task parameters were similar to the ones used for the fifth monkey. On the experimental day, this monkey performed 40 reaching movements during the critical five first minutes of the [^{14}C]DG measurement.

Figure 2. Schematics for behavioral paradigms and task events. (A) In the visual fixation paradigm, the monkey was rewarded for fixating a visual target (T_0) centered straight ahead. V and H, vertical and horizontal eye position, respectively. (B) In the cartoon of the horizontal saccades task, spatial locations of the targets are represented by gray circles and saccades by arrows. The monkey performed a sequence of visually guided horizontal saccades of 5 deg (from T_0 to T_1), 10 deg (from T_1 to T_2), and 15 deg (from T_2 to T_3) to the left, then two saccades of 30 deg (from T_3 to T_0, and from T_0 to T_4) to the right, and finally a saccade of 30 deg (from T_4 to T_0) to the left. Black arrows in the cartoon and black deflections in the horizontal eye position trace represent the 5, 10, 15 and 30 deg leftward saccades which were contraversive to the illustrated IPs in Figure 6C. Gray arrows and deflections represent the 30 deg ipsiversive saccades. (C) In the cartoon of the oblique saccades task, spatial locations of the targets are represented by gray circles and saccades by arrows. The monkey performed visually guided oblique saccades 20 deg in amplitude (from T_0 to T_1). (D) In the reaching in the light task, the monkey performed reaching movements with the left forelimb, from a central visual target (T_0) to a peripheral one (T_1) located 20 deg up left. The RL$_f$ monkey had to fixate at the illuminated T_0 and touch it with the index of its left forelimb until the onset of T_1. Then, the monkey had to touch T_1 while the eyes maintained fixation of T_0. (E) In the reaching in the dark task, the monkey performed reaching movements with the left forelimb, from the central target (T_0) to the peripheral one (T_1) located 20 deg up left. Vision of the screen and the forelimb was occluded.

A   Fixation task
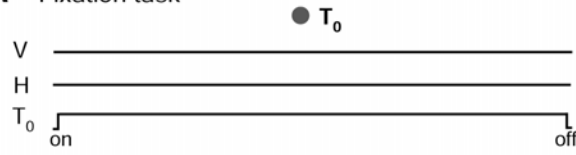
B   HorizontalSaccades task

15 deg
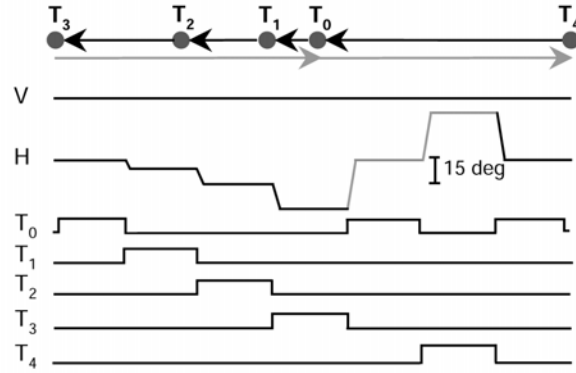
C   Oblique Saccades task

14 deg
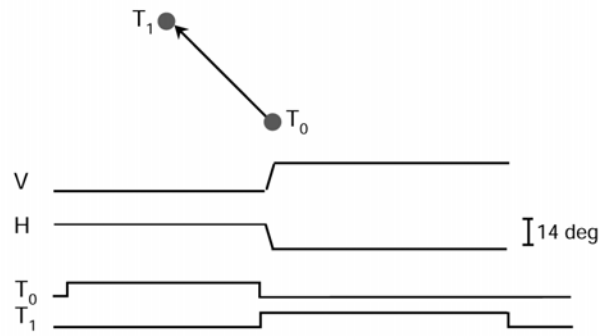
D   Reaching in the light task
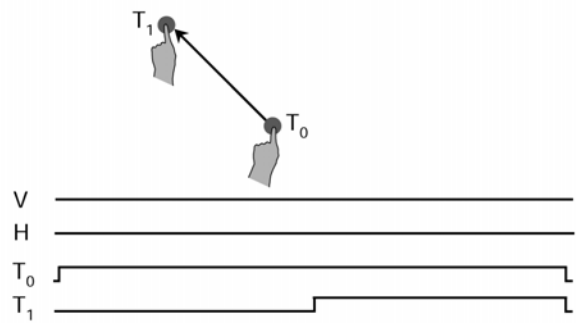
E   Reaching in the dark task
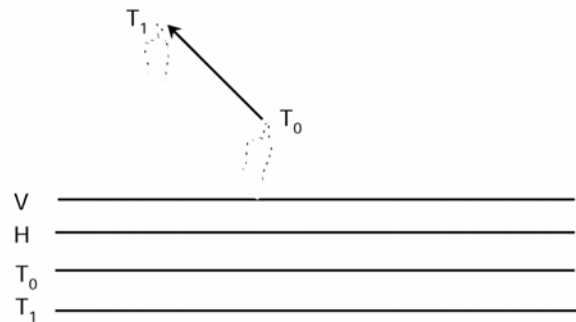
Reaching in the dark task.

The seventh monkey (RD monkey) remained in the dark, where it performed reaching movements with the left forelimb from a central to a peripheral position on the touchscreen, while the eyes maintained a straight ahead direction (Fig. 2E). View of its forelimb and of the touchscreen was occluded by a black barrier positioned vertically 10 cm in front of the monkey's eyes. The central and peripheral positions on the screen were at the same coordinates as the visual targets presented to the third monkey (same as in Fig. 2D). The monkey was required to hold eye and finger position within circular windows of 5 deg and 3.5 cm diameter, respectively. A speaker was placed 23 cm in front of the monkey, in the median sagittal plane, on top of the screen. Following an auditory cue (90 Hz), the monkey had to look straight ahead in the dark, towards a location corresponding to the central position of the screen. Then the monkey had to reach (within 3000 ms), touch the screen with the index and middle finger of its left forelimb at the central position and hold its forelimb there for 600-1000 ms, until a second auditory cue (180 Hz) signaled a reaching movement to the peripheral position on the screen. Then, the monkey had to reach (within 2000 ms) and touch the screen at the peripheral position and hold its forelimb there for 500-1000 ms, while the eyes maintained the straight ahead direction. The intertrial intervals ranged between 500 and 900 ms. On the experimental day, this monkey performed 40 reaching movements during the critical five first minutes of the [^{14}C]DG measurement.

**2.2 THE [^{14}C]DEOXYGLUCOSE AUTORADIOGRAPHIC METHOD FOR THE METABOLIC MAPPING OF FUNCTIONAL NEURAL PATHWAYS IN THE CENTRAL NERVOUS SYSTEM**

The brain exhibits a close relationship between energy metabolism and functional activity. The functions responsible for the brain's energy demands are mainly excitation, inhibition and conduction and these are reflected in the unceasing electrical activity of the brain. The electrical energy is ultimately derived from chemical processes and it is likely that most of the brain's energy consumption is utilized for active transport of ions to sustain and restore the membrane potentials discharged during the processes of excitation, inhibition, and conduction.

The brain's demands for energy are among the greatest of all body tissues and this is reflected in its relatively enormous rate of oxygen consumption (20% of the resting total body oxygen consumption in adults) which provides the energy required for its intense physiochemical activity. Oxygen is normally utilized in the brain almost entirely for the oxidation of carbohydrate and in the normal state the main substrate for cerebral energy metabolism is glucose taken up from the blood. Actually, the brain is normally restricted almost exclusively to glucose as the substrate for its energy metabolism. Given that energy metabolism and functional activity in the brain are interrelated it is possible to estimate the level of functional activity by measuring the rate of glucose consumption. Louis Sokoloff and his collaborators (Sokoloff et al., 1977) developed a method, which takes advantage of this relationship in order to map alterations in functional activity during physiological or experimentally induced changes of local functional activity. The method employs radioactive deoxyglucose ([^{14}C]deoxyglucose), an analogue of glucose, to trace glucose metabolism in the brain. It allows quantification of the rate of glucose utilization and also provides a high resolution (20 μm) pictorial representation of the relative glucose consumption in all components of the central nervous system, simultaneously. Therefore, functional maps of the brain in normal and experimental states can be obtained by using the [^{14}C]deoxyglucose method in laboratory animals.

2.2.1 Theoretical Basis of the Deoxyglucose Method

Although oxygen consumption is the most direct measure of energy metabolism, the volatility of oxygen and its metabolic products, as well as the short physical half-life of its radioactive isotopes, precluded measurement of oxidative metabolism by the autoradiographic technique. Although glucose is in most circumstances essentially the sole substrate for cerebral oxidative metabolism, and its utilization is stoichiometrically related to oxygen consumption, the use of radioactive glucose is not satisfactory either, because its labeled products are lost too rapidly from the cerebral tissues. The labeled analogue of glucose, 2-deoxy-D-1-[^{14}C]glucose (2-DG), was therefore selected because its biochemical properties make it particularly appropriate to trace glucose metabolism and to measure local cerebral glucose utilization by the autoradiographic technique. 2-DG differs from glucose only in the replacement of the hydroxyl group on the second carbon atom by a hydrogen atom. This single structural difference makes 2-DG suitable for this method.

The method is derived by analysis of a model based on the biochemical properties of 2-DG in the brain (Sokoloff et al., 1977) (Fig. 3). 2-DG is transported bidirectionally between blood and brain by the same carrier that transports glucose across the blood-brain barrier (Bidder, 1968; Bachelard, 1971). In the cerebral tissues 2-DG is phosphorylated by hexokinase to 2-deoxyglucose-6-phosphate (DG-6-P) just like glucose is phosphorylated to glucose-6-phosphate (G-6-P) (Sols and Crane, 1954). 2-DG and glucose are therefore competitive substrates for both blood-brain transport and hexokinase-catalyzed phosphorylation. However, unlike G-6-P, which is metabolized further eventually to CO_2 and water (and to a lesser degree via the hexosemonophosphate shunt), DG-6-P cannot be converted to fructose-6-phosphate due to the lack of the hydroxyl group on the second carbon atom, and it is also not a substrate for glucose-6-phosphate dehydrogenase (Sols and Crane, 1954). There is relatively little glucose-6-phosphatase activity in the brain (Hers, 1957) and even less deoxyglucose-6-phosphatase

activity (Sokoloff et al., 1977). DG-6-P can be converted into deoxyglucose-1-phosphate, then into UDP-deoxyglucose and eventually into glycogens, glycolipids, and glycoproteins, but these reactions are not only slow but also a very small fraction of the DG-6-P formed proceeds to these products in mammalian tissues (Nelson et al., 1984). In any case, these compounds are secondary, relatively stable products of DG-6-P, and all together represent the products of deoxyglucose phosphorylation. DG-6-P and its derivatives, once formed, are therefore essentially trapped in the cerebral tissues, at least long enough for the duration of the experimental period.

If the interval of time following the intravenous administration of $[^{14}C]DG$ is kept short enough (less than 1h) to allow the assumption of negligible loss of $[^{14}C]DG$-6-P and its secondary products from the tissues, then the quantity of $[^{14}C]DG$-6-P accumulated in the cerebral tissue at any given time following the introduction of $[^{14}C]DG$ into the circulation is equal to the integral of the rate of $[^{14}C]DG$ phosphorylation by hexokinase, in that tissue, during that interval of time. This integral is in turn related to the amount of glucose that has been phosphorylated over the same interval, depending on the time courses of the relative concentrations of $[^{14}C]DG$ and glucose in the precursor pools and the Michaelis-Menten kinetic constants for hexokinase with respect to both $[^{14}C]DG$ and glucose. With the cerebral glucose consumption in a steady state, the amount of glucose phosphorylated during the interval of time equals the steady state flux of glucose through the hexokinase-catalyzed step times the duration of the interval, and the net rate of flux of glucose through this step equals the rate of glucose utilization.

PLASMA	BRAIN TISSUE	
	Precursor Pool	Metabolic Products

GLYCOLIPIDS

$[^{14}C]$DEOXYGLYCOGEN ⬆ GLYCOPROTEINS

$[^{14}C]$UDPDG

$[^{14}C]$DEOXYGLUCOSE-1-PHOSPHATE

$[^{14}C]$Deoxyglucose C_P^* k_1^* / k_2^* $[^{14}C]$Deoxyglucose C_E^* k_3^* $[^{14}C]$Deoxyglucose-6-Phosphate C_M^*

TOTAL TISSUE ^{14}C CONCENTRATION $= Ci^* = C_E^* + C_M^*$

Glucose C_P k_1 / k_2 Glucose C_E k_3 Glucose-6-Phosphate C_M

$CO_2 + H_2O$

BLOOD-BRAIN BARRIER
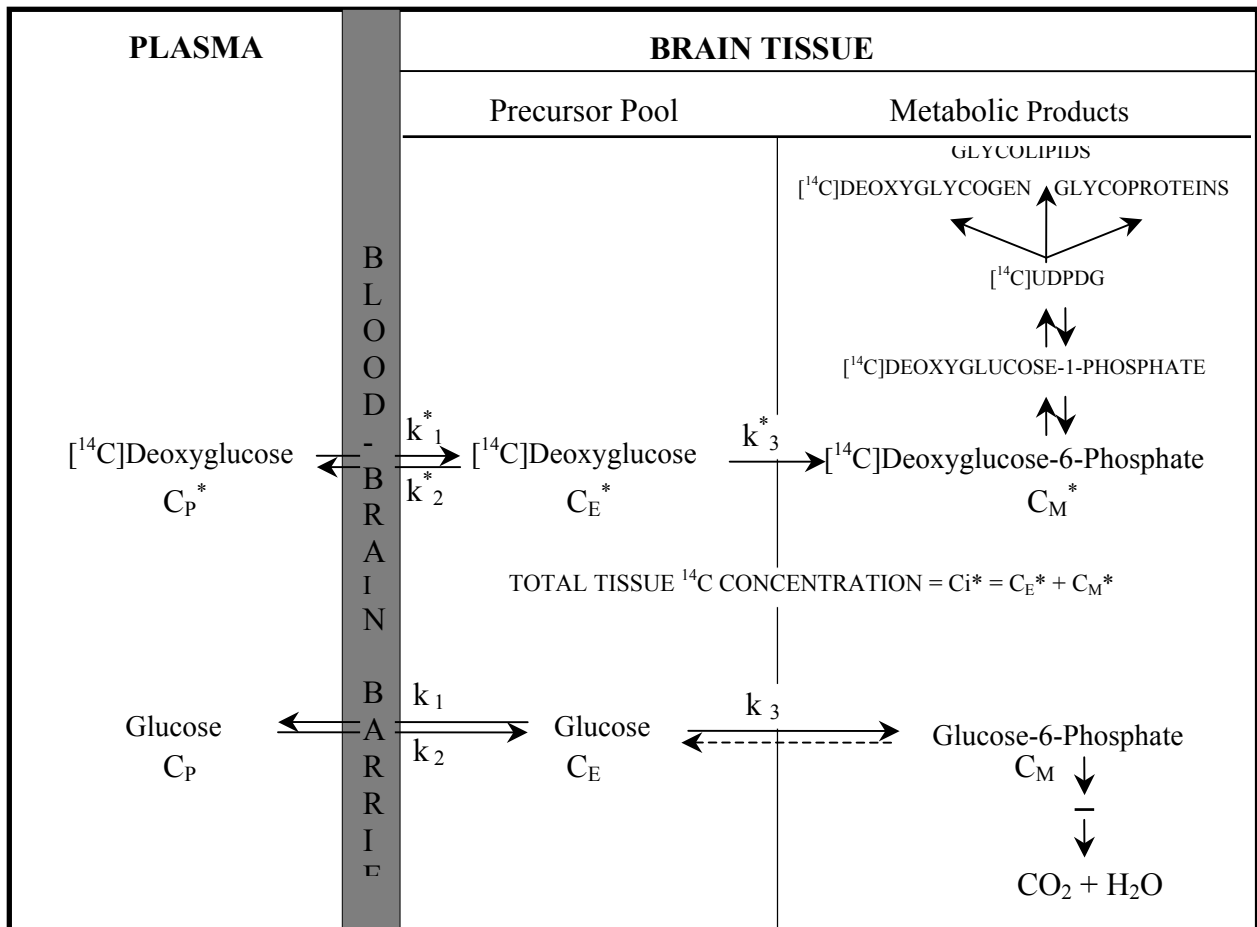
Figure 3. Theoretical basis of the radioactive deoxyglucose method for measurement of local cerebral glucose utilization (Sokoloff et al., 1977). Diagrammatic representation of the theoretical model. C_i^* represents the total tissue ^{14}C concentration in a single homogeneous area of the brain. C_P^* and C_P represent the concentrations of $[^{14}C]$deoxyglucose and glucose in the arterial plasma, respectively; C_E^* and C_E represent their respective concentrations in the tissue pools that serve as substrates for hexokinase. C_M^* represents the concentration of $[^{14}C]$deoxyglucose-6-phosphate in the tissue. The constants k_1^*, k_2^*, and k_3^* represent the rate constants for carrier mediated transport of $[^{14}C]$deoxyglucose from plasma to tissue, for carrier -mediated transport back from tissue to plasma, and for phosphorylation by hexokinase, respectively; the constants k_1, k_2, and k_3 are the equivalent rate constants for glucose. $[^{14}C]$deoxyglucose and glucose share and compete for the same carrier that transports both of them between plasma and tissue as well as for the hexokinase, which phosphorylates them to their respective hexose-6-phosphates. The dashed arrow represents the possibility of glucose-6-phosphate hydrolysis by glucose-6-phosphatase activity, if any.

These relationships can be mathematically defined and an operational equation can be derived if the following assumptions are made:

(a) a steady state for glucose (i.e. constant plasma glucose concentration and constant rate of glucose consumption) throughout the period of the procedure,

(b) homogeneous tissue compartment within which the concentrations of $[^{14}C]DG$ and glucose are uniform and exchange directly with the plasma and

(c) tracer concentrations of $[^{14}C]DG$ and $[^{14}C]DG$-6-P (negligibly small compared to those of glucose and glucose-6-P, respectively)

The operational equation which defines R_i, the rate of glucose utilization (R) per unit mass of tissue (i), in terms of measurable variables, is presented in Figure 4. This equation is essentially a general statement of the standard relationship by which rates of enzyme-catalyzed reactions are determined from measurements made with radioactive tracers. The numerator represents the amount of radioactive product formed in a given interval of time. This equals to C_i^*, the combined concentrations of $[^{14}C]DG$ and $[^{14}C]DG$-6-P in the tissue at time T (measured by the quantitative autoradiographic technique), minus a term that represents the free unmetabolized $[^{14}C]DG$ remaining in the tissue at time T. This way, the rate of chemical transformation of the labeled 2-DG can easily be measured. However this rate does not equal the rate of glucose phosphorylation. To derive the rate of the total reaction of a chemical substance from measurement of the reaction rate of its labeled species only, it is necessary to know the integrated specific activity (i.e. the ratio of labeled to total molecules) in the precursor pool. For this reason, the precursor pool specific activity is measured indirectly from measurements in the blood supplied to the tissue. The specific activity in the arterial blood or plasma can be directly measured and the precursor specific activity can be calculated by correcting for the lag in the equilibration of the precursor pool in the tissue with that of the plasma. Additionally, the labeled species often exhibits a kinetic difference from the natural compound, the so-called isotope effect. This isotope effect can be evaluated and corrected for. The denominator in the equation of Figure 4 represents the integrated specific activity of the precursor pool times a factor, the lumped constant, which is analogous to a correction factor for the isotope effect. The term with the exponential factor in the denominator takes into account the lag in the equilibration of the tissue precursor pool with that in the plasma.

In summary, with the use of the $[^{14}C]DG$ as a probe, a single biochemical reaction which is the first step in the pathway of glucose metabolism, has been isolated. This step is the hexokinase-catalyzed phosphorylation of glucose. The total amount of radioactive product formed and the integrated specific activity of the precursor at the enzyme site can be determined. From these data and the use of a correction factor (the lumped constant) for the difference in the kinetic behavior of deoxyglucose and glucose, the net rate of glucose phosphorylation can be calculated by the operational equation. In a steady state the net rate through any step in a pathway equals the net rate through the overall pathway. The deoxyglucose method therefore measures the net rate of glucose phosphorylation in vivo and the net rate of the entire glycolytic pathway in a steady state.

Functional Anatomy of the Operational Equation of the [^{14}C]Deoxyglucose Method

General Equation for Measurement of Reaction Rates with Tracers

$$\text{Rate of Reaction} = \frac{\text{Labeled Product formed in interval of time from 0 to T}}{\left[\begin{array}{c}\text{Isotope effect} \\ \text{correction factor}\end{array}\right]\left[\begin{array}{c}\text{Integrated specific} \\ \text{activity of precursor}\end{array}\right]}$$

Operational Equation of the [^{14}C]Deoxyglucose Method

Labeled product formed in interval of time 0 to T

$$R_i = \frac{\overbrace{C_i^*(T)}^{\substack{\text{Total }^{14}\text{C in} \\ \text{Tissue at time T}}} - \overbrace{k_1^*\, e^{-(k_2^*+k_3^*)T}\int_0^T C_p^*\, e^{(k_2^*+k_3^*)t}\, dt}^{\substack{^{14}\text{C in Precursor remaining in} \\ \text{Tissue at time T}}}}{\underbrace{\left[\frac{\lambda\, V_m^*\, K_m}{\Phi\, V_m^*\, K_m^*}\right]}_{\substack{\text{"Isotope Effect"} \\ \text{Correction} \\ \text{Factor}}}\left[\underbrace{\int_0^T\left(\frac{C_p^*}{C_p}\, dt\right)}_{\substack{\text{Integrated Plasma} \\ \text{Specific Activity}}} - \underbrace{e^{-(k_2^*+k_3^*)T}\int_0^T\left(\frac{C_p^*}{C_p}\right) e^{(k_2^*+k_3^*)t}\, dt}_{\substack{\text{Correction for Lag in Tissue} \\ \text{Equilibration with Plasma}}}\right]}$$

Integrated Precursor Specific Activity in Tissue

Figure 4. Operational equation of radioactive deoxyglucose method and its functional anatomy. T, represents the time at the termination of the experimental period; ë, equals the ratio of the distribution space of deoxyglucose in the tissue to that of glucose; Ö, equals the fraction of glucose which, once phosphorylated, continues down the glycolytic pathway; V_m^* and K_m^*, represent the maximal velocity and Michaelis-Menten constant of hexokinase for deoxyglucose, and V_m and K_m, represent the equivalent values for glucose. Other symbols as in Fig. 2.

2.2.2 Procedure for Measurement of Local Cerebral Glucose Utilization

The operational equation of the method specifies the variables to be measured in order to determine R_i, the local rate of glucose consumption in the brain. The following variables are measured in each experiment:

(a) the entire history of the arterial plasma [^{14}C]DG concentration, C_p^*, from zero time to the time of sacrifice T

(b) the steady state arterial plasma glucose level C_p, over the same interval and

(c) the local concentration of ^{14}C in the tissue at the time of killing $C_i^*(T)$.

The rate constants k_1^*, k_2^* and k_3^* and the lumped constant $\lambda \, V_m^* \, K_m / \Phi \, V_m \, K_m^*$ are not measured in each experiment; the values for these constants are species specific and have been determined separately in other groups of animals (rat (Sokoloff et al., 1977), monkey (Kennedy et al., 1978)).

The quantitative autoradiographic technique measures only total ^{14}C concentration in the tissue and does not distinguish between [^{14}C]DG-6-P and [^{14}C]DG. It is however, [^{14}C]DG-6-P concentration that must be known to determine glucose consumption. [^{14}C]DG-6-P concentration is calculated in the numerator of the operational equation, which equals the total tissue ^{14}C content $C_i^*(T)$ minus the [^{14}C]DG concentration remaining in the tissue (estimated by the term containing the exponential factor and the rate constants). In the denominator of the operational equation, there is also a term containing an exponential factor and rate constants. Both these exponential terms approach zero with increasing time, when C_p^* is also allowed to approach zero. The rate constants k_1^*, k_2^* and k_3^* are not measured in the same animals in which local glucose consumption is being measured and the standard normal rate constants used may not be equally applicable in all physiological and pathological states. One possible solution to this problem is to redetermine the rate constants for each condition to be studied. An alternative approach, which is the chosen one, is to administer the [^{14}C]DG as a single intravenous pulse at zero time and to allow sufficient time for the clearance of [^{14}C]DG from the plasma. This way, the terms containing the rate constants fall to levels too low to influence the final result. To wait until these terms reach zero is impractical because of the long time required and the risk of effects of the small but finite rate of loss of [^{14}C]DG-6-P from the tissues. A reasonable time interval is 45 min; by this time the plasma level has fallen to very low levels and the exponential factors have declined through at least 10 half-lives, at least under physiological conditions. An additional advantage derived from the use of a single pulse of [^{14}C]DG followed by a relatively long interval before sacrificing the animal is that by that time, most of the free [^{14}C]DG in the brain tissue has been either converted to [^{14}C]DG-6-P or transported back to the plasma (Fig. 2). Thus, the ^{14}C concentration in the tissue, which is measured in the autoradiographs, represents mainly the concentration of [^{14}C]DG-6-P and reflects directly the relative rates of glucose utilization.

In each experiment the following steps were taken:

(1) Preparation of the animal

(2) Administration of [^{14}C]deoxyglucose, and timed sampling of arterial blood during the succeeding 45 min

(3) Analysis of arterial plasma for [^{14}C]deoxyglucose and glucose concentrations

(4) Processing of brain tissue and preparation of autoradiographs

(5) Densitometric analysis of autoradiographs

Preparation of the animal

Each animal was subjected to femoral vein and artery catheterization under general anesthesia (ketamine hydrochloride, 20mg/kg, im.). The catheters were plugged at one end and filled with dilute heparin solution (100 U/ml) before their insertion. The animal was left to recover from anesthesia, restrained in a primate chair, for 4-5 hours.

Administration of [^{14}C] deoxyglucose and timed sampling of arterial blood

A dose of 100 μCi/kg of animal weight of [^{14}C]DG (specific activity 55mCi/ml, ARC) was used. Because [^{14}C]DG was supplied in an ethanol solution, it was evaporated to dryness and redissolved in 1ml of saline. The experimental period was initiated by the infusion of [^{14}C]DG as pulse, through the venous catheter, over a period of 30 s. With zero time marking the start of the infusion, blood sampling was begun from the arterial catheter to monitor the entire time course of the [^{14}C]DG concentration in the plasma. The samples were collected in heparinized tubes at predetermined times: 0 s, 15 s, 30 s, 45 s, 1min, 2 min, 3 min, 5min, 7.5 min, 10 min, 15min, 25 min, 35 min and 45 min. Care was taken to clear the dead space of the catheter prior to collection of each sample. The samples were immediately centrifuged in a small, high speed Beckman centrifuge and kept on ice until used for the analyses. Immediately after the last sample had been taken (at 45 min), the monkey was killed by an intravenous injection of 50 mg of sodium thiopental in 5 ml saline, followed by injection of a saturated KCl solution to stop the heart.

Analysis of arterial plasma for [^{14}C] deoxyglucose and glucose concentrations

To measure the concentration of deoxyglucose by means of counting its ^{14}C content in the plasma, 20 μl of each sample and 3 ml of scintillation liquid (Insta-Gel, Packard) were placed in each counting vial. The ^{14}C content of each sample was measured in a β-counter and the resulting cpm were transformed into dpm with the aid of an internal standard (calibrated [^{14}C]toluene). The plasma glucose concentration was assayed in a Spotchem dry glucose analyzer and was determined by reflectance spectrophotometry based on the glucose oxidase method (Kadish et al., 1968).

Processing of brain tissue and preparation of autoradiographs

Immediately after killing the animal, the brain was removed from the cranial cavity (each hemisphere separately) and frozen by immersion in isopentane maintained between -45° and -50°C with dry ice. Each hemisphere was kept for at least 15 min in the isopentane to ensure full and even freezing of the brain. When completely frozen, the tissue was covered with embedding medium (Lipshaw Manufacturing Co., M1) to protect from dehydration, and was stored at -80 °C until sectioned. Before sectioning, each hemisphere was fixed on an appropriate object holder for the microtome used. About 2500 serial horizontal brain sections of 20 μm thickness were obtained from each hemisphere in a cryostat (Cryopolycut, Reichert Jung) at -20 °C. The sections were picked from the knife surface on glass coverslips, to which they adhered by thawing, and were immediately transferred to a hotplate maintained at 60 °C on which the momentarily thawed sections became dry within 5-8 s. Intermediate sections (1 every 25) were taken on slides and were kept for Nissl staining. The ^{14}C-DG method requires cryostat temperature of -20 °C and immediate transfer of the coverslips to the hot plate in order to prevent movement of the label by diffusion. After sections were left for at least 30 min on the hotplate, the coverslips were glued on a paper board and were exposed in sets of 4-6 paper boards, with Kodak single coated X-ray medical films (EMC1), together with one strip of precalibrated ^{14}C standards of increasing ^{14}C concentration (Amersham). Exposure time ranged from 14-20 days depending mainly on exposure conditions and plasma glucose levels. The exposed films were developed in a Kodak X-OMAT 1000 processor automatic developer.

Densitometric analysis of autoradiographs

The autoradiographs provide a pictorial representation of the relative ^{14}C concentrations in the various cerebral structures; the darker the region, the higher the rate of glucose utilization. A calibration curve of the relationship between optical density and tissue ^{14}C concentration for each film

was obtained by measurements of the optical density corresponding to all different standards. The local tissue concentrations were then determined from the calibration curve and the optical densities of the cerebral regions of interest. Local cerebral glucose utilization was calculated from the local tissue concentrations of ^{14}C ($C_i^*(T)$ which is densitometrically determined from the autoradiographs) and the plasma [^{14}C]DG (C_p^*) and glucose concentration (C_p), according to the operational equation (Fig. 2) and the appropriate kinetic constants for the monkey (Kennedy et al., 1978). The densitometric analysis of the autoradiographs was carried out with a computerized image-processing system (Imaging Research Inc., Ontario, Canada), which allowed integration of the local cerebral glucose utilization (LCGU) values over the entire extent of each area of interest.

2.2.3 Theoretical and Practical Considerations

Although the deoxyglucose method has established its validity and worth through the years there are some potential problems in special situations that require further theoretical and practical considerations. The main potential sources of error are the rate constants and the lumped constant. The problem with them is that they are not measured in the same animals and at the same time when local cerebral glucose utilization is being measured. They are measured in separate groups of comparable animals and then used subsequently in other animals where glucose utilization is being measured.

Rate Constants

The rate constants k_1^*, k_2^* and k_3^* vary from structure to structure but the variation among gray structures and among white structures is considerably less than the differences between gray and white matter structures. The rate constants vary not only from structure to structure but also among different conditions. For example, k_1^* and k_2^* are influenced by both blood flow and transport of [^{14}C]DG across the blood-brain barrier, and because of the competition for the transport carrier, the glucose concentrations in the plasma and tissue affect the transport of [^{14}C]DG and will certainly change when glucose utilization is altered. If the [^{14}C]DG is given as an intravenous pulse and sufficient time is allowed for the plasma to be cleared of the tracer, then the influence of the rate constants, and the functions that they represent, on the final result diminishes with increasing time and ultimately becomes zero. As (C_p^*) in the operational equation of Figure 4 approaches zero, the terms containing the rate constants also approach zero with increasing time. Consequently, at short times after [^{14}C]DG injection enormous errors can occur if the values of the rate constants are not precisely known. On the contrary, negligible errors occur at 45 min, even over a wide range of rate constants of several-fold. In fact, this is precisely the reason why [^{14}C]deoxyglucose rather than [^{14}C]glucose is selected as the tracer of glucose metabolism. Because the products of [^{14}C]glucose metabolism are so rapidly lost from the tissues, it is necessary to limit the experimental period to short times, when enormous errors can occur if the rate constants are not precisely known. [^{14}C]deoxyglucose permits the prolongation of the experimental period to times when inaccuracies in rate constants have little effect on the final result. In pathological conditions, however, such as severe ischemia or hyperglycemia the rate constants may differ significantly and should be redetermined.

Lumped constant

The lumped constant is composed of six separate constants. Φ is the fraction of glucose which once phosphorylated continues down the glycolytic pathway and is, therefore, a measure of the steady-state hydrolysis of G-6-P to free glucose and phosphate. Because in normal brain tissue there is little such phosphohydrolase activity (Hers, 1957), Φ is normally approximately equal to unity. The other constants are arranged as three ratios: λ is the ratio of distribution spaces in the tissue for deoxyglucose and glucose; K_m / K_m^* and V_m^* / V_m; the ratios tend to remain the same under normal conditions

although each individual constant may vary from structure to structure and condition to condition. From measurements in a sufficiently large series of animals (Sokoloff et al., 1977), it has been confirmed that the lumped constant is a constant characteristic of the species of animal and does not differ significantly in different conditions in normal tissue (0.344 ± 0.036 for the monkey (Kennedy et al., 1978)). In pathological states, however, the lumped constant does change. In severe hypoglycemia there is a progressive increase in the lumped constant with falling plasma glucose concentration (Suda et al., 1981) and in severe hyperglycemia there is a small decrease (Schuier et al., 1981). Tissue damage could also alter the lumped constant value since λ (the ratio of distribution spaces for deoxyglucose and glucose) could differ in damaged and normal tissue. Finally in pathological states there may be release of lysosomal acid hydrolases, which may hydrolyze glucose-6-phosphate and thus alter the value of Φ.

Role of glucose-6-phosphatase

Glucose-6-phosphatase activity is known to be very low in the brain (Hers, 1957). Nevertheless, there is some activity present (although low) which appears to have no influence on the deoxyglucose method if the experimental period is limited to 45 min. If there was significant glucose-6-phosphatase activity the [^{14}C]DG-6-P would be hydrolyzed and there would be loss of product. The calculated glucose utilization rates over 20-, 30-, and 45-min periods remained constant (Sokoloff, 1982). Beyond this time the phosphatase effects began to appear, increasing in magnitude with increasing time. The time course of the effect was found to be compatible with the intracellular distribution of the [^{14}C]DG-6-P and phosphatase. The [^{14}C]DG-6-P is formed in the cytosol, but the phosphatase is on the inner surface of the cisterns of the endoplasmic reticulum. The [^{14}C]DG-6-P has to be transported from the cytosol across the endoplasmic reticular membrane by a specific carrier, before the phosphatase can act. This period is long enough because the carrier for G-6-P and DG-6-P is essentially absent in the brain (Fishman and Karnovsky, 1986). The substrate then has access to the enzyme only by slow diffusion through the membrane. If one extends the experimental period beyond 45 min then correction must be made for the effects of phosphatase by including a k_4^* rate constant for the phosphatase activity (Sokoloff, 1982).

Site and mechanisms of function-related changes in energy metabolism in the nervous system

There is good evidence that alterations in functional activity are reflected in the rates of glucose utilization. Decreased functional activity due to bilateral visual occlusion lowers the local rates of glucose consumption in all components of the primary visual pathway. Occlusion of one eye results in reduced input and therefore lower functional activity and rates of glucose utilization in the visual cortex ocular dominance columns served by that eye (Kennedy et al., 1976). The converse is also true; increases in local functional activity raise the local rates of glucose utilization in the brain. For example, tweaking the whiskers of rodents raises the rates of glucose utilization in the "whisker-barrel" regions of the contralateral somatosensory cortex (Hand, 1981). Moving an arm and hand increases glucose utilization in the contralateral motor cortex and in all components of the motor and sensory pathways that are involved in the task (Savaki et al., 1993). Regions rich in neuropil and not in cell bodies have been shown to exhibit greater changes in glucose utilization following alterations in local functional activity (Kennedy et al., 1976; Nordmann, 1977; Schwartz et al., 1979). To compare the effects of functional activation on local glucose utilization simultaneously in the perikarya and nerve terminals of the same pathway, the sciatic nerve of the anesthetized rat was electrically stimulated at different frequencies and the glucose utilization was measured by the [^{14}C]DG method in the body of the dorsal root ganglion (where perikarya devoid of neural processes are contained) and the dorsal horn of corresponding segments of the lumbar spinal cord (where the nerve terminal of the same pathway are contained) (Kadekaro et al., 1985). The results showed that glucose utilization in the

dorsal horn of the lumbar cord exhibited a linear increase in the rate of glucose utilization with increasing frequency of stimulation while the region of the cell bodies of the same pathway in the dorsal root ganglia showed no metabolic changes in response to the electrical stimulation, confirming that it is the glucose utilization in the region of the nerve terminals and not the cell bodies which is linked to the functional activity. Increased glucose utilization may be seen in structures in which inhibition of neuronal activity takes place because it is the electrical activity in the afferent nerve terminals that is associated with the energy consumption and this activity may be the same whether the terminals are releasing excitatory or inhibitory neurotransmitters. To determine whether the postsynaptic neurons are excited or inhibited, it is necessary to look downstream at the next relay station where these neurons project.

Which are the mechanisms that link energy metabolism to functional activity? It has been shown that activation of Na^+, K^+-ATPase activity by membrane depolarization provides a mechanism for coupling of energy metabolism to functional activity. When the rat posterior pituitary glands were electrically stimulated in vitro to secrete vasopressin, $[^{14}C]$deoxyglucose uptake was increased, indicating increased glucose utilization, which was completely blocked by addition of ouabain, a specific inhibitor of Na^+, K^+-ATPase (Mata et al., 1980). It is common knowledge that when extracellular K^+, and/or intracellular Na^+ concentrations are increased the activity of Na^+, K^+-ATPase is stimulated. ATPase is an enzyme that uses the energy of ATP to transport Na^+ out of the cell and K^+ into the cell to restore the ionic gradient to normal. ATPase activity lowers the ATP concentration and ATP/ADP ratio, and increases the ADP, phosphate acceptor and inorganic phosphate concentrations within the cell; these are all intracellular changes that can stimulate both glycolysis and electron transport in the respiratory chain. It appears then that the energy metabolism associated with the electrical and functional activities of the nervous tissue is not used directly in the generation and propagation of action potentials. The energy is used to restore the ionic gradients and resting membrane potentials that were partly degraded during the excitation phase. The reason why neuropil exhibits higher energy demands and therefore higher glucose utilization is probably due to the higher surface-to-volume ratio in nerve endings and dendrites compared to cell bodies. The higher the surface-to-volume ratio the greater the flux of ions per volume unit and per action potential, and thus the greater the activation of ATPase and the glucose utilization per volume unit.

2.3 TWO DIMENSIONAL RECONSTRUCTION OF THE METABOLIC ACTIVITY DISTRIBUTION WITHIN THE CORTEX.

The [^{14}C]DG method does not simply allow the estimation of the degree of activation of each separate region, but it also reveals the topographic organization of the affected neuronal populations. The main advantage of the application of the [^{14}C]DG method is that quantitative mapping of the distribution of metabolic activity in the entire brain is achieved in high resolution (100 μm). Two dimensional (2D) reconstruction of the spatio-intensive pattern of metabolic activity (local cerebral glucose utilization values, LCGU) within the rostrocaudal and the dorsoventral extent of the unfolded cortical area of interest (the intraparietal sulcus as well as the motor and premotor cortex) was generated in each hemisphere, based on a method developed in our laboratory as previously described (Dalezios et al., 1996; Savaki et al., 1997). According to this procedure, the distribution of activity in the rostrocaudal extent in each section was determined by measuring LCGU values pixel by pixel (resolution 45 μm/pixel for the intraparietal sulcus, 60 μm/pixel for the motor and premotor cortex and 65 μm/pixel for the mesial cortex) along a line parallel to the surface of the cortex, covering all cortical layers. Each data array (a series of LCGU values in each horizontal section), resulting from image segmentation in the rostrocaudal direction, was aligned with the arrays obtained from adjacent horizontal sections in the dorsoventral dimension of the brain. A specific anatomical point was used for the alignment of adjacent data arrays (the intersection of the intraparietal sulcus, IPs, with the parietoccipital sulcus, POs, in the intraparietal map; the anterior crown of the central sulcus, Cs, for the motor and premotor cortex map; the posterior tip of the cingulate sulcus, Cgs, for the mesial cortex map). The plotting resolution of both the rostrocaudal and the dorsoventral dimensions was 100 μm. Accordingly, each line parallel to the anteroposterior axis in the two dimensional reconstructed maps represents the distribution of activity averaged over five serial sections (of 20 μm thickness) along the rostrocaudal dimension. Occasional missing data arrays in the dorsoventral dimension were filled using linear interpolation between neighboring values.

Normalization of LCGU values was based on the average unaffected gray matter value (unaffected regions in the medial and lateral bank of the intraparietal cortex as well as in the ventral part of the precentral gyrus) pooled across all monkeys. Side to side percent differences within each monkey (%Dif in Table 2) were calculated as %Dif = [(Contra - Ipsi) / Ipsi] x 100, where Contra represents the LCGU average value in each cortical area of interest of the hemisphere contralateral to the moving forelimb, and Ipsi represents the respective ipsilateral LCGU value. Contra to Ipsi and experimental to control LCGU values were compared for statistical significances by the Student's unpaired t-test. Given that LCGU values for homologous areas in the two hemispheres of a normal resting monkey differ by up to 7% (Savaki et al., 1993) in the present study we adopted a conservative criterion accepting as significant only those hemispheric differences which exceeded 10% and also reached the 0.01 level of confidence by the Student's unpaired t-test. The Kolmogorov-Smirnov test was also used to check for statistically significant differences in the distribution of glucose utilization values.

Occasionally, to directly compare the activation foci between different hemispheres and different animals, and because the geometry of cortical areas obtained from different hemispheres is not identical, we transformed part of our maps which contained the region of interest. The transformation resulted in equivalent maps of the same dimensions for each region in all hemispheres. The dorsoventral extent of this region (DV_{max}) in each hemisphere was used as reference to express the dorsoventral value of each section (DV_s). Thus, DV_s was expressed as a ratio of DV_{max} (DV_s / DV_{max}). The anteroposterior value AP_x of each pixel was similarly expressed as a ratio of the anteroposterior length AP_s, of the area measured in that section (AP_x / Ap_s). The result of the transformation was a rectangular map for each hemisphere.

3. RESULTS

3.1 METABOLIC ACTIVITY PATTERNS WITHIN THE INTRAPARIETAL SULCUS

We used the $[^{14}C]DG$ quantitative method to map the distribution of metabolic activity in the IPs of one control and four experimental monkeys performing one of four tasks: (i) fixation of a central visual target (Fig. 2A), (ii) horizontal saccades of different amplitudes to visual targets (Fig. 2B), (iii) reaching in the light during fixation of the central visual target (Fig. 2D), and (iv) reaching in the dark while the eyes maintained a straight ahead direction (Fig. 2E). Two-dimensional reconstruction of the spatio-intensive pattern of metabolic activity (LCGU) within the rostrocaudal and the dorsoventral extent of the unfolded IPs was generated in each hemisphere, as described in the methods section. LCGU values were measured pixel by pixel (resolution 45 μm/pixel) along a line parallel to the surface of the cortex, as shown in Figure 5A. Each data array was aligned with the arrays obtained from adjacent horizontal sections (the total of 550 sections of 20 μm thickness which contained the whole extent of IPs) in the dorsoventral dimension of the brain. The caudalmost part of the IPs (the intersection of IPs with the parietoccipital sulcus, POs) was used for the alignment of adjacent data arrays (point b in Figure 5A, and line b in Figure 5B). The plotting resolution of both the caudorostral and the dorsoventral dimensions was 100 μm. Accordingly, each vertical line at a given dorsoventral level on the left half of the metabolic maps (Figs 6 and 7) represents the distribution of the average activity in the medial bank along the rostrocaudal dimension in five serial sections. The vertical line at the same dorsoventral level on the right half of the metabolic maps represents the rostrocaudal distribution of the average activity in the lateral bank within the same five sections.

The medial and the lateral banks of IPs were subdivided into different subregions on the basis of the activations induced by the performance of the different tasks (Fig. 5B). This parcellation has been used in previous studies (Savaki et al., 1997; Savaki and Dalezios, 1999) and was presented in detail in a recent study (Gregoriou and Savaki, 2001). The nomenclature used to describe this parcellation differs from what other authors have reported in recent literature. However, the use of this nomenclature is necessary in order to present quantitative results in activated regions, which extend beyond the already reported ones. Area 5DIP covers the dorsalmost three fifths of the medial bank. Its rostral subregion (5DIP-rostral) is defined as the rostralmost three fourths of the entire rostrocaudal extent of the medial bank, reaching the fundus in the rostral tip of the bank. The remaining caudalmost one fourth (5DIP-caudal) extends caudally up to the intersection of the POs with the IPs. The delineation of areas 5DIP-rostral and 5DIP-caudal is based on the fact that the former area displayed major activations in contrast to the latter one in the reaching monkeys (Fig. 8). Area 5VIP covers the ventralmost two fifths of the medial bank (4 mm adjacent to the fundus) extending rostrally for 21 mm starting from the IPs-POs intersection. The parts corresponding to 5VIP-rostral and 5VIP-caudal cover the rostralmost two thirds and the caudalmost one third of area 5VIP, respectively. The same spatial relations are valid for the homologous subregions in the lateral bank of the IPs, i.e. for areas 7DIP-rostral, 7DIP-caudal, 7VIP-rostral, and 7VIP-caudal. The delineation of rostral and caudal regions within the lateral bank is based on the differential activations induced by eye movements in these regions (Fig. 6). In most of the illustrated hemispheres (Figs 6C, 7A,B,C,D) the fundus of the IPs is almost parallel to the horizontal plane of sectioning and thus overlaps with the line of zero dorsoventrality. However, in two of the IPs maps (Fig. 6A,B) the rostral part of both banks 5 and 7 deviates from the line of zero dorsoventrality, apparently due to a different geometry of these sulci.

Fixation and saccade related regions in the IPs of the monkey brain
The 2D reconstructed map of metabolic activity in the IPs of the right hemisphere in the monkey performing fixation of a central visual target displays a restricted region of enhanced

metabolic activity in the lateral bank (Fig. 6B), which is not present in the respective IPs map of the untrained control monkey (Fig. 6A). This activation is located almost in the middle of the dorsoventral extent of the lateral bank (3-4 mm from the fundus) and rather rostrally (10-12 mm from its anterior tip). It lies within both areas 7DIP-rostral and 7VIP-rostral. The same activation was observed in the IPs map of the left hemisphere of the fixating monkey and not in the respective map of the untrained control subject (maps similar to those of the right hemispheres in Figs. 6B and 6A, respectively, and thus not illustrated). The absence of such activation in the IPs of the untrained control monkey indicates that the activated region in Figure 6B may be related to either the fixation itself or to the performance of small amplitude saccades (0-2.5 deg) around the point of fixation. We will refer to this area as the parietal fixation region (PFR). Quantification of the average LCGU value within (i) the activated PFR in the fixating monkey (outlined by rectangle in Fig. 6B) and (ii) the corresponding region in the control monkey reveals a 47% increase in metabolic activity within the activated PFR.

The right hemisphere of the monkey performing contraversive horizontal saccades of 5, 10, 15 and 30 deg displays activations within an extended region in the lateral bank of IPs (Fig. 6C). We will refer to this region as the parietal saccade region (PSR). The activations within PSR appear as bands of increased metabolic activity, which cover part of areas 7DIP-rostral and 7VIP-rostral. The most active subregion within the PSR of the monkey performing saccades (outlined by rectangle in Fig. 6C) overlaps topographically with the PFR of the fixating monkey, and is most probably related to the multiple short fixations of all visual targets for saccades required by the task.
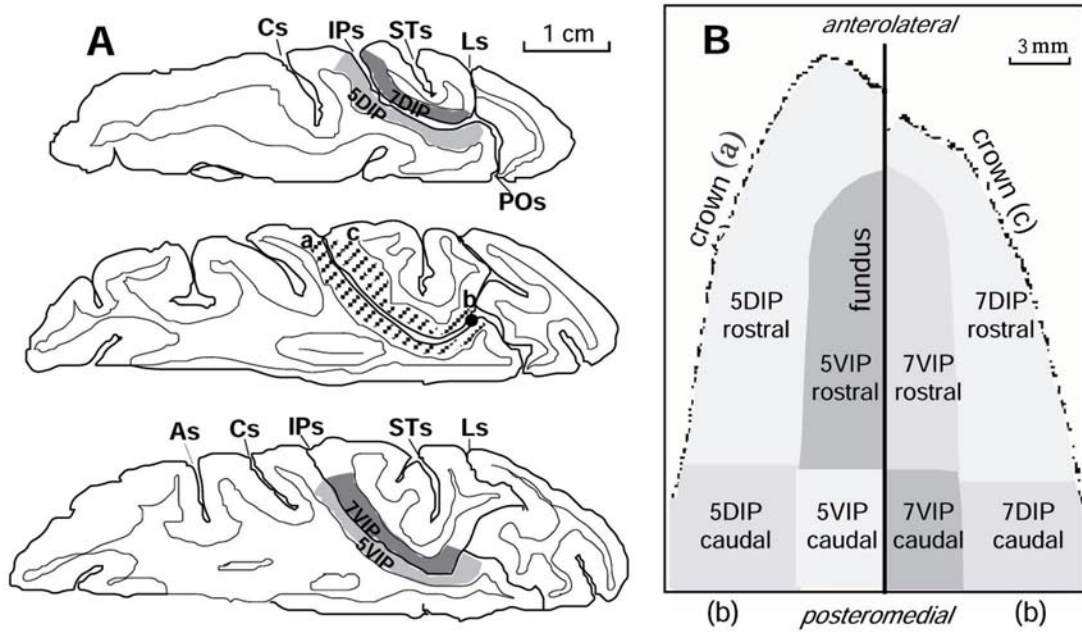
Figure 5. Reconstruction of the medial and lateral banks of IPs. (A) Schematic representations of three horizontal sections through the right hemisphere of a monkey brain at different dorsoventral levels (top corresponds to dorsal and bottom to ventral sections). In the first and third sections, the light and dark dotted areas outline the cortex of the medial (dorsal, 5DIP and ventral, 5VIP) and the lateral (7DIP and 7VIP) banks of IPs, respectively. In the middle section, the striped area indicates the caudorostral extent of the reconstructed cortex. The solid circle (b) within the striped area indicates the point of alignment of adjacent sections, which corresponds to the intersection of the IPs with the POs. Letters a-c indicate the same landmarks in both Figures 2A and 2B. As, arcuate sulcus; Cs, central sulcus; IPs, intraparietal sulcus; Ls, lunate sulcus; POs, parietoccipital sulcus; STs, superior temporal sulcus. (B) Schematic representation of 2D maps. Zero caudorostral level (line b) corresponds to the most posterior and medial part of IPs, used for alignment of adjacent sections. Solid line in the middle of the map indicates the fundus of the IPs. Dotted lines a and c indicate the crowns of the medial and lateral banks of IPs, respectively. Different shades represent caudal and rostral subregions. DIP, dorsal intraparietal cortex; VIP, ventral intraparietal cortex. (From Gregoriou and Savaki, 2001)
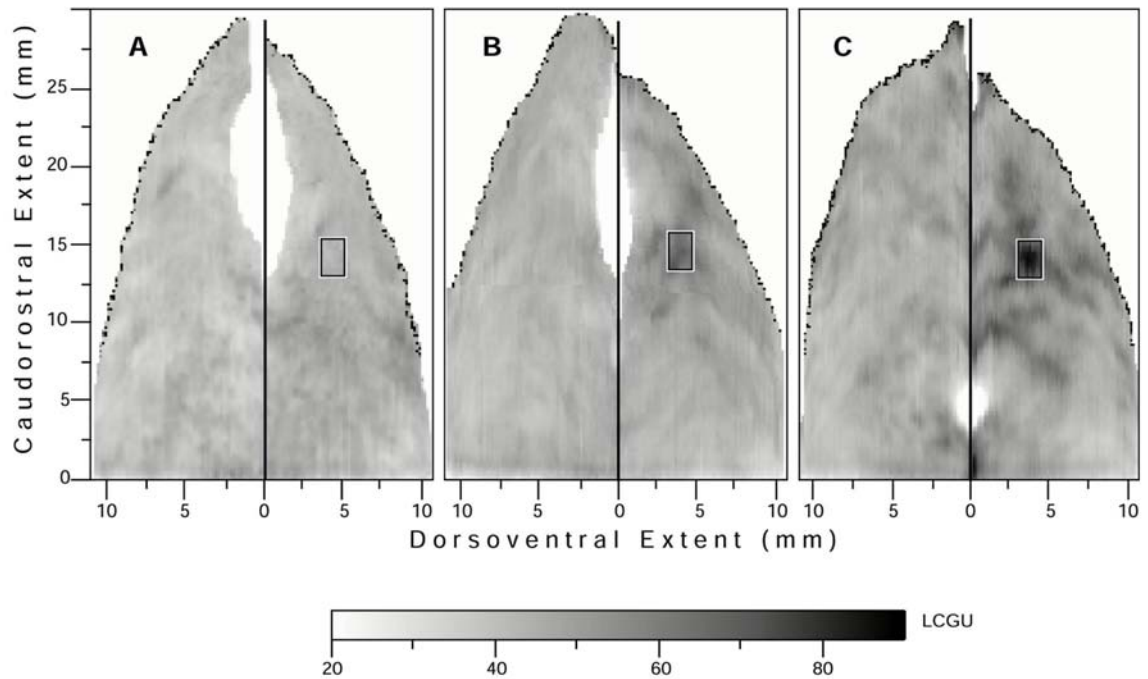
Figure 6. Activations in the IPs induced by fixation and saccades to visual targets. (A) The 2D spatial reconstruction of the LCGU values (μmol/100g/min) of metabolic activity in the IPs of the right hemisphere of the untrained control monkey. (B) The 2D map of metabolic activity in the IPs of the right hemisphere of a monkey fixating at a central visual target. (C) The 2D map of metabolic activity in the IPs of the right hemisphere of a monkey performing contraversive horizontal saccades of 5, 10, 15 and 30 deg to visual targets. Rectangles in the lateral bank of IPs outline the surface used for quantification of the LCGU values in PFR, which are reported in Table 1. (From Gregoriou and Savaki, 2001)

The activation in 7IP of the left hemisphere in the RL$_f$ monkey (Fig. 7A), which lies approximately 4 mm from the fundus and 12 mm from the anterior tip of the lateral bank, overlaps topographically with the PFR of the fixating monkey. PFR is activated in the RL$_f$ monkey because this animal performed reaching during central visual fixation. Thus, by using complementary tasks, the activated PFR is demonstrated not only in the two hemispheres of the fixating monkey but also in the two hemispheres of the saccading and the RL$_f$ monkeys. Rectangles of the same dimensions positioned at corresponding coordinates to those indicated in Figure 6 were used for quantification of the LCGU within the PFR of all the analyzed hemispheres. Of interest is the gradual decrease of the PFR activation in the hemispheres of (i) the saccading monkey, S$_h$(right), (ii) the left, F(left), and (iii) the right hemispheres, F(right), of the fixating monkey, (iv) the ipsilateral, RL$_f$(ipsi), and (v) the contralateral hemispheres, RL$_f$ (contra), of the RL$_f$ monkey, as well as (vi) the control (C) monkey (74, 64, 63, 59, 49 and 43 μmol/100g/min, respectively). Regression analysis was performed in order to reveal any possible correlation between the intensity of the PFR activation and several different behavioral parameters (Table 1). The intensity of PFR activation in the different hemispheres is not correlated with the duration of fixation during the critical five first minutes of the [^{14}C]DG experiment (regression coefficient, r=0.08, p>0.1). In contrast, the intensity of the PFR activation is well correlated with the number of small amplitude contraversive saccades performed around the point of fixation during the five first minutes of the experiment (r=0.92, p<0.05). When the total number of small amplitude (contraversive and ipsiversive) saccades is used for the comparison, the r drops to 0.76 (p>0.1). This decrease of the regression coefficient is due to the inclusion of small amplitude ipsiversive saccades, which are not correlated with the intensity of the PFR activation (r=0.04, p>0.1). Similarly, when the total number of contraversive (small and large amplitude) saccades is used for the comparison the r drops to 0.72 (p>0.1). Finally, we examined the relationship between the intensity of the PFR activation and the state of attention of the animal. Agreeably, the percentage of successful trials could reflect the state of attention of the monkey. Regression analysis demonstrates that the intensity of the PFR activation in the different hemispheres is not correlated with the percentage of successful trials during the five first minutes of the experiment (r=0.06, p>0.1). In conclusion, the results of the linear regression analysis indicate that 85% of the variance of the dependent variable (intensity of the PFR activation) can be accounted for by the number of small amplitude contraversive saccades performed around the point of fixation.

In summary, the metabolic effects induced by the performance of visual fixation and saccades to visual targets were confined in the intraparietal area 7 of the lateral bank in the IPs. The absence of any remarkable activation in the medial bank of the monkeys performing the fixation and saccade tasks indicates that intraparietal area 5 has no major involvement in the visual and saccadic aspects of these tasks.

Table 1
Fixation effect and related behavioral parameters

	S$_h$(right)	F(left)	F(right)	RL$_f$(ipsi)	RL$_f$(contra)
Intensity (μmoles/100g/min)	74	64	63	59	49
Fixation Duration (min)	2.8	3.6	3.6	2.9	2.9
Small amplitude contraversive saccades	168	82	138	63	18
Small amplitude (contra+ipsi) saccades	211	220	220	81	81
Small amplitude	43	138	82	18	63

ipsiversive saccades					
Contraversive saccades (small + large amplitude)	345	121	178	197	143
% Successful trials	80	45	45	70	70

F, fixation; **S_h**,saccades , **RL_f**, reaching in the light
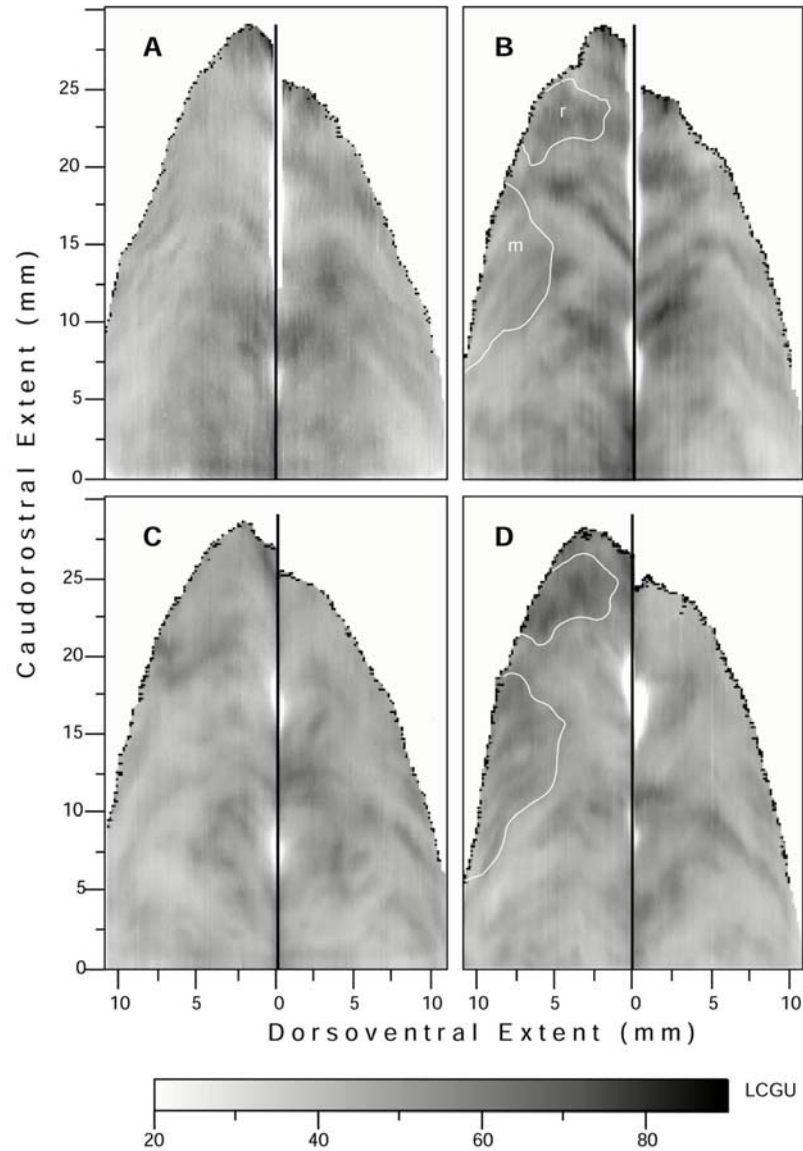
Figure 7. Activations in the IPs induced by reaching in the light and reaching in the dark during fixation. (A) Cortical 2D map of metabolic activity in the IPs of the left hemisphere, ipsilateral to the moving forelimb, in a monkey reaching from a central to a peripheral visual target in the light during fixation of the central target. (B) The 2D map of cortical activity in the IPs of the right hemisphere, contralateral to the moving forelimb, in the same monkey as in case A. r, rostralmost and m, medial activated regions, outlined in the medial bank of IPs. (C) The 2D map of cortical activity in the IPs of the left hemisphere, ipsilateral to the moving forelimb, in a monkey which remained in complete darkness and performed acoustically triggered reaching from a central to a peripheral position while the eyes maintained a straight ahead direction. (D) The 2D map of cortical activity in the IPs of the right hemisphere, contralateral to the moving forelimb, in the same monkey as in case C. (From Gregoriou and Savaki, 2001)

Reaching related regions in the IPs of the monkey brain

The medial bank of the IPs was activated more strongly in the monkeys performing the reaching tasks, and mainly in the hemisphere contralateral to the moving forelimb (Fig. 7B,D).

Figures 7A and 7B represent the distribution of metabolic activity in the hemispheres ipsilateral and contralateral to the moving forelimb, respectively, of the monkey reaching from a central to a peripheral target in the light during fixation of the central visual target (RL_f). Both areas 5DIP and 5VIP are strongly activated in the hemisphere contralateral to the moving forelimb (Fig. 7B). Two activated regions are focused within area 5DIP-rostral in the contralateral hemisphere of the RL_f monkey (r and m outlined in Fig. 7B). The first one (r), which is located in the rostralmost part of area 5DIP, is more pronounced and displays 32% higher activity in the contralateral as compared to the ipsilateral hemisphere (Table 2, 5DIP-rostralmost). The second one (m), which is located caudally within the limits of area 5DIP-rostral, is higher by 24% in the contralateral than in the ipsilateral hemisphere (Table 2, 5DIP-medial). Several activations within area 5VIP of the RL_f monkey were bilateral, with the most pronounced ones running almost parallel to each other and covering the entire rostrocaudal extent in the hemisphere contralateral to the reaching forelimb. Some activations within area 7VIP of the RL_f monkey were also bilateral, with the most intense and extended ones running parallel to each other in the contralateral 7VIP-rostral.

Figures 7C and 7D represent the distribution of metabolic activity in the hemispheres ipsilateral and contralateral to the moving forelimb, respectively, of the monkey performing acoustically triggered reaching movements from a central to a peripheral position, in complete darkness, while the eyes maintained a straight ahead direction (RD). Area 5DIP-rostral in the RD monkey displays two activated regions (the 5DIP-rostralmost and the 5DIP-medial) in the hemisphere contralateral to the moving forelimb (outlined in Fig. 7D), same way as in the RL_f monkey. Thus, by using complementary tasks, the activated regions 5DIP-rostralmost and 5DIP-medial are demonstrated not only in the RL_f but also in the RD monkey. These activations in the RD monkey display higher glucose consumption in the contralateral hemisphere as compared to the corresponding regions of the ipsilateral hemisphere by 39% and 30%, respectively. Comparison of these two effects in 5DIP-rostral in the RD and RL_f monkeys demonstrated that the activations were slightly higher in the RD monkey (Table 2). In contrast, area 5VIP of the RD monkey (Fig. 7D) did not display the pronounced activations observed in the RL_f monkey (Fig. 7B). A spatially restricted, moderately activated band is present in the lateral bank of the IPs in the RD monkey, bilaterally. Given that reaching was performed in complete darkness while the eyes remained stationary, this activated band cannot be attributed to visual stimulation or to voluntary saccades. This activation may be related to eye drifting during fixation in the dark. However, it cannot be excluded that this activation may be related to the auditory signals used as cues for reaching, because neuronal responses to auditory signals used as cues for saccades have been reported in the lateral bank of the IPs (Mazzoni et al., 1996).

The map generated after subtracting the cortical activity in the IPs ipsilateral to the moving forelimb (Fig. 7C) from that in the IPs contralateral to the moving forelimb (Fig. 7D) in the RD monkey is shown in Figure 8A. The fundus as well as the crowns of IPs were used for alignment of the maps used for subtraction. In the map of Figure 8A, the two activated regions 5DIP-rostralmost and 5DIP-medial are clearly delineated and demonstrate the unilaterality of the effect induced by RD. The outlines of these two activations in Figure 8A were used to delimit the corresponding regions (r and m) in Figure 7B,D. In the absence of visual input, these activations can only be attributed to somatosensory information used to guide the forelimb in the dark.

Both somatosensory and visual information is used to guide reaching in the light, whereas only somatosensory input is available to guide reaching in the dark. In order to reveal the regions associated with the visual guidance of reaching, we subtracted the map of the contralateral IPs in the RD monkey (Fig. 7D) from the equivalent map in the RL_f monkey (Fig. 7B). The so generated map illustrates activated zones mainly in the ventral intraparietal cortex around the fundus of IPs (Fig. 8B).

Quantitative comparison of the effects in the different subregions of the ventral intraparietal cortex demonstrated activations higher by 15% in area 5VIP-rostral, 27% in 5VIP-caudal, and 14% in 7VIP-rostral in the RL_f as compared to the RD monkey. All these differences were statistically significant.

Based on the results of the two subtraction maps we conclude that the dorsal part of intraparietal area 5 is involved in the somatosensory guidance of the reaching forelimb, whereas the ventral intraparietal cortex is implicated in the visual guidance of reaching.
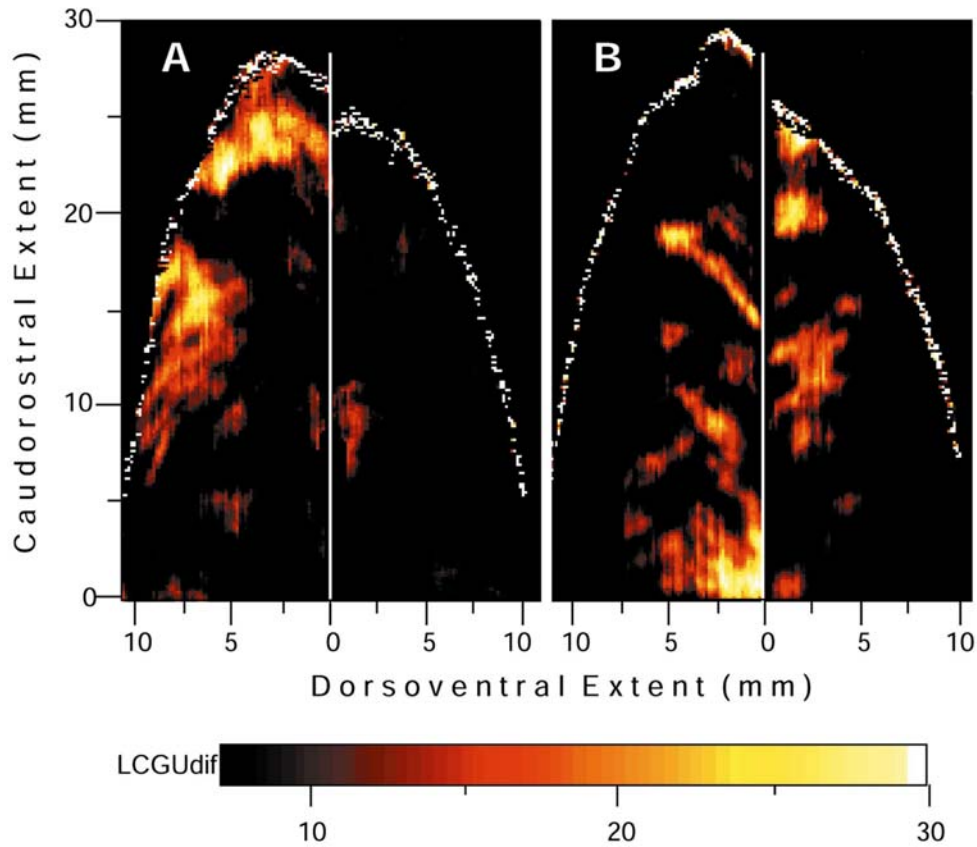
Figure 8. Subregions of IPs involved in the somatosensory and visual guidance of reaching. (A) Map generated after subtracting the cortical activity in the left IPs (ipsilateral to the moving forelimb, Fig. 7C) from that in the right IPs (contralateral to the moving forelimb, Fig. 7D) of the monkey reaching in the dark, to illustrate areas involved in somatosensory guidance of reaching. (B) Map generated after subtracting the cortical activity in the right IPs (contralateral to the moving forelimb, Fig. 7D) of the monkey reaching in the dark from that in the respective IPs of the monkey reaching in the light (Fig. 7B), to illustrate areas involved in visual guidance of reaching. Colour bar indicates the difference in local cerebral glucose utilization (LCGUdif). (From Gregoriou and Savaki, 2001)

Table 2

Metabolic effects in subregions of the intraparietal cortex

AREA (n)	C	F	S_h Contra	RL_f Ipsi	Contra	%Dif	RD Ipsi	Contra	%Dif
5DIP-rostral (105)	38±2	42±2	46±2	43±2	50±5	16*	45±4	55±5	22*
5DIP-rostralmost (45)				44±2	58±2	32*	46±1	64±3	39*
5DIP-medial (29)				42±1	52±3	24*	43±1	56±2	30*
5DIP-caudal (65)	39±2	40±1	42±3	42±6	46±4	10*	40±2	42±2	5
5VIP-rostral (43)	38±1	42±1	46±1	47±2	53±3	13*	46±3	46±2	0
5VIP-caudal (43)	41±1	44±1	48±3	52±2	57±6	10*	45±1	45±3	0
7DIP-rostral (103)	43±4	48±3	51±3	46±4	47±6	2	46±2	45±3	-2
PFR (18)	43±1	63±2	74±4	59±2	49±2				
7DIP-caudal (66)	41±2	41±2	43±3	39±5	38±3	-2	42±5	40±3	-5
7VIP-rostral (42)	42±1	47±1	57±4	50±3	56±5	12*	49±2	49±1	0
7VIP-caudal (42)	44±1	43±1	50±5	46±2	50±3	8	46±2	48±4	4

Values represent the normalized mean of glucose utilization (LCGU) expressed in μmol/100g/min ± standard deviation obtained from one control (**C**) and four experimental monkeys performing one of the following tasks: fixation (**F**), saccades (S_h), reaching in the light (RL_f), and reaching in the dark (**RD**).
n, number of sets of five adjacent horizontal sections used in obtaining mean LCGU values for each region in each hemisphere.
%Dif, contra-to-ipsi percent difference calculated as (Contra - Ipsi) / Ipsi x 100.
PFR, parietal fixation region.
*All side to side differences above 10% were statistically significant by the Student's unpaired *t*-test at the level of p<0.01 and comparison of the respective distributions of glucose utilization values by the Kolmogorov-Smirnov test also demonstrated statistically significant differences at the level of p<0.01.

### 3.2 METABOLIC ACTIVITY PATTERNS WITHIN THE AGRANULAR FRONTAL CORTEX

The distribution of metabolic activity in the agranular frontal cortex of a naive control and five experimental monkeys was also mapped by means of the [^{14}C]DG quantitative method. The five animals performed one of the following five tasks: (i) fixation of a central visual target (F), (ii) visually guided upward oblique saccades 20 deg in amplitude (S$_o$), (iii) reaching in the light from a central to a peripheral target (RL) (iv) reaching in the light during fixation of the central visual target (RL$_f$), and (v) reaching in the dark while the eyes maintained a straight ahead direction (RD). Two dimensional reconstruction of the spatio-intensive pattern of metabolic activity (LCGU) within the rostrocaudal and the dorsoventral extent of the cortex comprising the premotor and primary motor areas, lying on the lateral cortical convexity and buried within the arcuate (As) and central (Cs) sulcus, was generated in each hemisphere, as described in the methods section. LCGU values were measured pixel by pixel (resolution 60 µm/pixel) along a line parallel to the surface of the cortex, as shown in Figure 9B. Each data array, was aligned with the arrays obtained from adjacent horizontal sections (the total of about 1200 sections of 20 µm thickness which contained the whole dorsoventral extent of Cs and As). The anterior crown of the Cs and its ventral extension was used for the alignment of adjacent data arrays (point g in Fig. 9B, and line g in Fig. 9A). The plotting resolution of both the caudorostral and the dorsoventral dimensions was 100 µm. Accordingly, each horizontal line at a given dorsoventral level on the metabolic maps (Figs. 10-12) represents the distribution of the average activity along the anteroposterior dimension in five serial sections. Maps corresponding to left hemispheres are shown after reflection so that anterior is always shown to the left and posterior to the right.

The different cytoarchitectonic subdivisions of the agranular frontal cortex were identified on Nissl stained horizontal brain sections of the monkeys used. Area F1 is characterized by low cellular density, poor lamination, absence of granular layer IV and prominent giant pyramidal cells (Betz cells) in layer V. The posterior border of F1 with the primary somatosensory cortex (SI) is easily identified since SI displays a higher cellular density, a prominent granular layer IV and no giant pyramidal cells. This border lies close to the fundus of the Cs. The anterior border of F1 towards F2 and F4, on the lateral convexity, is more difficult to define since the cytoarchitectonic features do not change abruptly but rather gradually. An increase in cellular density in lower layer III together with the gradual decrease in density of giant pyramidal cells, defines the transition from the primary motor cortex to the premotor cortex. In the dorsal premotor cortex, area F2 is poorly laminated with scattered giant pyramidal cells present only in its caudal part, towards the border with F1. In lower layer III at the border with layer V, a narrow band of medium-sized pyramids can be found. Rostral to F2, area F7 is clearly laminated and has a prominent layer V. In the ventral premotor cortex, area F4 is poorly laminated with pyramids increasing in size from upper to lower layer III, similarly to area F2. The overall cellular density in F4 is lower than in F2. Scattered, large pyramids can be found in the caudal part (towards the border with F1) of dorsal area F4. Rostral to F4, area F5, is clearly laminated, with a prominent layer V and a higher than F4 cellular density. Area F5 borders rostrally with the prefrontal cortex, which is characterized by the existence of the granular layer IV. Overall, the known cytoarchitectonic differences between areas F1, F2, F4, F5, and F7 (Matelli et al., 1991; Matelli et al., 1996; Geyer et al., 2000) allowed the delineation of these anatomically distinct areas on the 2D functional maps (Figs. 10-16).

The 2D reconstructed map of the distribution of metabolic activity in the frontal cortex of the right hemisphere of the F monkey displays restricted metabolic activations (Fig. 10A). Regions of enhanced metabolic activity can be seen 1) in the anterior bank and the fundus of the As, 2) in area F4, 3) in dorsal SI, around the fundus of Cs, in a region corresponding to the trunk representation (Woolsey et al., 1952), 4) in ventral F1 where the mouth representation has been described (Woolsey et al., 1952) and 5) in the corresponding mouth representation in ventral SI (Woolsey et al., 1952). The latter SI-mouth effect corresponds to the saturated (black) region of the reconstruction.   The   right

hemisphere (contralateral to the moving forelimb) of the RL_f monkey performing visually guided reaching from a central to a peripheral (20 deg up left) target during fixation of the central target, displays extended activations which are shown in Figure 10C. In addition to the ones illustrated in the map of the fixating monkey (Fig. 10A), intense activations are also displayed in the forelimb representation in areas F1 and SI (dorsal to the mouth representation (Woolsey et al., 1952), which are evident within the Cs as well as in area F5. The activated band in F5, running from dorso-caudal (posterior crown of As) to ventro-rostral (fundus of As), is also present in the map of the ipsilateral to the moving forelimb hemisphere (Fig. 10B), although it is much less intense.

Similar is the picture obtained from the RL animal performing visually guided reaching from a central to a peripheral target, which was located 20 deg away from straight ahead in an oblique direction 45 deg up (Fig. 11B). This monkey was free to move its eyes during the trial period. Band-like activations are evident in the forelimb representation of areas F1 and SI and in area F5, when compared to the corresponding control case (Fig. 11A). The monkey serving as a control (S_o) performed visually guided saccades 20 deg in amplitude, from the central to the peripheral target.
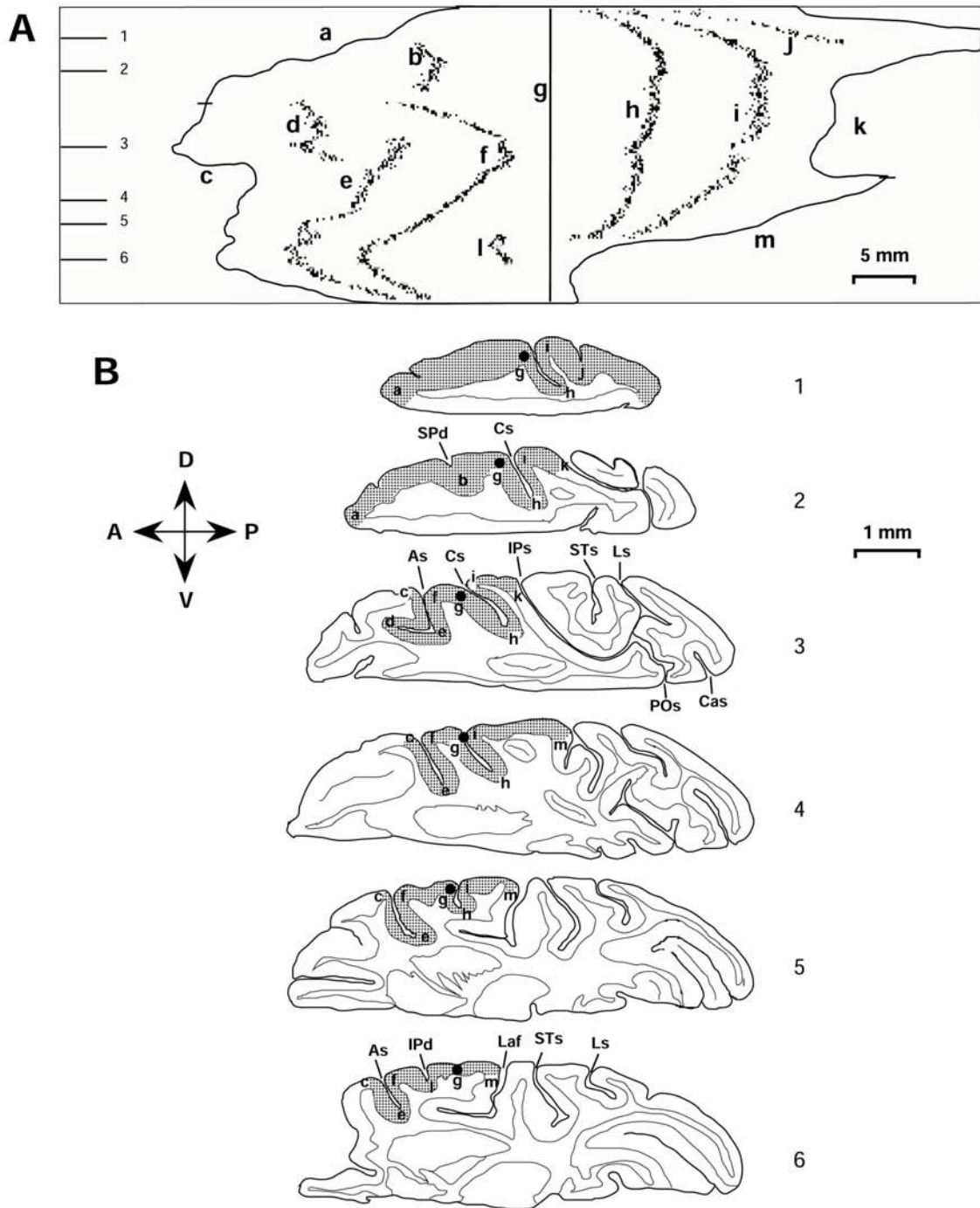
Figure 9. Reconstruction of the primary motor and lateral premotor areas around and within the As and the Cs. (A) Schematic representation of 2D maps. Zero anteroposterior level (line g) corresponds to the anterior crown of Cs, used for alignment of adjacent sections. Line a corresponds to the rostralmost tip of each horizontal section; line b corresponds to the superior precentral dimple; line c corresponds to the anterior crown of As; line d corresponds to the anterior tip of the floor of As; line e corresponds to the posterior tip of the floor of As dorsally and the fundus of As more ventrally; line f corresponds to the posterior crown of As; line h corresponds to the fundus of Cs; line i corresponds to the posterior crown of Cs; line j corresponds to the superior postcentral dimple; line k corresponds to the anterior crown of IPs; line l corresponds to the inferior precentral dimple; line m corresponds to the anterior crown of Laf. Lines 1-6 on the right part of the figure indicate the approximate dorsoventral location of the sections shown in B. (B) Schematic representations of six horizontal sections through the right hemisphere of a monkey brain at different dorsoventral levels; D, dorsal; V, ventral; A, anterior; P, posterior. The shaded areas outline the cortical region measured and reconstructed. The solid circle (g) within the shaded area indicates the point of alignment of adjacent sections, which corresponds to the anterior crown of Cs. Letters a-m indicate the same landmarks in both Figures 9A and 9B. As, arcuate sulcus; Cas, calcarine sulcus; Cs, central sulcus; IPd, inferior precentral dimple IPs, intraparietal sulcus; Laf, lateral fissure; Ls, lunate sulcus; POs, parietoccipital sulcus; SPd, superior precentral dimple; STs, superior temporal sulcus.
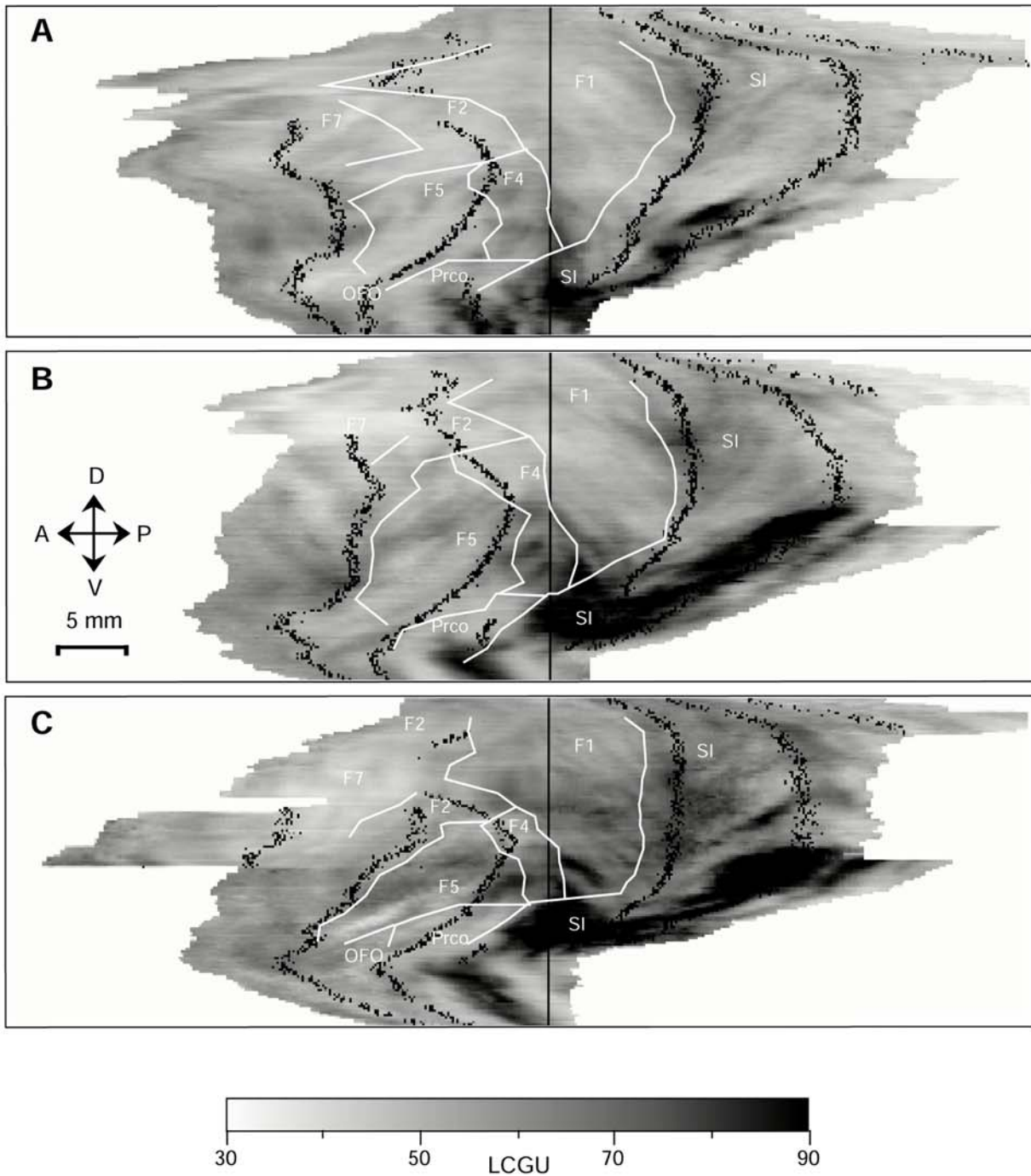
Figure 10. Activations in the As, Cs and the lateral cortical convexity induced by fixation and visually guided reaching. (A) The 2D spatial reconstruction of the LCGU values (μmol/100g/min) of metabolic activity in the right hemisphere of the fixating monkey. (B) The 2D map of metabolic activity in the ipsilateral to the moving forelimb hemisphere of the monkey performing visually guided reaching under fixation. (C) The 2D map of metabolic activity in the contralateral to the moving forelimb hemisphere of the monkey performing visually guided reaching during fixation. White lines indicate the borders of the cytoarchitectonically distinct subregions of the frontal lobe. Other conventions as in Figure 9.
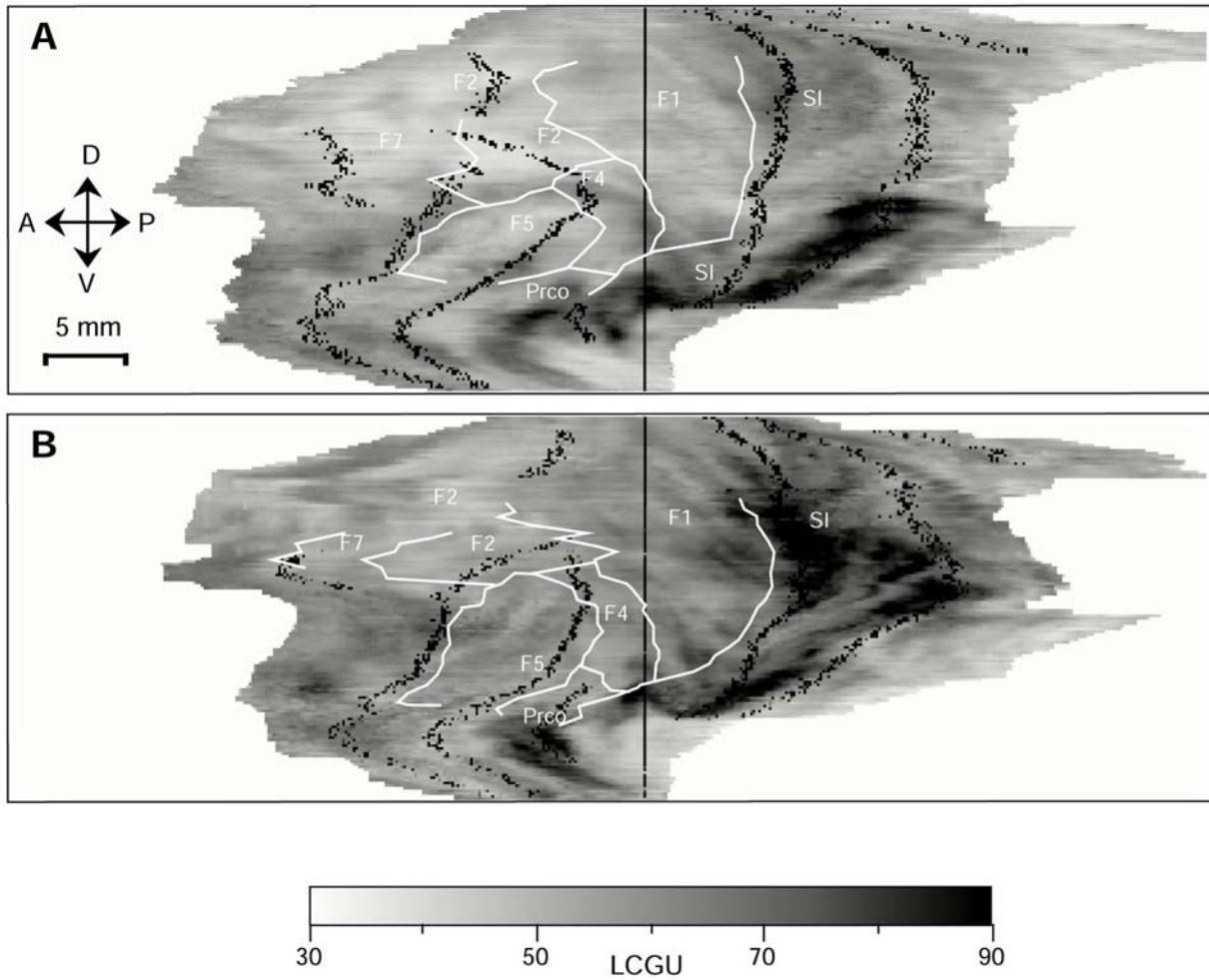
Figure 11. Activations in the As, Cs and the lateral cortical convexity induced by visually guided saccades and visually guided reaching. (A) The 2D spatial reconstruction of the LCGU values (μmol/100g/min) of metabolic activity in the right hemisphere of the monkey performing saccades from a central to a peripheral visual target located 20 deg up left. (B) The 2D map of metabolic activity in the contralateral to the moving forelimb hemisphere of the monkey performing visually guided reaching from the central to the peripheral target located 20 deg up left. Other conventions as in Figure 10.

52
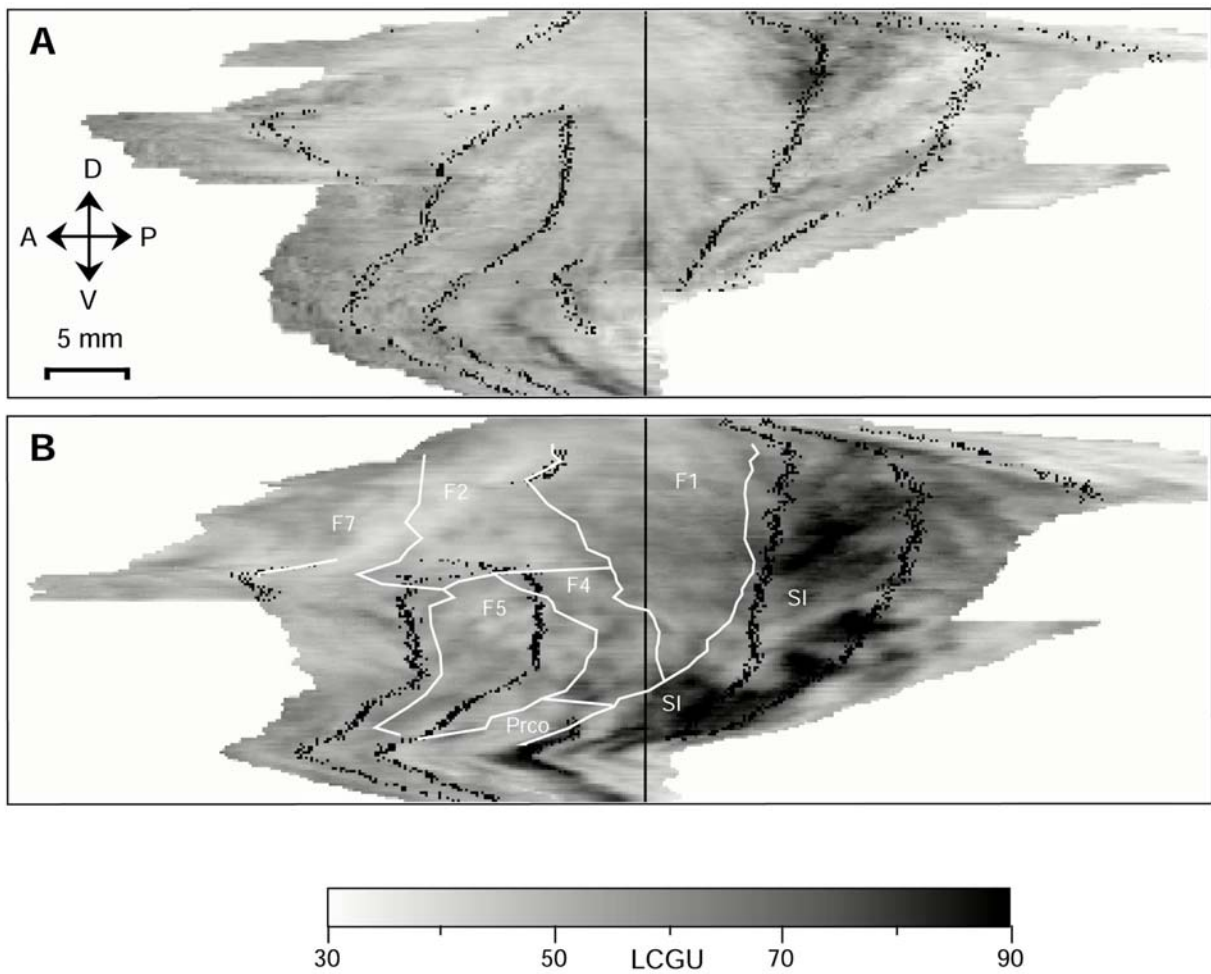
Figure 12. Activations in the As, Cs and the lateral cortical convexity induced by reaching under somatosensory guidance. (A) The 2D spatial reconstruction of the LCGU values (μmol/100g/min) of metabolic activity in the right hemisphere of the untrained control monkey sitting in the dark. (B) The 2D map of metabolic activity in the contralateral to the moving forelimb hemisphere of the monkey performing reaching in the dark. Other conventions as in Figure 10.

The fifth monkey (RD) was rewarded for performing reaching in the dark from the learned central to the learned peripheral location of the targets used in the previous cases, in response to auditory cues used as go-signals. The eyes had to maintain a straight ahead direction during the trial period. No visual information about the target or the forelimb position was available. The monkey had learned the central and peripheral locations. The 2D map of the distribution of metabolic activity in the contralateral to the moving forelimb hemisphere is shown in Figure 12B. Compared to the map of the naive control monkey (C), which remained in the dark and did not receive any reward or visual stimulation (Fig. 12A), the map in Figure 12B displays widespread activations within the motor, premotor and primary somatosensory cortices. More specifically, similarly to Figures 10C and 11B intense and extended activation is evident in the forelimb and mouth representations in areas F1 and SI. The activation in area F5 is moderate while several activation foci can also be seen in area F4.

Overall, the metabolic activity maps shown in Figures 10-12 demonstrate massive involvement of areas SI, F1, F2, F4 and F5 in reaching movements. Furthermore, the two control monkeys, F and S_o, displayed activation in regions related to the processing of visual information and execution of saccadic eye movements, respectively. Part of the anterior bank of As which appears activated in all visually stimulated animals (Figs. 10 and 11) when compared to the C monkey (Fig. 12A), belongs to the FEF, the cortical center which controls eye movements. Neurons in this area display visual as well as motor properties. Comparison of the LCGU values in the whole anterior bank of the As between the visually stimulated monkeys and the C monkey, which remained in the dark, demonstrates a statistically significant increase of activity in the visually stimulated animals (Table 3). Moreover, a region within the As, which lies close to its fundus and has been suggested to be involved in fixation of visual targets (Burman and Bruce, 1997) is activated in the hemispheres of the animals fixating visual targets (Fig. 10). The intensity of the effect within this area in the F and RL_f monkeys displays over 20% increase in activity as compared to the C monkey (Table 4). Area F4 is also activated in the F and S_o monkeys as compared to the C monkey (Table 5; F4), a fact which may reflect the well known visual properties of neurons in this area.

In order to evaluate both the topographical organization and the intensity of the effects in further detail and in order to make direct comparisons between different animals we isolated and analyzed separately (i) the ventral premotor cortex, (ii) the dorsal premotor cortex and (iii) the central sulcus, as described below.

Table 3

Metabolic activation in the anterior bank of the As

HEMISPHERE (n)	LCGU	%Dif
C (33)	54±2	-
RD(ipsi) (34)	56±1	4
RD(contra) (61)	52±4	-4
F(left) (63)	62±2	15*
F(right) (40)	60±2	11*
S_o (52)	62±3	15*
RL_f(ipsi) (47)	62±3	15*
RL_f(contra) (58)	61±3	13*
RL(ipsi) (44)	65±2	20*
RL(contra) (57)	65±3	20*

Values represent the normalized mean of glucose utilization (LCGU) expressed in μmol/100g/min ± standard deviation obtained from one control (**C**) and five experimental monkeys performing one of the following tasks: reaching in the dark (**RD**), fixation (**F**), saccades (**S_o**), reaching in the light under fixation (**RL_f**), and reaching in the light (**RL**).

n, number of sets of five adjacent horizontal sections used in obtaining mean LCGU values in each hemisphere.

%Dif, experimental-to-control percent difference calculated as [(H - C) /C] x 100, where H represents each one of the reported hemispheres. Contra and ipsi refer to the contralateral and ipsilateral to the moving forelimb hemispheres in the reaching monkeys.

* All differences above 10% were statistically significant by the Student's unpaired *t*-test at the level of $p < 0.01$ and comparison of the respective distributions of glucose utilization values by the Kolmogorov-Smirnov test also demonstrated statistically significant differences at the level of $p < 0.01$.

Table 4

Metabolic activation of the fixation related region in the anterior bank of As close to the fundus.

HEMISPHERE (n)	LCGU	%Dif
C (28)	52±2	-
F(left) (23)	64±2	23*
F(right) (20)	63±1	21*
RL_f(ipsi) (15)	69±4	33*
RL_f(contra) (15)	66±3	27*

All conventions as in Table 3.

Activated regions within the ventral premotor cortex

In order to make direct comparisons between different hemispheres and because the geometry of the As and the lateral convexity is not identical in different animals we generated isodimensional maps of the area of interest in the different hemispheres by transforming the anteroposterior and dorsoventral dimensions as ratios of their maximal values. More specifically, we transformed the region outlined in Figure 13A between lines a and c. This region extends anteroposteriorly from the fundus of As (line a) to the anterior crown of Cs (line c) and dorsoventrally from the dorsalmost border of area F4 to approximately the ventralmost border of area F5. The dorsoventral extent of this region (DV_{max}) in each hemisphere was used as reference to express the dorsoventral value of each section (DV_s). Thus, DV_s was expressed as a ratio of DV_{max} (DV_s /DV_{max}). The anteroposterior value AP_x of a pixel located in the posterior bank of As was similarly expressed as a ratio of the anteroposterior length of the posterior bank, $AP_{pb,s}$, in that section ($AP_x / AP_{pb,s}$). The anteroposterior value AP_y of a pixel located in the convexity between the posterior crown of As and the anterior crown of Cs was expressed as a ratio of the anteroposterior length of the convexity $AP_{c,s}$, in that section ($AP_y / AP_{c,s}$) and its value on the map was calculated as $1+ (AP_y / AP_{c,s})$. This way the anteroposterior values on the convexity were added to the length of the posterior bank of As. The left half in each transformed map of Figures 13-16 represents the posterior bank of As whereas the right half represents the cortical convexity between the posterior crown of As and the anterior crown of Cs. Thus, the line separating the two halves represents the posterior crown of As. The relationship between the anteroposterior and the dorsoventral extent of the transformed region was respected so that in the transformed maps the anteroposterior dimension is 1.5 times the dorsoventral one.

The distribution of metabolic activity in the transformed maps of the two hemispheres of the F monkey is shown in Figure 13B, C. Apart from the intense activation in the SI mouth representation, in the lower right part of the maps, which is related to licking of water as a reward, there are clear activations in area F4 and toward the fundus of As in the left part of the maps, in a region which we believe is part of the FEF-fixation region. Subtraction of Figure 13B map from the corresponding one in Figure 13C results in the map shown in Figure 16A.

Moreover, subtraction of the corresponding map of the C monkey (Fig. 15A) from the one in Figure 13C results in the map shown in Figure 16B. This map should, by definition, demonstrate the effects induced by fixation of a visual target, in the posterior bank of As and the cortical convexity. These effects are confined in area F4 and in a restricted region close to the fundus of As.

The transformed maps of the ipsilateral and the contralateral to the moving forelimb hemispheres of the RL_f monkey are shown in Figure 13D and E, respectively. Enhanced activation is displayed (1) in area F4, (2) in area F5 within the posterior bank of As as well as on the lateral convexity and (3) close to the fundus of As. These effects are much more pronounced in the hemisphere contralateral to the moving forelimb (Fig. 13E). The activations could be attributed to the visual processing and/or the reaching movement. To reveal the activations related to reaching we subtracted the map corresponding to the F monkey (Fig 13C) from the one of the hemisphere contralateral to the moving forelimb in the RL_f monkey (Fig. 13E). The result of the subtraction is shown in Figure 16D. The activated foci are confined in area F4, in the part of F5 lying on the cortical convexity and in the part of F5 within the posterior bank of As.

Similar, but less intense, are the results obtained from the RL monkey. The maps corresponding to the hemispheres ipsilateral and contralateral to the moving forelimb are shown in Figure 14B and C, respectively. Enhanced metabolic activity is evident within F4, F5 and a region close to the fundus of As. To reveal the effects related to reaching we subtracted the map of the monkey performing visually guided 20 deg up-left saccades (Fig.14A) from the map of the hemisphere contralateral to the moving forelimb in the RL monkey (Fig. 14C). The resulting subtraction map displays activation in both areas F4 and F5 (Fig. 17A).

Quantitative comparison of the effects induced in area F4 of the hemisphere contralateral to the moving forelimb in the RL and RL_f monkeys with their corresponding control values (S_o and F, respectively) demonstrated that the activations are higher in the reaching animals by 13% and 17%, respectively (Table 5; F4). In contrast, no statistically significant difference was found between the contralateral and the ipsilateral hemisphere of each monkey, suggesting a bilateral involvement of F4 in reaching. When similar quantitative comparisons were made in F5, it was found that both the convexity (Table 5; F5convexity) and the posterior bank of the As (Table 5; F5bank) displayed higher glucose consumption by 37% and 22%, respectively, as compared to the F monkey. The glucose consumption within the activated zone in the posterior bank of the As was increased by 21% in the contralateral hemisphere of the RL_f monkey as compared to the control values of the equivalent area (Table 5; F5zone). Similar were the results obtained from the comparison between the RL and S_o monkey. The RL monkey displayed 18% increase in glucose consumption in the posterior bank of the As and the cortical convexity and 23% increase within the F5 activated zone as compared to the S_o monkey (Table 5). Based on these data and the subtraction maps of Figures 16D and 17A we conclude that during reaching in the light both areas F4 and F5 are markedly activated.

58
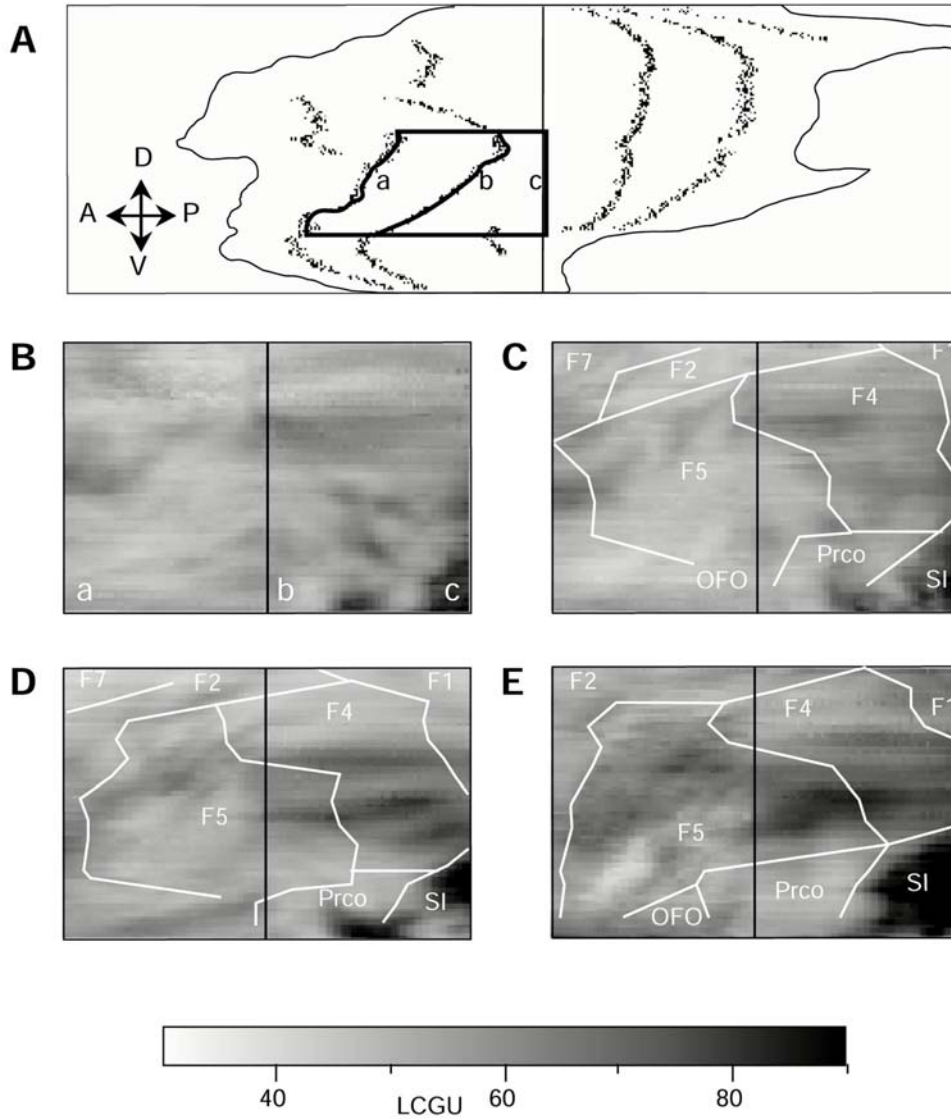
Figure 13. Activations in the ventral premotor cortex induced by fixation and visually guided reaching. (A) The outlined region (between lines a and c) on the 2D schematic map indicates the borders of the area transformed and illustrated in Figures 13-15. Line a corresponds to the fundus of As; line b corresponds to the posterior crown of As; line c corresponds to the anterior crown of Cs. (B) The 2D spatial reconstruction of the LCGU values (µmol/100g/min) of metabolic activity in the transformed map of the left ventral premotor cortex of the fixating monkey. Letters a-c indicate the same landmarks in both A and B. (C) The 2D transformed map of metabolic activity in the right ventral premotor cortex of the fixating monkey. (D) The 2D transformed map of metabolic activity in the ventral premotor cortex ipsilateral to the moving forelimb in the monkey performing visually guided reaching under fixation. (E) The 2D transformed map of metabolic activity in the ventral premotor cortex contralateral to the moving forelimb in the monkey performing visually guided reaching during fixation. Other conventions as in Figure 10.
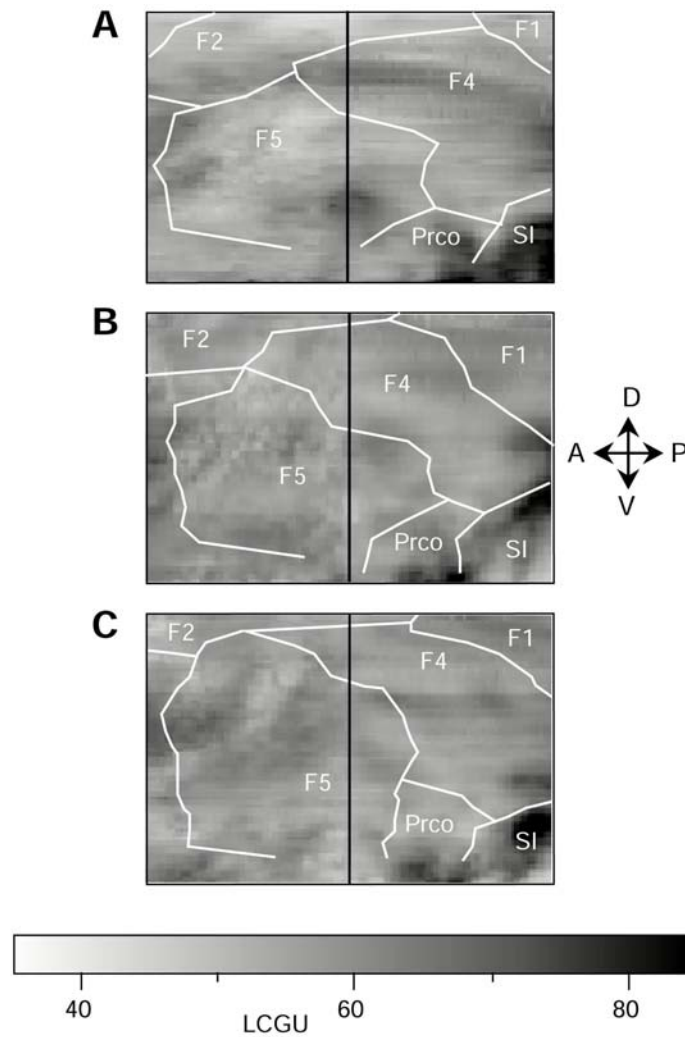
Figure 14. Activations in the ventral premotor cortex induced by visually guided saccades and visually guided reaching. (A) The 2D spatial reconstruction of the LCGU values (μmol/100g/min) in the transformed map of the right ventral premotor cortex of the saccading monkey. (B) The 2D transformed map of metabolic activity in the ventral premotor cortex ipsilateral to the moving forelimb in the monkey performing visually guided reaching. (C) The 2D transformed map of metabolic activity in the ventral premotor cortex contralateral to the moving forelimb in the monkey performing visually guided reaching. Other conventions as in Figure 13.
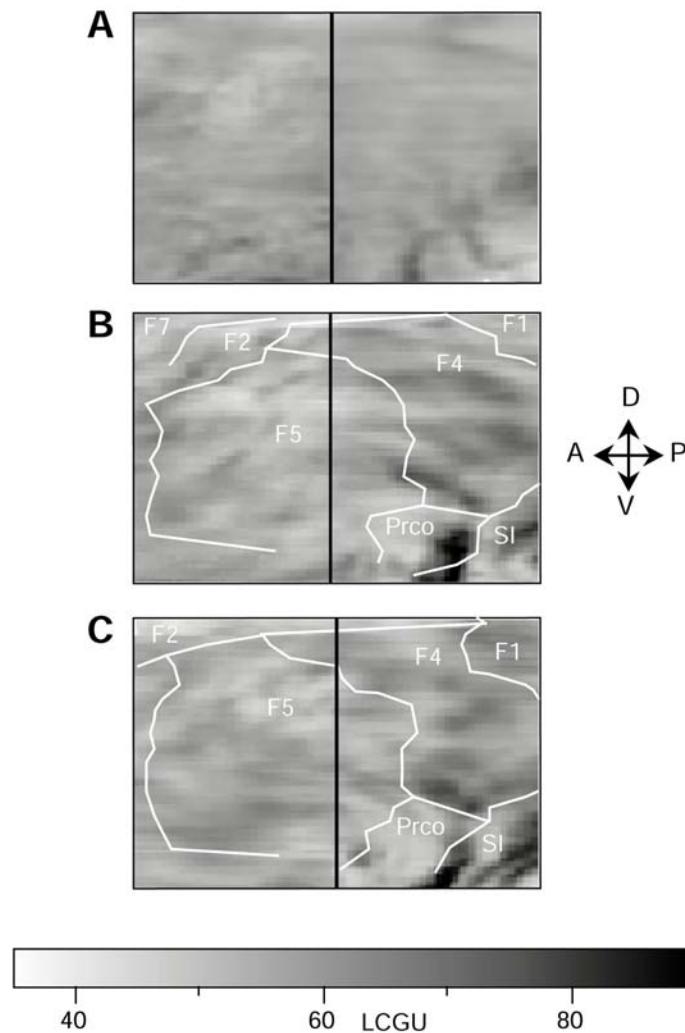
Figure 15. Activations in the ventral premotor cortex induced by reaching under somatosensory guidance. (A) The 2D spatial reconstruction of the LCGU values (μmol/100g/min) in the transformed map of the right ventral premotor cortex of the untrained control monkey. (B) The 2D transformed map of metabolic activity in the ventral premotor cortex ipsilateral to the moving forelimb in the monkey performing reaching in the dark. (C) The 2D transformed map of metabolic activity in the ventral premotor cortex contralateral to the moving forelimb in the monkey performing reaching movements in the dark. Other conventions as in Figure 13.
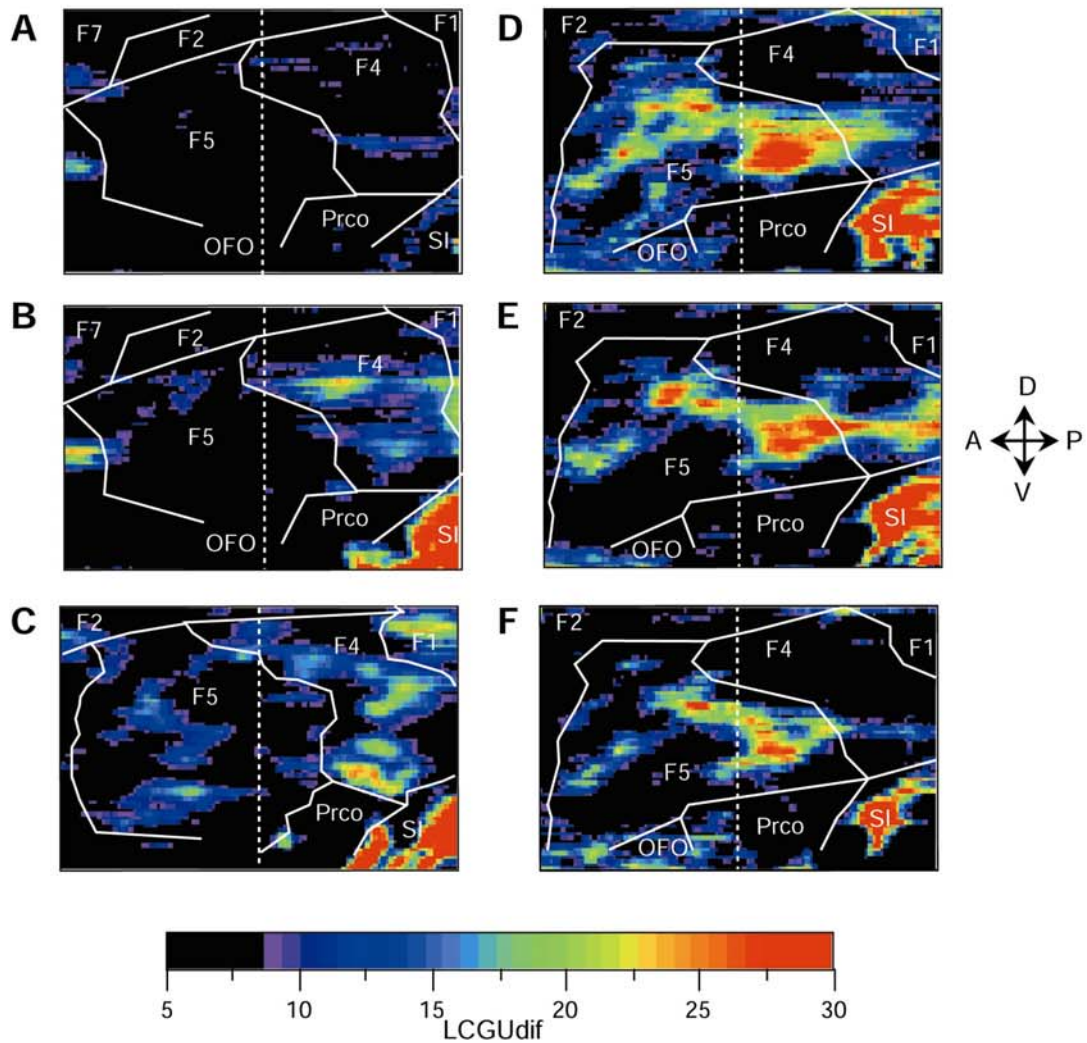
Figure 16. Subregions of the ventral premotor cortex activated during fixation, reaching under somatosensory guidance and reaching under visual guidance. (A) Map generated after subtracting the cortical activity in the left ventral premotor cortex (Fig. 13B) of the fixating monkey from that in the right ventral premotor cortex of the same monkey (Fig. 13C). (B) Map generated after subtracting the cortical activity in the right ventral premotor cortex of the untrained control monkey (Fig. 15A) from the respective map of the right hemisphere of the fixating monkey (Fig. 13C), to illustrate areas activated during fixation. (C) Map generated after subtracting the metabolic activity of the right ventral premotor cortex of the untrained control monkey (Fig.15A) from the one in the ventral premotor cortex contralateral to the moving forelimb in the monkey reaching in the dark (Fig. 15C), to illustrate areas involved in reaching under somatosensory guidance. (D) Map generated after subtracting the cortical activity in the right ventral premotor cortex of the fixating monkey (Fig. 13C) from the one in the ventral premotor cortex contralateral to the moving forelimb in the monkey reaching in the light during fixation (Fig. 13E) to illustrate areas involved in reaching uder both visual and somatosensory guidance. (E) Map generated after subtracting the cortical activity in the ventral premotor cortex contralateral to the moving forelimb in the monkey reaching in the dark (Fig. 15C) from that in the ventral premotor cortex contralateral to the moving forelimb in the monkey reaching in the light during fixation (Fig. 13E), to illustrate areas invovled in fixation and visual guidance of reaching. (F) Map generated after subtracting the map illustrated in B from that illustrated in E, to show areas involved in the visual guidance of reaching. Dashed line indicates the posterior crown of the arcuate sulcus. Colour bar indicates the difference in local cerebral glucose utilization (LCGUdif).
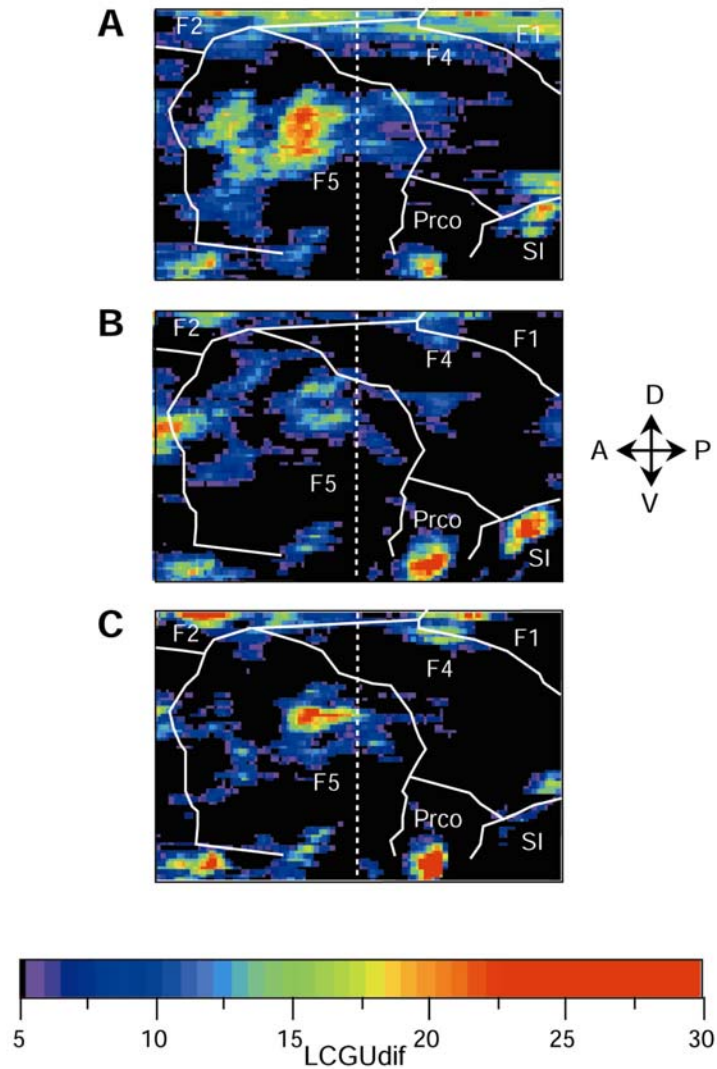
Figure 17. Subregions of the ventral premotor cortex activated during visually guided reaching from a second animal. (A) Map generated after subtracting the cortical activity in the right ventral premotor cortex of the saccading monkey (Fig. 14A) from the one in the ventral premotor cortex contralateral to the moving forelimb in the monkey reaching in the light (Fig. 14C), to illustrate areas involved in reaching under both visual and somatosensory guidance. (B) Map generated after subtracting the cortical activity in the ventral premotor cortex contralateral to the moving forelimb in the monkey reaching in the dark (Fig. 15C) from that in the ventral premotor cortex contralateral to the moving forelimb in the monkey reaching in the light (Fig. 14C), to illustrate areas activated during visually guided saccades and visually guided reaching. (C) Map generated after subtracting the maps shown in Figures 15A and 14A, from the map illustrated in B, to show areas involved in the visual guidance of reaching. Other conventions as in Figure 16.

Reaching movements are usually accomplished under both visual and somatosensory guidance. Vision provides information about the target and limb location, whereas somatosensory input provides information about the current "felt" position of the limb. The transformed maps of the hemispheres ipsi- and contra-lateral to the moving forelimb in the RD monkey, which had only somatosensory and no visual information available to guide the forelimb, are shown in Figure 15B and C. The effects induced by reaching under somatosensory guidance are shown in the subtraction map of Figure 16C. In this map pronounced activations are illustrated in area F4 and moderate activations in area F5. The latter ones are mainly concentrated within the posterior bank of the As and not in the convexity. We quantitatively compared the effects induced in the different subregions of the ventral premotor cortex in the RD monkey with the corresponding values in the C monkey. Area F4 and the part of area F5 which lies in the posterior bank of the As displayed significant activations in the hemisphere contralateral to the moving forelimb as compared to the C monkey (Table 5; F4, F5bank). No difference was found in the part of the F5 which lies on the cortical convexity. These results confirm that areas F4 and F5 are involved in reaching movements under somatosensory guidance and also indicate that it is the F5-bank region, which is more directly involved rather than the F5-convexity.

To separately evaluate the contribution of visual and somatosensory information in the guidance of reaching we subtracted the map of Figure 15C (reaching in the dark under somatosensory guidance) from the maps of Figures 13E and 14C (reaching in the light under both visual and somatosensory guidance). The resulting subtraction maps (Figs. 16E and 17B) should illustrate the neuronal populations related to reaching under visual guidance using peripheral vision in the case of fixation (Fig. 16E), and central vision in the case of saccades (Fig. 17B). These subtraction maps demonstrate activated populations within areas F4 and F5, the activations being more pronounced in the case of visual guidance under fixation. Furthermore, in order to exclude any effect of visual information unrelated to reaching, we subtracted the map corresponding to the effect of visual fixation (Fig. 16B) from the one of Figure 16E. The result of this subtraction is shown in Figure 16F, which illustrates the activated regions associated with visual guidance of reaching in the RL_f monkey. In a similar way Figure 17C illustrates the areas associated with visual guidance of reaching in the RL monkey. Thus, both maps of Figures 16E and 17C illustrate the spatial distribution of neurons related to the visual guidance of reaching. The most intense activated foci are concentrated within F5, both on the convexity and in the posterior bank of the As, around the posterior crown of As.

Based on the results of the subtraction maps of Figures 16 and 17 we conclude that within the ventral premotor cortex area F4 is activated during visual processing (Fig. 16B) and during reaching under somatosensory guidance (Fig. 16C). On the other hand, area F5 is involved in reaching under both visual (Fig. 16F and Fig. 17C) and somatosensory guidance, with neurons related to the visual guidance concentrated closer to the crown rather than the fundus of As (Fig. 16F and Fig. 17C).

Table 5
Metabolic effects in subregions of the ventral premotor cortex

AREA (n)	C	RD				F			RLf				So	RL			
		Ipsi	Contra	%Dif	%RD/C	Left	Right	%Dif	Ipsi	Contra	%Dif	%RLf/F		Ipsi	Contra	%Dif	%RL/So
F4	49±2	58±4	58±2	0	18*	56±5	58±5	4	65±9	68±9	5	17*	53±5	58±3	60±3	3	13*
	(65)	(76)	(57)			(69)	(69)		(85)	(48)			(81)	(48)	(63)		
F5convexity	51±2	56±3	53±1	-5	4	51±1	51±2	0	61±7	70±8	15*	37*	50±2	55±1	59±3	7	18*
	(17)	(13)	(23)			(21)	(14)		(30)	(18)			(26)	(27)	(14)		
F5bank	50±2	54±2	56±3	4	12*	49±2	49±2	0	53±3	60±5	13*	22*	51±2	56±2	60±3	7	18*
	(35)	(39)	(44)			(41)	(41)		(50)	(44)			(36)	(36)	(37)		
F5zone	49±2	57±1	58±1	2	18*	53±4	56±3	6	60±2	68±3	13*	21*	53±2	58±2	65±2	12*	23*
	(33)	(23)	(24)			(29)	(32)		(32)	(35)			(23)	(24)	(30)		

%Dif, side-to-side percent difference calculated as [(Contra-Ipsi)/Ipsi]*100

%RD/C, %RLf/F, %RL/So, contra-to-control percent differences calculated as [(RDcontra-C)/C]*100, [(RLfcontra-Fright)/Fright]*100,

[(RLcontra-So)/ So]*100, respectively.

Numbers in parentheses show number of sets of five adjacent horizontal sections used in obtaining mean LCGU values in each region of each hemisphere.

All other conventions as in Table 3.

Activated regions within the dorsal premotor cortex

The dorsal premotor cortex is comprised of areas F2 posteriorly and F7 anteriorly (Matelli et al., 1991). To study in further detail the role of these areas in the visual and somatosensory guidance of movement, we focused on the part of the metabolic maps which includes areas F2 and F7 (outlined in Fig. 18A). This region extends anteroposteriorly from the rostralmost tip of each horizontal section (for the sections dorsal to the appearance of As) and from the anterior crown of As (in more ventral sections), to the anterior crown of Cs. Dorsoventrally, this region extends from about 2mm from the dorsalmost section of the hemisphere to the genu of As, where the ventral border of F2 lies.

To evaluate the effects (shown in Figs. 10-12) induced by the different behaviors used in our study, we first subtracted the map of the F animal from that of the hemisphere contralateral to the moving forelimb in the RL_f animal. The anterior crown of Cs and the superior precentral dimple were used as reference points for the alignment of the individual maps. The resulting subtraction map (Fig. 18B) illustrates the regions, which are activated during visually guided reaching. The intense activation within F1 corresponds to the extension of the forelimb representation on the lateral convexity of the primary motor cortex. Within F2, less marked activations are illustrated (i) dorsally, below the superior precentral dimple, and (ii) ventrally, close to the As. The latter activation covers part of the lateral convexity and the floor of As. The ventral activation is more intense than the dorsal one. Both of these activated regions displayed significantly higher LCGU values in the contralateral hemisphere of the RL_f and the RL monkeys when compared with the corresponding control values (Table 6, F2dimple, F2AS). Moreover, the dorsal activation (below the superior precentral dimple) is also significantly higher in the contralateral hemisphere as compared with its ipsilateral homologue in both the RL_f and the RL monkeys.

Given that during visually guided reaching both visual and somatosensory information is used to guide the forelimb, the two different activation foci revealed in the subtraction map of Figure 18B could represent two distinct neuronal populations being selectively involved in either the visual or the somatosensory guidance of reaching. In that case, only one of these two neuronal populations should be activated in the equivalent map of the RD monkey. Figure 18C is the result of subtraction of the map of the C monkey from the map in the hemisphere contralateral to the moving forelimb of the RD monkey. As expected, there is only one activated region within F2, which lies dorsal and close to the superior precentral dimple. This region displays significantly higher glucose consumption compared to its equivalent in the ipsilateral hemisphere and in the control monkey (Table 6, F2dimple). No significant activation is evident in the ventral part, close to the As. These results suggest that within F2 there is a segregation of visual and somatosensory input used for reaching. Neurons related to visual guidance of reaching are ventrally located around and within the As, whereas neurons related to somatosensory guidance are dorsally located, below the superior precentral dimple.

Finally, within F7 no significant differences were revealed between the different tasks used in the present study.
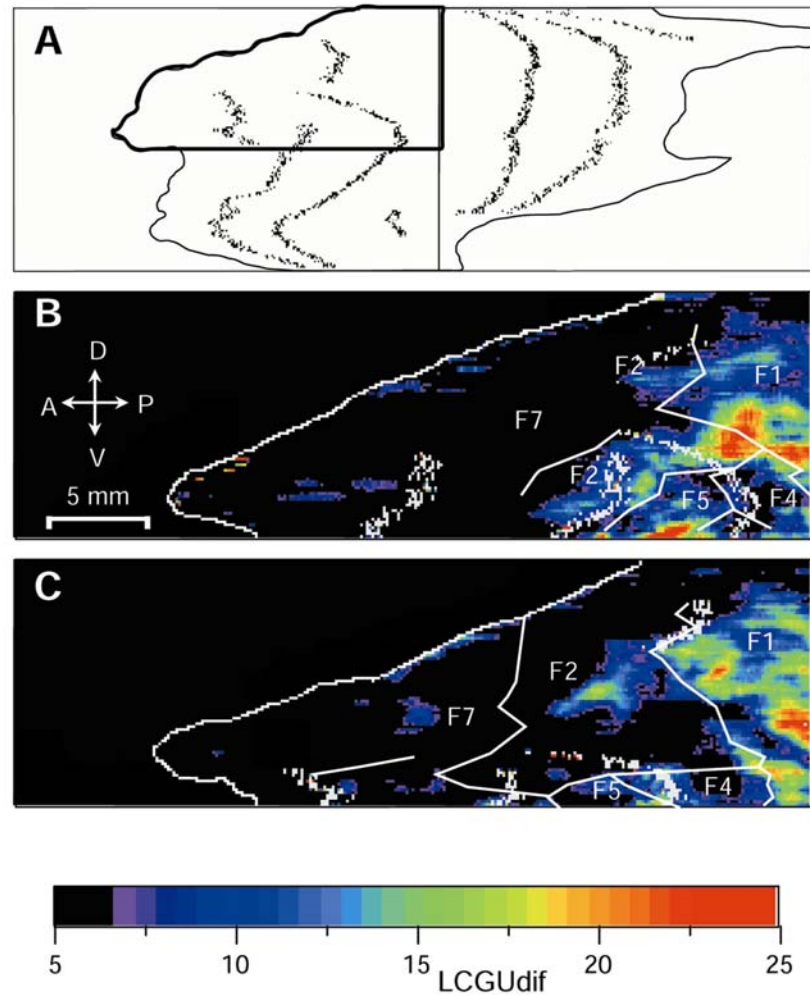
Figure 18. Subregions of the dorsal premotor cortex activated during reaching under visual guidance and under somatosensory guidance. (A) The region outlined on the schematic representation of the 2D map corresponds to the dorsal premotor cortex shown in B and C. (B) Map generated after subtracting the cortical activity in the right dorsal premotor cortex of the fixating monkey (Fig. 10B) from the one in the dorsal premotor cortex contralateral to the moving forelimb in the monkey reaching in the light under fixation (Fig. 10C), to illustrate areas involved in reaching under both visual and somatosensory guidance. (C) Map generated after subtracting the cortical activity in the right dorsal premotor cortex of the untrained control monkey (Fig. 12A) from that in the dorsal premotor cortex contralateral to the moving forelimb in the monkey reaching in the dark (Fig. 12B), to illustrate areas involved in reaching under somatosensory guidance. Colour bar indicates the difference in local cerebral glucose utilization (LCGUdif).

Table 6
Metabolic effects in subregions of the dorsal premotor cortex

AREA (n)	C	RD				F			RL_f				S_o	RL			
		Ipsi	Contra	%Dif	%RD/C	Left	Right	%Dif	Ipsi	Contra	%Dif	%RL/F		Ipsi	Contra	%Dif	%RL/S_o
F2dimple	42±3 (21)	45±2 (17)	52±1 (13)	16*	24*	47±2 (22)	47±1 (22)	0	48±2 (15)	55±2 (16)	15*	17*	46±3 (18)	48±1 (20)	56±1 (17)	17*	22*
F2AS	47±4 (35)	47±3 (32)	49±3 (26)	4	4	46±1 (27)	45±1 (26)	-2	52±2 (21)	57±3 (30)	10	27*	46±7 (28)	50±4 (25)	54±1 (21)	8	17*
F7	45±3 (20)	44±1 (27)	44±2 (22)	0	-2	46±2 (26)	46±2 (24)	0	44±3 (25)	45±2 (23)	2	-2	45±3 (26)	49±2 (27)	48±2 (22)	-2	7

All conventions as in Table 5.

Activated regions within the central sulcus

      The Cs contains part of the primary motor cortex (F1) in its anterior bank and part of the primary somatosensory cortex (SI) in its posterior bank. An orderly topographic representation of all body parts exists in each area and the two representations display a mirror image relationship. Overall, lower body parts (leg, lower trunk) are represented dorsally and upper body parts (upper trunk, forelimb, face) are represented ventrally in a orderly manner.

      To study in detail the activations induced by the different tasks presently used, we transformed the part of the maps of Figures 10-12 which contained the Cs (outlined in Fig. 19A), in order to overcome the individual geometrical irregularities and to make direct comparisons possible. The transformation was based on the same principles which were used for the ventral premotor cortex and resulted in equivalent maps of standard dimensions. In summary, the area taken into consideration extended in the anteroposterior dimension from the anterior crown to the posterior crown of Cs, and in the dorsoventral dimension from the dorsalmost section in our maps (corresponding to about 2mm from the top of the hemisphere) to the ventralmost section of Cs. The dorsoventral extent of this region (DV_{max}) in each hemisphere was used as reference to express the dorsoventral value of each section (DV_s). Thus, DV_s was expressed as a ratio of DV_{max} (DV_s / DV_{max}). The anteroposterior value AP_x of a pixel located in the anterior bank of Cs was similarly expressed as a ratio of the anteroposterior length of the posterior bank, $AP_{ab,s}$, in that section ($AP_x / AP_{ab,s}$). The anteroposterior value AP_y of a pixel located in the posterior bank of Cs was expressed as a ratio of the anteroposterior length of the posterior bank $AP_{pb,s}$, in that section ($AP_y / AP_{pb,s}$) and its value on the map was calculated as $1+ (AP_y / AP_{pb,s})$. This way the anteroposterior values on the posterior bank were added to the length of the anterior bank of Cs. The two halves in each transformed map of Figures 19-20 represent the anterior bank of Cs (left half) and the posterior bank (right half) with the line in between representing the fundus of Cs.

      The distribution of metabolic activity within the Cs in the six hemispheres of the three monkeys performing reaching movements (RL, RL_f, RD) as well as in the two hemispheres of the F monkey are shown in Figure 19. The most intense activation in the lower part of each map corresponds to the mouth representation and is due to licking of the water in the rewarded trials. The bilateral activation in the upper half of each map, around the fundus of Cs, corresponds to the trunk representation and is due to postural involvement. Extended activated bands within F1 and SI are evident in the hemispheres contralateral to the moving forelimb in the RL, RL_f, and RD monkeys when compared (a) to their ipsilateral hemispheres (compare maps E, G, I to maps D, F, H, respectively, in Fig. 19) and (b) to the hemispheres of the F monkey (Fig. 19B, C).

      Since the forelimb is thought to be controlled by the contralateral hemisphere whereas both trunk and mouth representations are controlled bilaterally, subtraction of the map corresponding to the ipsilateral hemisphere from the equivalent map in the contralateral hemisphere of the reaching monkeys should allow us to visualize the forelimb representation within the Cs. The result of these subtractions for the RL_f and the RL monkeys is shown in Figures 20A and B, respectively.

      To evaluate quantitatively the activations induced in the different hemispheres within the Cs, we measured separately the glucose consumption within the subregions corresponding to the mouth, trunk and forelimb representations. The values are shown in Table 7. The forelimb representation is markedly activated contralateral to the moving forelimb in all reaching animals in both SI and F1 (Table 7; SI-forelimb, F1-forelimbCS). When the glucose consumption in these regions was compared to the corresponding regions of the control monkeys all increases were over 40% and statistically significant (Table 7; %RD/C, %RL_f/F, %RL/S_o). When they were compared to the equivalent regions in the ipsilateral hemispheres all increases were over 25% and statistically significant (Table 7; %Dif). This fact confirms a major contralateral involvement of both F1 and SI forelimb regions in reaching. The F1 forelimb representation extending in the

lateral convexity demonstrates similar effects with those in the anterior bank of Cs (Figs. 10-12; Table 7, F1-forelimbconv).

As far as the trunk representation is concerned, of interest is the fact that it displayed higher glucose consumption in the reaching monkeys compared to the control ones (Table 7; SI-trunk, F1-trunk, %RD/C, %RL$_f$/F, %RL/S$_o$). These differences were statistically significant and are attributed to postural adjustment during reaching. The absence of any side to side differences is compatible with the fact that during postural adjustments the trunk representation is bilaterally activated in both areas SI and F1.

Finally, the mouth activation in both SI and F1 was not significantly different in any pair of hemispheres of the monkeys receiving liquid reward. Statistically significant differences were found only between the monkeys receiving reward and the C monkey, which did not receive any reward during the experimental period (e.g. Table 7; SI-mouth, F1-mouth, %RD/C)

An interesting feature of the RD map in Figure 19I is the surprisingly broad SI activation. To directly compare its intensity and extent with those in the RL$_f$ map of Figure 19G we subtracted the latter from the former map. The result of the subtraction (Fig. 20C) confirms that in the RD monkey somatosensory activation is higher than in the RL$_f$ monkey. Similar was the result obtained from the RL monkey, after subtraction of Figure 19E from Figure 19I map. These data indicate that during reaching in the dark, when no visual information is available to guide the forelimb, processing of somatosensory input is enhanced. This enhancement could be used as a compensatory mechanism to the absence of visual information, in order to accurately guide reaching.
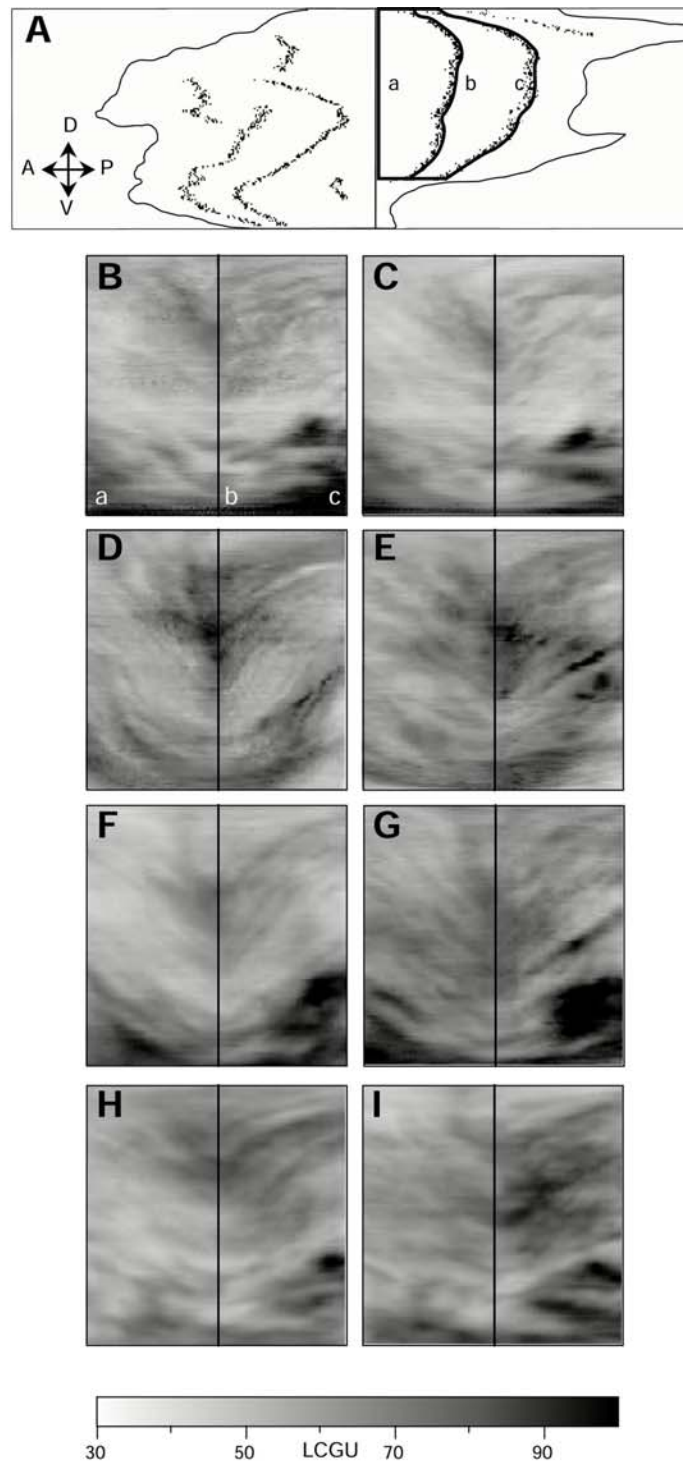
Figure 19. Activations within the Cs induced by reaching. (A) The outlined area on the 2D schematic map indicates the borders of the area transformed and shown in (B)-(I). Line a corresponds to the anterior crown of Cs; line b corresponds to the fundus of Cs; line c corresponds to the posterior crown of Cs. (B) The 2D spatial reconstruction of the LCGU values (μmol/100g/min) of metabolic activity in the transformed map of the left Cs of the fixating monkey. Letters a-c indicate the same landmarks in both A and B. (C) The 2D transformed map of metabolic activity in the right Cs of the fixating monkey. (D) The 2D transformed map of metabolic activity in the Cs ipsilateral to the moving forelimb in the monkey performing visually guided reaching. (E) The 2D transformed map of metabolic activity in the Cs contralateral to the moving forelimb in the monkey performing visually guided reaching. (F) The 2D transformed map of metabolic activity in the Cs ipsilateral to the moving forelimb in the monkey performing visually guided reaching during fixation. (G) The 2D transformed map of metabolic activity in the Cs contralateral to the moving forelimb of the monkey performing visually guided reaching during fixation. (H) The 2D transformed map of metabolic activity in the Cs ipsilateral to the moving forelimb in the monkey performing reaching in the dark. (I) The 2D transformed map of metabolic activity in the Cs contralateral to the moving forelimb in the monkey performing reaching in the dark.
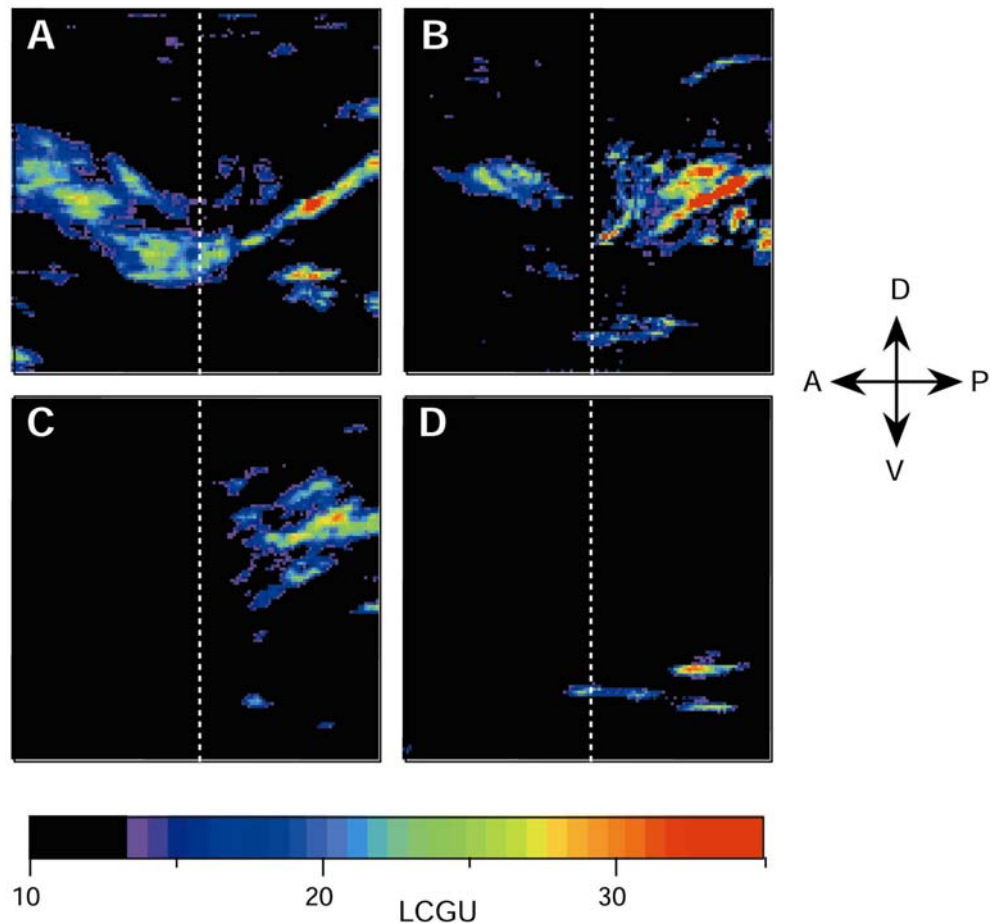
Figure 20. Subregions within the Cs activated during reaching. (A) Map generated after subtracting the cortical activity in the Cs ipsilateral to the moving forelimb in the monkey reaching in the light during fixation (Fig. 19F) from the one in the Cs contralateral to the moving forelimb in the same monkey (Fig. 19G), to illustrate the forelimb representation within the Cs. (B) Map generated after subtracting the cortical activity in the Cs ipsilateral to the moving forelimb in the monkey reaching in the light (Fig. 19D) from that in the Cs contralateral to the moving forelimb in the same monkey (Fig. 19E), to illustrate the forelimb representation within the Cs in a second animal. (C) Map generated after subtracting the cortical activity in the Cs contralateral to the moving forelimb in the monkey reaching in the light during fixation (Fig. 19G) from that in the Cs contralateral to the moving forelimb in the monkey reaching in the dark (Fig. 19I), to illustrate the enhanced somatosensory activation during reaching in the dark. (D) Map generated after subtracting the cortical activity in the left Cs of the fixating monkey (Fig. 19B) from the one in right Cs of the same monkey (Fig. 19C). Colour bar indicates the difference in local cerebral glucose utilization (LCGUdif).

In summary, during reaching the forelimb representation in both F1 and SI was found to be markedly activated in the hemisphere contralateral to the moving forelimb. This activation was illustrated within the Cs and also extended in the lateral convexity. The trunk representation was also activated, dorsally within the Cs, in both hemispheres of the reaching monkeys. The activation of the trunk representation is due to postural adjustments made during reaching with the forelimb. Finally, the mouth representation was activated bilaterally in all monkeys receiving reward during the experimental period as compared to the nonrewarded control monkey.

Table 7
Metabolic effects in subregions of the Cs

AREA (n)	C	RD				F			RL$_f$				S$_o$	RL			
		Ipsi	Contra	%Dif	%RD/C	Left	Right	%Dif	Ipsi	Contra	%Dif	%RL/F		Ipsi	Contra	%Dif	%RL/S$_o$
SI-mouth	57±5 (38)	88±5 (38)	89±3 (43)	1	56*	92±6 (36)	89±5 (39)	-3	92±3 (37)	98±6 (52)	7	10*	87±4 (42)	82±5 (28)	88±5 (41)	7	1
SI-trunk	63±3 (40)	74±2 (39)	74±5 (34)	0	19*	66±2 (36)	64±2 (36)	-4	70±4 (42)	74±2 (25)	6	16*	65±1 (36)	75±9 (48)	77±4 (41)	3	19*
SI-forelimb	49±2 (33)	68±1 (25)	85±2 (27)	25*	75*	54±7 (33)	53±4 (34)	-2	63±3 (35)	80±4 (23)	27*	51*	56±3 (35)	62±4 (34)	82±6 (44)	32*	47*
F1-mouth	52±3 (27)	73±2 (22)	70±2 (12)	-3	35*	76±4 (29)	74±3 (29)	-2	74±3 (13)	77±4 (9)	4	3	71±1 (11)	76±2 (21)	76±2 (13)	-1	6
F1-trunk	44±1 (35)	59±2 (36)	56±3 (31)	-5	27*	52±2 (32)	50±2 (33)	-4	53±3 (56)	56±3 (27)	6	13*	53±3 (29)	60±3 (39)	61±1 (31)	2	16*
F1-forelimbCS	45±1 (27)	51±1 (38)	68±2 (37)	32*	49*	51±3 (31)	51±1 (28)	0	52±2 (34)	73±2 (22)	40*	43*	50±1 (35)	58±2 (24)	76±2 (23)	32*	51*
F1-forelimbconv	44±2 (30)	52±1 (35)	63±1 (35)	21*	44*	50±3 (29)	51±2 (26)	2	49±3 (26)	68±4 (26)	39*	34*	49±1 (35)	53±3 (25)	62±3 (27)	17*	28*

All conventions as in Table 4.

Activated regions within the mesial motor cortex

Two dimensional reconstruction of the spatio-intensive pattern of metabolic activity (LCGU) within the rostrocaudal and the dorsoventral extent of the mesial cortex including the mesial surface and the cortex buried within the cingulate sulcus (Cgs) was generated in each hemisphere, as described in the methods section. LCGU values were measured pixel by pixel (resolution 65 μm/pixel) along a line parallel to the surface of the cortex, as shown in Figure 21B. Each data array, was aligned with the arrays obtained from adjacent horizontal sections (the total of about 650 sections of 20 μm thickness). The posterior tip of the Cgs was used for the alignment of adjacent data arrays (point c in Figure 21B, and line c in Figure 21A). Thus, the dorsal bank of the Cgs is represented on the left and the ventral bank on the right of the reconstructed maps (Figs. 21-23). The ventral border of the gray matter in the lower part of the maps corresponds to the fundus of the Cgs. The plotting resolution of both the caudorostral and the dorsoventral dimensions was 100 μm. Accordingly, each horizontal line at a given dorsoventral level on the metabolic maps (Fig. 22) represents the distribution of the average activity along the anteroposterior dimension in five serial sections. Maps corresponding to left hemispheres are shown after reflection so that the anterior tip of the hemisphere (point a) is always shown to the left.

The different cytoarchitectonic subdivisions of the mesial frontal cortex were identified on Nissl stained horizontal brain sections of the monkeys used on the basis of the known cytoarchitectonic differences (Matelli et al., 1991). Because the horizontal plane of sectioning is parallel to the Cgs, identification of the cytoarchitectonically distinct cingulate motor areas was not possible. We will therefore show only the borders separating areas SI, F1, F3 and F6 on the mesial surface, and will rely on the data from the literature to estimate the location of cingulate motor areas 23 and 24. Area F1 on the mesial surface displays the same cytoarchitectonic characteristics with the ones described for F1 on the lateral convexity. In summary, it is characterized by low cellular density in lower layer III, poor lamination and prominent giant pyramidal cells in layer V. Caudal to area F1 lies area SI with a clear granular recipient layer IV. Rostral to F1, area F3 is poorly laminated like F1, with an increasing cellular density in lower layer III which fuses with upper layer V. Scattered giant pyramidal cells in layer Vb are present only in the caudal part of area F3 toward its border with F1. More rostrally located, area F6 is clearly laminated, unlike areas F1 and F3, and has a prominent layer V which distinguishes it from F3.

The 2D metabolic maps of representative hemispheres of the monkeys used are shown in Figure 22. Activated regions are evident in the dorso-rostral part of area F3 where an orofacial representation has been described (Luppino et al., 1991). This can be easily identified in the dorso-rostral edge of the map of the F monkey (Fig. 22A). In the same map additional activations are evident in area SI and in the rostral part of the dorsal bank of the Cgs. Similar is the picture obtained from the S_o monkey (map not shown).

Compared to the control cases, the maps of the hemispheres contralateral to the moving forelimb in the reaching monkeys show an additional activation zone within F3, which runs obliquely from dorso-rostral to ventro-caudal as a continuation of the rostrally located orofacial activation (Figs. 22C, D, E). This band corresponds, both in location and direction, to the described forelimb representation in F3 (Luppino et al., 1991). This band is absent in the maps of the hemispheres ipsilateral to the moving forelimb (e.g. Fig. 22B) and displays significantly higher glucose consumption in the contralateral hemispheres compared to the ipsilateral ones on the reaching monkeys (Table 8; F3-forelimb %Dif RD, RL_f, RL). This fact demonstrates that during reaching the forelimb representation in F3 is activated mainly contralaterally to the moving forelimb.

To further evaluate the effects induced by reaching we subtracted the maps corresponding to the F, S_o, and C monkeys from the maps of RL_f, RL and RD monkeys, respectively. The caudal tip and the crowns of the Cgs were used as points of alignment for the subtractions. An oblique band in the rostral part of F3 is visible in all three subtraction maps (Fig. 23). This band corresponds to the forelimb representation in F3 as it has been described on the basis of microstimulation and anatomical data (Luppino et al., 1991; Luppino et al., 1993). The glucose consumption within this band in our study

was significantly higher in the contralateral hemispheres of the reaching monkeys as compared to the control ones (Table 8; F3-forelimb %RD/C, %RL$_f$/F, %RL/S$_o$).

Furthermore, below area F3 there are significant activations located in the dorsal bank (Fig. 23 left half of the reconstructed maps, below the dotted line) as well as in the corresponding locations of the ventral bank of the Cgs (mirror image site in the right half of the map). Although histological identification of the area including the latter activation was not possible on the basis of its cytoarchitectonic characteristics, its location with respect to areas F3 and F6 indicates that it corresponds to area 24 and possibly to its caudal part, area 24d. Area 24d is situated around the fundus of the Cgs in both the dorsal and the ventral bank of the sulcus. Quantitative comparison of the glucose consumption values within the dorsal and the ventral bank of the Cgs in the reaching monkeys with those in the equivalent regions of their control monkeys demonstrated statistically significant differences, only in the dorsal bank (Table 8; 24-dorsalbank, %RD/C, %RL$_f$/F, %RL/S$_o$). This activation is bilateral since no significant side to side differences were found in the reaching monkeys. The part of area 24 lying in the ventral bank displayed increased activation in the contralateral hemispheres of the monkeys reaching in the light by 11% as compared to the control cases (Table 8; 24-ventral bank, %RL$_f$/F, %RL/S$_o$).

Finally, activation foci are also evident within SI and in a circumscribed region in the ventral bank of the Cgs toward the fundus of the sulcus and next to the line of alignment (Fig. 23A and B). This activation seems to be within the limits of granular area 23. No significant activations were induced in area F6 by the tasks used in the present study.
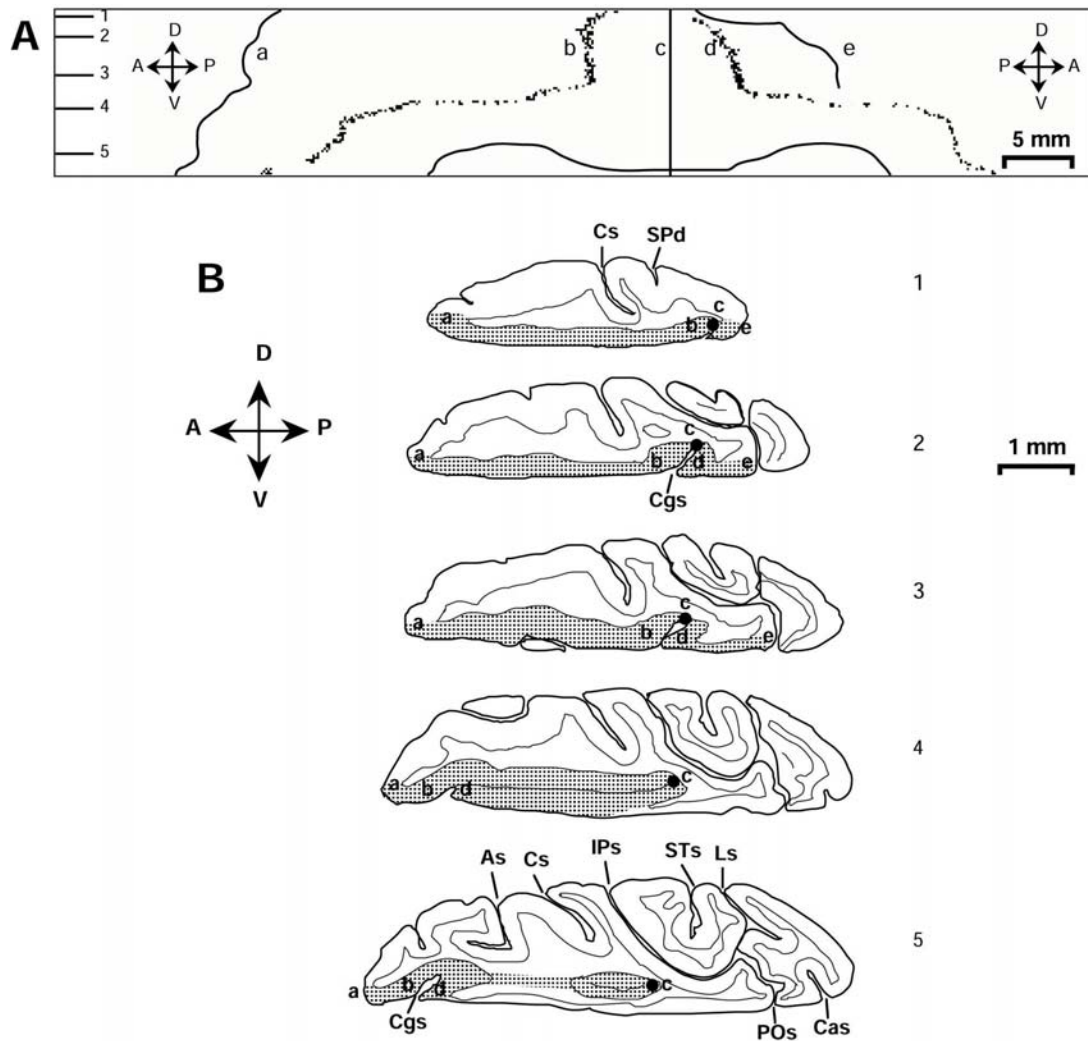
Figure 21. Reconstruction of the mesial surface and cingulate motor areas (A) Schematic representation of 2D maps. Line c corresponds to the posterior tip of Cgs which was used for alignment of adjacent sections; line a corresponds to the rostralmost tip of each horizontral section; line b corresponds to the anterior (dorsal) crown of Cgs; line d corresponds to the posterior (ventral) crown of Cgs; line e corresponds to the posterior end of the measurement on the mesial surface of the dorsal sections. Lines 1-5 on the right part of the figure indicate the approximate dorsoventral location of the sections shown in B. (B) Schematic representations of five horizontal sections through the right hemisphere of a monkey brain at different dorsoventral levels (top corresponds to dorsal and bottom to ventral sections). The shaded areas outline the cortical region measured and unfolded in the reconstruction maps. The solid circle (c) within the shaded area indicates the point of alignment of adjacent sections, which corresponds to the posterior tip of Cgs. Letters a-e indicate the same landmarks in both A and B. As, arcuate sulcus; Cas, calcarine sulcus; Cgs, cingulate sulcus; Cs, central sulcus; IPs, intraparietal sulcus; Ls, lunate sulcus; POs, parietoccipital sulcus; SPd, superior precentral dimple;STs, superior temporal sulcus.
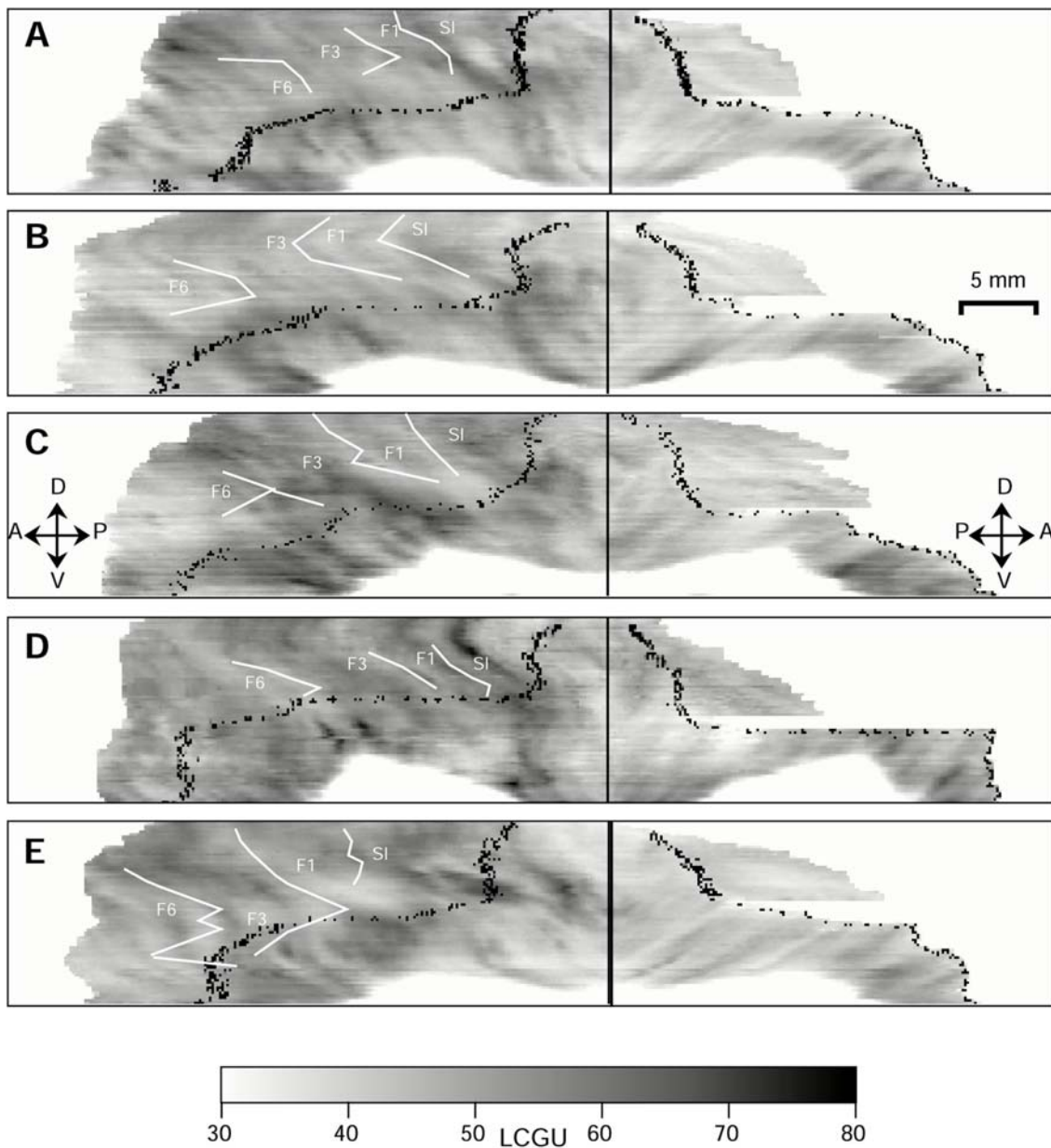
Figure 22. Activations in the mesial surface and the cortex within the Cgs induced by visual fixation and forelimb reaching. (A) The 2D spatial reconstruction of the LCGU values (μmol/100g/min) of metabolic activity in the right hemisphere of the fixating monkey. (B) The 2D map of metabolic activity in the hemisphere ipsilateral to the moving forelimb in the monkey performing visually guided reaching under fixation. (C) The 2D map of metabolic activity in the hemisphere contralateral to the moving forelimb in the monkey performing visually guided reaching during fixation. (D) The 2D map of metabolic activity in the hemisphere contralateral to the moving forelimb in the monkey performing visually guided reaching. (E) The 2D map of metabolic activity in the hemisphere contralateral to the moving forelimb in the monkey performing reaching in the dark. White lines indicate the borders of the cytoarchitectonically distinct subregions of the mesial cortex. Other conventions as in Figure 21.
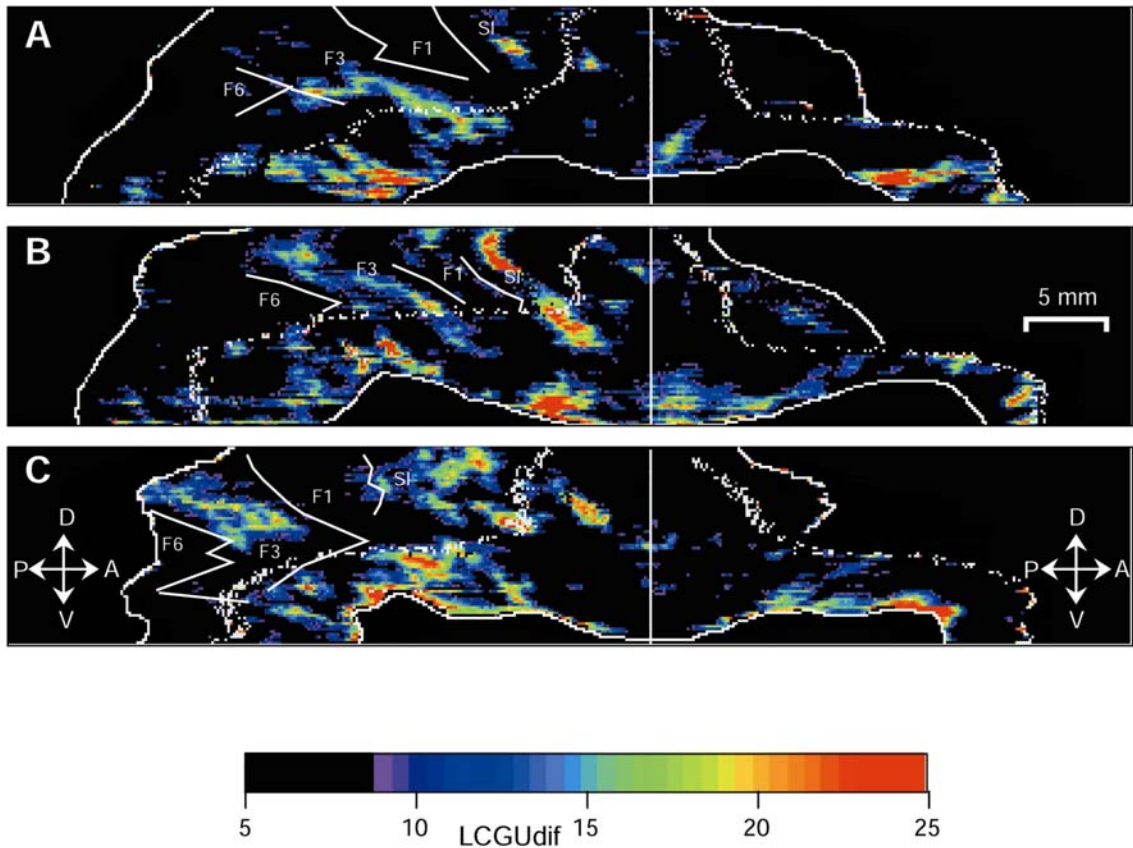
Figure 23. Subregions of the mesial cortex activated during reaching. (A) Map generated after subtracting the cortical activity in the right hemisphere of the fixating monkey (Fig. 22A) from the one in the contralateral to the moving forelimb hemisphere of the monkey reaching in the light under fixation (Fig. 22C). (B) Map generated after subtracting the cortical activity in the right hemisphere of the saccading monkey from that in the hemisphere contralateral to the moving forelimb in the monkey reaching in the light (Fig. 22D). (C) Map generated after subtracting the cortical activity in the right hemisphere of the untrained control monkey from that in the hemisphere contralateral to the moving forelimb in the monkey reaching in the dark (Fig. 22E). Colour bar indicates the difference in local cerebral glucose utilization (LCGUdif). Other conventions as in Figure 21.

Table 8

Metabolic effects in subregions of the mesial surface and the Cgs

AREA (n)	C	RD Ipsi	Contra	%Dif	%RD/C	F Right	RL_f Ipsi	Contra	%Dif	%RL/F	S_o	RL Ipsi	Contra	%Dif	%RL/S_o
F3-orofacial	46±2	61±3	60±2	-2	30*	59±2	53±1	58±3	9	-2	53±2	58±2	58±1	0	9
	(22)	(20)	(24)			(26)	(17)	(30)			(21)	(16)	(19)		
F3-forelimb	43±1	51±2	58±2	12*	35*	50±2	50±2	64±1	28*	28*	45±2	52±2	58±2	12*	29*
	(24)	(20)	(21)			(27)	(23)	(25)			(24)	(26)	(22)		
F3-unaffected	45±1	49±1	48±1	-2	7	46±1	44±1	47±2	7	2	47±1	47±1	50±1	6	6
	(11)	(11)	(23)			(11)	(16)	(20)			(20)	(11)	(14)		
F6	44±1	46±2	49±1	7	11	49±1	44±2	48±3	9	-4	51±2	43±2	47±1	9	-8
	(17)	(16)	(19)			(31)	(17)	(21)			(17)	(18)	(14)		
24-dorsalbank	46±4	55±3	56±2	2	22*	51±4	54±2	59±4	9	16*	47±2	55±4	56±2	2	19*
	(49)	(50)	(53)			(48)	(49)	(48)			(49)	(48)	(69)		
24-ventralbank	46±4	50±4	47±3	-6	2	47±4	49±2	52±7	6	11*	47±5	51±7	52±4	2	11*
	(41)	(48)	(43)			(38)	(35)	(50)			(36)	(39)	(43)		
23	44±6	43±3	43±1	0	-2	41±4	48±5	47±2	-2	15*	38±1	46±3	47±6	2	24*
	(23)	(25)	(29)			(26)	(29)	(27)			(31)	(13)	(35)		

All conventions as in Table 4.

4. DISCUSSION

This study was undertaken to examine the role of specific parietofrontal networks in reaching movements. To this end we employed simple tasks in order to dissociate the different aspects of this rather complex behavior which requires perception of the world surrounding us, orientation toward the targets of our actions and execution of the appropriate actions. We used the [^{14}C]deoxyglucose method to map the metabolic activity in the brain of monkeys performing 1) fixation of a visual target, 2) saccades to visual targets, 3) reaching in the light with the eyes either fixed or free to move and 4) reaching in the dark with the eyes fixed. Our results demonstrate that distinct subregions within the monkey intraparietal and frontal cortices are involved in different aspects of goal directed movements. This is the first time that high resolution maps of the spatial distribution of metabolic activity in the entire intraparietal and frontal cortex have been generated to reveal the specific regions involved in visual fixation, voluntary saccades, reaching in the light, and reaching in the dark.

4.1 THE INTRAPARIETAL CORTEX

Subregions in the lateral bank of IPs involved in fixation and saccades

PSR, a region associated with saccades to visual targets, was found in the lateral bank of IPs. The PSR is located in the rostral sector of 7IP and covers (i) part of area LIP as this has been defined on the basis of single unit recording (Andersen et al., 1990; Barash et al., 1991) and microstimulation (Thier and Andersen, 1996), and (ii) the part of area VIP lying in the lateral bank of IPs close to the fundus (Colby et al., 1993). The activation of PSR in our study during visually guided saccades is consistent with the well established saccadic (Barash et al., 1991; Colby et al., 1996; Thier and Andersen, 1996) and visual (Blatt et al., 1990; Colby et al., 1993; Colby et al., 1996; Thier and Andersen, 1996) properties of areas LIP and VIP. However, the PSR as outlined in the present study, may cover only a part of the saccade related intraparietal area since its activation was induced by single directional (only horizontal) saccades of different amplitudes. Indeed, preliminary observations in our lab indicate that upward saccades to targets on a line inclined by 45 deg with respect to the horizontal plane activate a region which extends caudal to the presently illustrated PSR. In order to reveal the full extent of the saccade related intraparietal area, experiments with execution of saccades of different amplitudes in several directions are required.

PFR, a region associated with fixation of a visual target, was found in the rostral sector of the lateral bank of IPs. The PFR lies in the anterior part of PSR, and posterior to AIP as this has been defined on the basis of neurophysiological and anatomical studies (Sakata et al., 1995; Luppino et al., 1999; Murata et al., 2000). The location of PFR appears to be in register with the recently reported foveal representation in the rostral part of intraparietal area 7 (Ben Hamed et al., 2001). Its activation was consistent in both hemispheres of the monkey performing fixation of a visual target as well as in both hemispheres of the RL monkey. The PFR was also active in the monkey performing sequential horizontal saccades of different amplitudes, whereas it was not active in the control monkey. Because the intensity of the PFR activation varied in the different experimental hemispheres, we used linear regression analysis to examine whether this activation was correlated with certain behavioral parameters. No significant correlations were obtained with (i) the duration of fixation, (ii) the total number of small amplitude (contraversive and ipsiversive) saccades, (iii) the number of small amplitude ipsiversive saccades, (iv) the total number of contraversive (small and large amplitude) saccades, and (v) the percentage of successful trials. Taking into account that only the number of small amplitude contraversive saccades was significantly correlated with the intensity of the PFR activation in the different

hemispheres, we suggest that the PFR activation is associated with the performance of small amplitude contraversive saccades around the point of fixation.

In conclusion, this is the first time that a high resolution map of functional activity induced by visually guided saccades of different amplitudes is generated, and a region related to fixation of a visual target is mapped in the lateral intraparietal area 7.

Subregions in the IPs involved in the visual and somatosensory guidance of reaching

The rostral part of the ventral intraparietal cortex (areas 5VIP-rostral and 7VIP-rostral) in our study largely overlaps with area VIP as this has been defined on the basis of single unit recording (Colby et al., 1993). The present data demonstrate that area 5VIP (including 5VIP-rostral and 5VIP-caudal) is activated by visually guided reaching (Fig. 7B) and not in response to visual stimuli used as targets for saccades (Fig. 6C). Given that cells in area VIP display visual properties (Colby and Duhamel, 1991; Colby et al., 1993), the present finding indicates that visual information in this area is used to guide reaching and not to code target location per se. On the other hand, the activation of area 7VIP during both visually guided forelimb movements (Fig. 7B) and visually guided eye movements (Fig. 6C) indicates that this area encodes visual information about the location of stimuli used as targets for motor acts, whatever the effector employed.

In the reaching tasks, area 5DIP-rostral was activated in the hemisphere contralateral to the moving forelimb in both the RL and RD monkeys. These two monkeys had in common only proprioceptive-somatosensory information available to guide the forelimb. Therefore, the activation of 5DIP-rostral should be attributed to the somatosensory guidance of reaching. Moreover, this activation was higher in the RD monkey, in which only somatosensory (and no visual) information was available to guide the forelimb. The higher activation of area 5DIP-rostral in the RD monkey as compared to that in the RL monkey may act as a compensatory mechanism to the absence of any visual information, in accordance with the findings and suggestion of a previous study (Savaki et al., 1993). The ventral intraparietal cortex (including both 5VIP and 7VIP) was activated mainly in the RL_f monkey, which was the only one with visual information available to guide the forelimb. Therefore, the activation of the ventral intraparietal cortex should be attributed to the visual guidance of reaching. Indeed, a similar activation to that around the fundus of IPs in the RL_f monkey was also observed in the RL monkey. The less lateralized effect in the ventral intraparietal cortex associated with visual processing as compared to that in dorsal intraparietal area 5 associated with somatosensory processing is consistent with previous findings (Colby et al., 1993; Savaki and Dalezios, 1999).

The functional dissociation of the dorsal intraparietal area 5 related to somatosensory guidance of reaching from the ventral intraparietal cortex related to visual guidance proves an earlier hypothesis regarding the differential contribution of IPs cortical subregions in the control of reaching (Savaki et al., 1993; Savaki and Dalezios, 1999). Moreover, this dissociation is consistent with the anatomical data supporting a differential distribution of visual and somatosensory input within the medial bank of the IPs. Area VIP receives visual input from areas MT, MST, FST (Maunsell and Van Essen, 1983; Ungerleider and Desimone, 1986; Boussaoud et al., 1990) and PO (Colby et al., 1988), and projects to the ventral premotor cortex (Luppino et al., 1999). More dorsally located areas within the medial bank of IPs, area MIP and area PEip receive somatosensory input (Pandya and Seltzer, 1982; Pearson and Powell, 1985) and project to the dorsal premotor cortex (Matelli et al., 1998). Area MIP has been described as the middle one-third of the caudal half of the medial bank (Colby et al., 1988; Matelli et al., 1998). Accordingly, area MIP must cover part of our areas 5DIP and 5VIP, a fact consistent with the reported convergence of visual and somatosensory input in this area (Pandya and Seltzer, 1982; Colby et al., 1988; Caminiti et al., 1996). Area PEip occupies the dorsalmost one-third of the caudal half, and the whole rostral part of the medial bank (Matelli et al., 1998), thus overlapping with most of

our area 5DIP-rostral. Two neuronal populations were labeled in PEip following tracer injection in the dorsal premotor F2 arm field (Matelli et al., 1998). These two neuronal populations correspond topographically to subregions 5DIP-rostralmost and 5DIP-medial, which were both markedly activated in our study (Fig. 8A).

Furthermore, the functional dissociation of the dorsal intraparietal area 5 related to somatosensory guidance of reaching from the ventral intraparietal cortex related to visual guidance is complemented by the following electrophysiological data. Many neurons in VIP respond to visual stimuli located in the near extrapersonal space (Duhamel et al., 1998). Area MIP displays a range of properties from purely visual to bimodal to purely somatosensory, as the electrode moves from the fundus to the crown of the medial bank (Colby and Duhamel, 1991). The dorsal intraparietal area 5 responds to somatosensory stimuli (Mountcastle et al., 1975) and controls arm movements (Kalaska et al., 1990). Cells with movement-related activity associated with the execution of reaching are located around the crown of the medial bank of IPs, while cells with set- and signal-related activity associated with the planning of reaching are located deeper in the medial bank (Johnson et al., 1996). Finally, our data are consistent with the results of a lesion study which has demonstrated that removal of the dorsal part of the medial bank causes misreaching in the dark but has little effect on reaching in the light (Rushworth et al., 1997).

In conclusion, quantitative high-resolution maps of functional activity in the intraparietal cortex demonstrate, for the first time, the spatially distinct neuronal populations, which are associated with the visual and the somatosensory guidance of reaching.

4.2. THE MOTOR AND PREMOTOR CORTEX

The premotor cortex has been subdivided into a dorsal and a ventral sector based on cytoarchitectonic (Barbas and Pandya, 1987), immunocytochemical (Matelli et al., 1985), functional (Weinrich and Wise, 1982) and lesion data (Kurata and Hoffman, 1994). Moreover, it has been now established that each of these sectors is comprised by at least two distinct subdivisions. Given the geometrical complexity and the variability of the extent of the various brain areas in different monkeys it would be difficult, if not highly speculative, to attribute the activations in our functional maps to any of these different areas on the basis of anatomical landmarks, such as the crowns and fundus of the relevant sulci. Thus, based on the data of the literature we identified the cytoarchitectonic differences of the various areas in Nissl stained horizontal brain sections of the monkeys used. It was, therefore, feasible to draw the borders of the histologically identified areas on our functional maps and attribute the activations induced by the different behaviors to each of the cytoarchitectonically identified areas.

Furthermore, in order to make direct comparisons possible, we occasionally transformed the 2D unfolded brain areas in a way that isodimensional maps were generated for all hemispheres. This allowed us to make subtractions between different hemispheres and different monkeys and thus to overcome the geometrical irregularities.

Subregions in the anterior bank of the arcuate sulcus involved in fixation, visual processing and saccades
The anterior bank of the As displayed enhanced activation in all hemispheres of the visually stimulated monkeys compared to the untrained control monkey which remained in the dark. This is in accordance with the physiological data coming from this region. The anterior part of the arcuate sulcus belongs to a portion of the FEF, which further extend on the prearcuate cortex. The majority of neurons in the FEF has visual and oculomotor properties (Bruce and

Goldberg, 1985; Bruce et al., 1985) and is therefore expected to respond even to the visual targets used in our tasks for both saccading and fixating monkeys.

Moreover, a region around the fundus of the As, extending into both banks of the sulcus, displayed significantly higher glucose consumption in the hemispheres of the fixating monkeys compared to the untrained control. This region corresponds to the area, which has been described to result in suppression of saccades when microstimulated and which has been suggested to be involved in a fixation process (Burman and Bruce, 1997).

Subregions in the ventral premotor cortex involved in visual processing and reaching.

The ventral premotor cortex is considered to be comprised of at least two areas, F4 and F5. This distinction is based on both anatomical (Matelli et al., 1985; Matelli et al., 1996; Geyer et al., 2000) and functional data (Rizzolatti et al., 1987; Gentilucci et al., 1988). These two areas displayed functional differences, which were revealed by the tasks employed in the present study. More specifically, area F4 was activated in visually stimulated monkeys and in monkeys performing reaching movements. Subtractions of several different maps allowed us to distinguish among subregions associated with different signals. The results of the subtractions demonstrated that within F4 significant visual processing occurs regardless of whether a reaching movement is associated with the visual stimulus. This is in agreement with the reported visual properties of neurons in F4 (Gentilucci et al., 1988; Fogassi et al., 1996; Graziano et al., 1997; Graziano and Gross, 1998). These studies suggest that 3D objects and moving stimuli are necessary to elicit visual responses from area F4 neurons. However, visual responses to spots of light have also been reported (Boussaoud et al., 1993).

Moreover, significant activation in F4 was found in all reaching monkeys, including the monkey reaching in the dark. Given the absence of visual stimulation in the latter case, this activation demonstrates that area F4 is involved in reaching under somatosensory guidance. It should be noted that somatosensory stimulation during reaching could not be dissociated from the motor act of reaching. Somatosensory responses are dominant in area F4. More than 80% of the neurons in area F4 respond to somatosensory (mainly tactile) stimuli (Gentilucci et al., 1988; Fogassi et al., 1996; Graziano et al., 1997). In addition to the tactile responses, proprioceptive and deep responses are evoked by trunk and arm stimulation in area F4 (Fogassi et al., 1996; Graziano et al., 1997; Graziano, 1999). Thus, somatosensory stimulation of the trunk and the moving forelimb could activate area F4 during reaching. Furthermore, there is evidence that area F4 is directly linked to the movement itself. Intracortical microstimulation evokes movements of the forelimb at low thresholds (Gentilucci et al., 1988; Godshalk et al., 1995), and neuronal responses during reaching movements have been recorded in one study (Gentilucci et al., 1988). Our finding is also compatible with anatomical studies demonstrating that the forelimb field of F4 is directly connected to the forelimb representation of F1 and also to the spinal cord (Dum and Strick, 1991; He et al., 1993). Finally, the auditory responses recorded from few neurons in area F4 (Graziano et al., 1997; Graziano and Gandhi, 2000) may contribute to the activation observed in the monkey reaching in the dark, which used auditory cues as go-signals.

In contrast to area F4, area F5 was activated only in the reaching monkeys and is therefore not related to purely visual processing. Activation was moderate in the case of the monkey reaching in the dark and was confined within the posterior bank of the As. On the contrary, the activation was intense in the case of the monkeys reaching in the light. The result of the subtractions suggests that F5 neurons in the posterior bank of As and on the lateral convexity, around the posterior crown of As, are involved in the visual guidance of reaching. Thus, our data indicate that area F5 is mainly involved in the visual guidance of reaching movements and is less associated with reaching performed under somatosensory guidance. In contrast, area F4 is mainly associated with reaching under somatosensory guidance.

The results in F5 are supported by several reports in the literature. The motor role of F5 neurons is supported by anatomical data demonstrating the direct projections of area F5 to the spinal cord (He et al., 1993) and to the primary motor cortex (Matelli et al., 1986). Moreover, the activated band, which runs from the caudomedial to the rostrolateral part of F5 in the monkeys reaching in the light, resembles the pattern of corticospinal neurons labeled in the ventral premotor cortex after injections in the cervical segments of the spinal cord (Dum and Strick, 1991). Corticospinal neurons around the As tended to shift from a more superficial position in the sulcus at caudomedial levels, to the depths of the sulcus at more rostrolateral levels. Furthermore, neurons in F5 fire in response to reaching movements although these responses are rare compared to the ones during grasping (Rizzolatti et al., 1987; Rizzolatti et al., 1988). The fact that somatosensory stimuli activate F5 neurons (Rizzolatti et al., 1988) could contribute to the moderate activation observed in the monkey reaching in the dark. Our results are also compatible with the reports that about half of the reaching neurons can be activated by visual stimuli (Rizzolatti et al., 1988), that neurons within F5 have visuomotor properties (Murata et al., 1997) and that F5 plays a role in space coding (Schieber, 2000; Fogassi et al., 2001).

Given that area F5 has traditionally been implicated in the control of distal movements, it cannot be excluded that part of the activation observed in this study is due to the involvement of distal together with proximal parts of the forelimb in the reaching movement. However, the consistent F5 activation in all animals performing reaching movements regardless of the distal configuration used in the different tasks of the present study, indicates that the activated F5 region reflects a population of cells related to reaching rather than grasping.

Subregions in the dorsal premotor cortex involved in visual and somatosensory guidance of reaching

The dorsal premotor cortex is comprised of two distinct areas, area F2 and F7 (Matelli et al., 1991). No significant activations were observed within F7 in the present study. Although movement-related responses have been described in F7 (di Pellegrino and Wise, 1991) this area does not send direct projections neither to the primary motor cortex (Barbas and Pandya, 1987; Luppino et al., 1990) nor to the cervical segments of the spinal cord (Keizer and Kuyepers, 1989). The part of F7 corresponding to the SEF (Schlag and Schlag-Rey, 1985; Schlag and Schlag-Rey, 1987) may have been missed with the sampling procedure of the present study, and will be considered separately.

Area F2 was activated in our study contralateral to the moving forelimb in the reaching monkeys. The involvement of F2 in reaching has been extensively described in the literature. More specifically, a forelimb representation has been demonstrated below the superior precentral dimple on the basis of recording experiments (Weinrich and Wise, 1982; Kurata and Tanji, 1986; Kurata, 1989; Caminiti et al., 1990), microstimulation studies (Godshalk et al., 1995) and anatomical data (Dum and Strick, 1991; He et al., 1993). The activity of F2 neurons has been shown to be broadly tuned to the direction of movement (Georgopoulos et al., 1982; Georgopoulos et al., 1988; Caminiti et al., 1990; Caminiti et al., 1991).

In our study we employed tasks, which aimed to elucidate the role of F2 in reaching under visual and under somatosensory guidance. The results of the comparison between monkeys reaching in the light and reaching in the dark demonstrate that within F2 there are two segregated populations related either to the visual or to the somatosensory guidance of movement. Specifically, the monkeys performing reaching in the light, which had both visual and somatosensory information available to guide the forelimb, displayed two activated regions within F2; the first one lying ventrally and close to the As (also extending in the floor of the sulcus) and the second one located more dorsally and caudally, just below the superior precentral dimple. On the contrary, the monkey reaching in the dark, which had only somatosensory information available to guide the forelimb, displayed activations only in the region below the

superior precentral dimple. These results suggest that the dorsocaudal F2 region, below the superior precentral dimple, is mainly involved in reaching under somatosensory guidance, whereas the ventrorostral F2 region close to the As is involved in the visual guidance of reaching.

The functional dissociation of F2 into a dorsocaudal region related to somatosensorily guided reaching and a ventrorostral region related to visually guided reaching is supported by anatomical data. It has been shown that the dimple region of F2 receives projections from the parietal area PEip which processes mainly somatosensory information (Matelli et al., 1998), whereas the ventrorostral part of F2 receives projections from parietal area MIP which conveys mainly visual information (Matelli et al., 1998). Moreover, proprioceptive responses were recorded recently from neurons in F2 and visual neurons were found in the rostrolateral sector of the forelimb representation of F2 (Fogassi et al., 1999).

The dissociation of a ventrorostral part of F2 involved in reaching under visual guidance from a dorsocaudal part involved in reaching under somatosensory guidance complements the equivalent dissociation demonstrated in the intraparietal cortex. Within the medial bank of IPs we demonstrated that its dorsal and rostral part (5DIP) is mainly involved in the somatosensory guidance of movement. This region of IPs together with the dorsocaudal F2 share reciprocal connections forming a parieto-frontal network associated with somatosensory guidance of reaching movements. Moreover, more ventrally within the medial bank of IPs, the ventral part of area MIP, was activated during visually guided reaching. This area and the ventrorostral F2 are anatomically connected forming a different parietofrontal network which is associated with visual guidance of reaching movements. In conclusion, the present data illustrate for the first time in high-resolution functional maps the differential contributions of distinct F2 subregions in reaching.

Subregions within the central sulcus involved in reaching

The two dimensional reconstruction of the metabolic activity pattern within the unfolded central sulcus showed significant side-to-side differences in the forelimb representation of the reaching animals in both areas F1 and SI. Comparison of our maps with preexisting functional maps of the representation of the different body parts within the Cs (Woolsey et al., 1952; Woolsey, 1958) showed that the trunk representation is activated bilaterally in the reaching animals. This fact is consistent with previous data (Dalezios et al., 1996; Savaki et al., 1997). The lower trunk activation during reaching is attributed to postural adjustment during the forelimb movement, while the bilateral mouth activation is due to the liquid uptake after completion of successful trials. The largely unilateral activation of the forelimb representation reflects control of the reaching movement mainly by the contralateral F1 in accordance to previous findings and suggestions (Savaki et al., 1993; Dalezios et al., 1996). The symmetrical activation of the forelimb representation revealed in the subtraction maps is also in agreement with the somatotopic pattern of the Woolsey's homunculus. According to that the representation of body movements within the primary motor cortex is a mirror image of the sensory representation of the body in the primary somatosensory cortex.

An interesting finding was the enhanced activation observed in the somatosensory cortex of the monkey reaching in the dark. This activation included mainly the SI forelimb representation and part of the upper trunk representation. This activation is attributed to the increased sensitivity to somatosensory input due to the absence of visual input, which is mainly used to guide the movement under normal conditions. When no visual input is available somatosensory processing may be enhanced in order to guide the forelimb accurately. This finding in the Cs is equivalent to that reported in the IPs. In the IPs we found that areas involved in the somatosensory guidance of movement displayed enhanced activation in the monkey reaching in the dark as compared to the monkey reaching in the light.

Subregions within the mesial cortex involved in reaching

The mesial frontal cortex is comprised of areas F1, F3 and F6 on the mesial wall and the dorsal bank of the Cgs and areas 23, 24c and 24d within the Cgs (Matelli et al., 1991). We identified the different areas on the mesial wall based on their distinct cytoarchitectonic characteristics on the Nissl stained horizontal sections. The most striking activation in the 2D metabolic maps of the unfolded Cgs and mesial wall in the present study was a band spanning the rostral part of F3, running from rostrodorsal to caudoventral. This band was present in the hemisphere contralateral to the moving forelimb of all reaching animals. Its position within F3 fits well with the representation of the forelimb, which has been described on the basis of microstimulation and anatomical data (Mitz and Wise, 1987; Luppino et al., 1991; Luppino et al., 1993; Luppino et al., 1994; He et al., 1995). Activation within this forelimb representation displayed significant side-to-side differences. In the somatotopic map of F3, caudal to the forelimb representation, lies the hindlimb representation, which did not display significant activation in our study. Moreover, a restricted activation in the rostralmost part of F3 illustrated in our maps corresponds to the orofacial representation of F3 (Mitz and Wise, 1987; Luppino et al., 1991; Luppino et al., 1994) and displays bilateral activation in all monkeys receiving reward during the experiment. This activation was statistically significant when compared to the untrained control, which received no reward throughout the experiment.

Area F3 together with area F6 have been implicated in the execution of sequences of movements (Tanji and Shima, 1994; Tanji et al., 1996; Picard and Strick, 1997) and in memorized motor tasks (Mushiake et al., 1991; Picard and Strick, 1997). The present study, however, shows that the forelimb representation in F3 is strongly activated during simple, single directional reaching movements performed either under visual guidance or under somatosensory guidance. This result is in agreement with the reported somatosensory properties of F3 neurons (Matsuzaka et al., 1992; Rizzolatti et al., 1996). Moreover, it is in agreement with the motor properties of this area. Most F3 neurons discharge in association with active movements and the discharge onset is typically time-locked to the movement onset (Alexander and Crutcher, 1990; Matsuzaka et al., 1992).

The anatomical data also support the activation of area F3 during reaching. F3 receives somatotopically organized projections from somatosensory areas SII, PEci, PE and cingulate area 23 (Petrides and Pandya, 1984; Luppino et al., 1993). Cortical afferents to area F3 originate also from areas F2, F4, F5, F6 and F7 (Luppino et al., 1993). Moreover, area F3 is directly connected to F1, and has descending corticospinal and corticobulbar connections. The caudal part of F3 projects to the thoracolumbar segments, whereas the rostral part to the cervicothoracic segments of the spinal cord (Keizer and Kuyepers, 1989; Luppino et al., 1994; He et al., 1995).

No significant differences in activation were found within areas F6, same way as in area F7. Both these areas are connected with the prefrontal cortex and are thought to exert a control action upon movements (Rizzolatti et al., 1990; Rizzolatti and Luppino, 2001). Their exact role in reaching is not very clear and apparently, more complex tasks are required to establish their role.

Within the cingulate sulcus, significant activations were found in the dorsal bank of the Cgs of the reaching monkeys, in a part corresponding to area 24 (Matelli et al., 1991). Unfortunately, the plane of sectioning did not allow us to histologically identify area 24 with its different subdivisions. Area 24, in the dorsal bank of the Cgs, displayed bilateral activations, which were significantly higher, compared to the control cases. Increased activation was also seen in the same area on the ventral bank, in the reaching in the light animals. The activation of area 24 in our study complements the described forelimb representations in area 24 (Luppino et al., 1991) and its anatomical connections with areas F1, F3 and the spinal cord (Luppino et al., 1993; Luppino et al., 1994; He et al., 1995). The dorsal bank of the Cgs (named CMAd) was

reported to be activated during the performance of a remembered sequence of movements (Picard and Strick, 1997). The results presented here indicate that this area is activated even during simple reaching movements performed either in the light or in the dark.

Finally, an activated region within the ventral bank located posteriorly and close to the fundus of the Cgs was evident in the reaching in the light monkeys. We believe that this activation, which was statistically significant as compared to the control, belongs to granular area 23. This part of area 23 at the border with area 24 is connected to the F3 arm field (Luppino et al., 1993) and also projects to the cervical segments of the spinal cord (Luppino et al., 1994). Although there are not many functional data in the literature to support area's 23 involvement in reaching, the converging evidence seem to establish such a role at least for that part of area 23 which lies in the ventral bank, close the fundus, at the border with area 24d.

4.3. CONCLUSION

Areas SI, F1, F3, and 24 were found to be involved in reaching movements under both visual and somatosensory guidance. In contrast, specific populations within the intraparietal and the ventral premotor cortex were found to be preferentially involved in reaching under either visual or somatosensory guidance. Area 5DIP, in the dorsal part of the medial bank of the intraparietal sulcus, the part of area F2 lying rather dorsally close to the superior precentral dimple, area F4 and the part of area F5 lying on the posterior bank of the arcuate sulcus are part of a network which controls reaching movements under somatosensory guidance. On the other hand, the ventral part of the intraparietal cortex corresponding to areas 5VIP and 7VIP, the part of area F2 which lies rather ventrally close to the arcuate sulcus, the part of area F5 around the posterior crown of the arcuate sulcus and area 23 are part of a network which controls reaching movements under visual guidance.

Overall, although neurophysiological studies indicate that neurons in most association cortical regions, such as the intraparietal cortex, display multimodal properties (processing visual, tactile, proprioceptive, acoustic signals etc.), our imaging method demonstrates that at the population level specific functions can predominantly be attributed to these regions.

FUNCTIONAL MAPPING OF THE MONKEY PARIETO-FRONTAL CIRCUITS INVOLVED IN THE VISUAL AND SOMATOSENSORY GUIDANCE OF REACHING MOVEMENTS.
A quantitative autoradiographic study using the [^{14}C]-2-deoxyglucose method

Laboratory of Functional Brain Imaging, Department of Basic Sciences, Division of Medicine, School of Health Sciences, University of Crete.

ABSTRACT

The functional activity of the intraparietal, agranular frontal and mesial motor cortex was mapped with the [^{14}C]deoxyglucose method in one untrained control monkey and in six monkeys performing (i) fixation of a central visual target, (ii) saccades to visual targets, (iii) reaching in the light during fixation of a central visual target or without fixation, and (iv) acoustically triggered reaching in the dark while the eyes maintained a straight ahead direction. In the intraparietal sulcus different subregions of the intraparietal cortical area 7 were activated by fixation, saccades to visual targets, and acoustically triggered reaching in the dark. A region associated with fixation was revealed within the rostral part of the lateral bank of the intraparietal sulcus. The saccade related region covered almost the entire dorsoventral extent of the lateral bank in the rostral sector of intraparietal area 7. Subregions in the ventral part of the intraparietal cortex (around the fundus of the intraparietal sulcus) were activated only during reaching in the light, in which case visual information was available to guide the moving forelimb. In contrast, subregions in the dorsal part of the intraparietal cortical area 5 were activated during both reaching in the light and reaching in the dark, in which cases somatosensory information was the only one available in common. Activation in the dorsal intraparietal area 5 was enhanced in the monkey reaching in the dark probably acting as a compensatory mechanism to the absence of visual input to guide the forelimb. We conclude that within the intraparietal sulcus visual guidance of reaching is associated with the ventral intraparietal cortex, whereas somatosensory guidance, based on proprioceptive information about the current forelimb position, is associated with the dorsal intraparietal area 5.

In the premotor cortex, dorsal premotor area F2 was activated contralateral to the moving forelimb in the reaching monkeys. The dorsocaudal-F2 subregion, below the superior precentral dimple, was activated in reaching under both visual and somatosensory guidance. A different subregion, the ventrorostral-F2, close to the arcuate sulcus and within its floor, was activated only in the monkeys reaching in the light. Thus, the dimple region of F2 is involved in reaching under somatosensory guidance whereas the arcuate sulcus region of F2 is involved in reaching under visual guidance. In the ventral premotor cortex, caudally located area F4 was activated in all visually stimulated and reaching monkeys. Subtractions of the maps corresponding to the different cases showed that area F4 is involved in visual processing and in reaching under somatosensory guidance. On the contrary, the rostrally located area F5 was not activated during visual processing in the absence of movement and showed only moderate activations (within the posterior bank of the arcuate sulcus) during reaching in the dark. However, area F5 displayed significant activations in the monkey reaching in the light in both the posterior bank of the arcuate sulcus and the lateral convexity close to the posterior crown of the arcuate sulcus. Thus, within the ventral premotor cortex area F4 is mainly involved in reaching under somatosensory guidance whereas area F5 is mainly involved in reaching under visual guidance.

In the anterior bank of the arcuate sulcus, which is part of the frontal eye fields, the cortical center that controls eye movements, metabolic activity was increased in all visually stimulated monkeys. Moreover, a region around the fundus of the arcuate sulcus extending to

both banks was activated in all hemispheres of fixating monkeys and is related to fixation of visual targets.

Within the central sulcus bilateral activations of the trunk representation in both the primary somatosensory and motor cortex were observed in all reaching monkeys as a result of postural adjustment during the forelimb movement. Bilateral activation of the mouth representation in the central sulcus was related to licking during rewarded trials. The forelimb representation was symmetrically activated within the central sulcus in the hemisphere contralateral to the moving forelimb of the reaching monkeys. The activation of the primary somatosensory forelimb representation in the monkey reaching in the dark was higher as compared to the reaching in the light monkeys. This enhancement of somatosensory processing, when no visual information is available to guide the forelimb, could act as a compensatory mechanism to the absence of visual input.

In the mesial wall the forelimb representation of area F3 was activated in the contralateral to the moving forelimb hemisphere in all reaching monkeys. Moreover, the dorsal bank of the cingulate sulcus corresponding to part of area 24 was bilaterally activated in the reaching monkeys. This result suggests a role of area 24 in reaching behavior. A circumscribed activation within area 23 was also observed in the ventral bank of the cingulate sulcus close to the fundus at the border with area 24. This activation was significant only in the reaching in the light monkeys.

In summary, the parietal and frontal areas involved in reaching under visual and somatosensory guidance are revealed in the present study. The topographical organization of the neuronal populations involved in fixation, visual processing, execution of saccadic eye movements, reaching in the light and reaching in the dark is illustrated in functional maps of high resolution. Our results demonstrate that distinct parietofrontal networks are activated during reaching under visual and under somatosensory guidance.

ΧΑΡΤΟΓΡΑΦΗΣΗ ΤΩΝ ΒΡΕΓΜΑΤΟ-ΜΕΤΩΠΙΑΙΩΝ ΝΕΥΡΩΝΙΚΩΝ ΚΥΚΛΩΜΑΤΩΝ ΕΓΚΕΦΑΛΟΥ ΠΙΘΗΚΟΥ, ΤΑ ΟΠΟΙΑ ΕΜΠΛΕΚΟΝΤΑΙ ΣΤΗΝ ΟΠΤΙΚΑ ΚΑΙ ΣΩΜΑΤΑΙΣΘΗΤΙΚΑ ΚΑΘΟΔΗΓΟΥΜΕΝΗ ΚΙΝΗΣΗ ΤΟΥ ΑΝΩ ΑΚΡΟΥ
Μελέτη με τη χρήση της ποσοτικής αυτοραδιογραφικής μεθόδου της [^{14}C]-2-δεοξυγλυκόζης

Εργαστήριο Λειτουργικής Απεικόνισης του Εγκεφάλου, Τομέας Βασικών Επιστημών, Τμήμα Ιατρικής, Σχολή Επιστημών Υγείας, Πανεπιστήμιο Κρήτης.

ΠΕΡΙΛΗΨΗ

Η μεταβολική δραστηριότητα στο φλοιό της ενδοβρεγματικής αύλακας, στον ακοκκιώδη μετωπιαίο φλοιό και στο φλοιό της έσω επιφάνειας των εγκεφαλικών ημισφαιρίων χαρτογραφήθηκε με την αυτοραδιογραφική μέθοδο της [^{14}C]δεοξυγλυκόζης σε έναν μη εκπαιδευμένο πίθηκο ελέγχου και σε έξι πιθήκους που είχαν εκπαιδευθεί και εκτελούσαν μία από τις παρακάτω συμπεριφορές: α) εστίαση του βλέμματος σε κεντρικό οπτικό στόχο, β) σακκαδικές κινήσεις σε οπτικούς στόχους, γ) κινήσεις του άνω άκρου στο φώς κατά τη διάρκεια εστίασης του βλέμματος ή χωρίς εστίαση του βλέμματος και δ) κινήσεις του άνω άκρου στο σκοτάδι ως απάντηση σε ακουστικά ερεθίσματα ενώ το βλέμμα παρέμενε ακίνητο ίσια μπροστά. Η κατανάλωση της γλυκόζης κατά μήκος των υπό εξέταση περιοχών μετρήθηκε με τη βοήθεια υπολογιστικά υποστηριζόμενου συστήματος ανάλυσης εικόνας στις αυτοραδιογραφικές εικόνες που ελήφθησαν από τις οριζόντιες τομές των διαφορετικών ημισφαιρίων. Η κατανομή της μεταβολικής δραστηριότητας στις διάφορες φλοϊκές περιοχές αναπαραστάθηκε με τη μορφή δισδιάστατων χαρτών που συγκεντρώνουν τα δεδομένα από σειριακές εγκεφαλικές τομές και καλύπτουν ολόκληρη τη ραχιαιοκοιλιακή και προσθιοπίσθια έκταση των αναλυόμενων περιοχών. Οι χάρτες αυτοί επιτρέπουν τη σύγκριση της κατανομής της μεταβολικής δραστηριότητας σε εγκεφάλους διαφορετικών πιθήκων.

Εντός της ενδοβρεγματικής αύλακας διαφορετικές υποπεριοχές της ενδοβρεγματικής φλοϊκής περιοχής 7 ενεργοποιήθηκαν κατά την εστίαση του βλέμματος, κατά την εκτέλεση σακκαδικών κινήσεων σε οπτικούς στόχους και κατά την εκτέλεση ακουστικά καθοδηγούμενων κινήσεων του άνω άκρου στο σκοτάδι. Μια περιοχή σχετιζόμενη με την εστίαση του βλέμματος εντοπίστηκε σχετικά πρόσθια εντός της πλάγιας όχθης της ενδοβρεγματικής αύλακας. Η σχετιζόμενη με σακκαδικές κινήσεις περιοχή βρέθηκε να εκτείνεται σε όλη σχεδόν τη ραχιαιοκοιλιακή έκταση της πλάγιας όχθης και εντοπίσθηκε στο πρόσθιο τμήμα της ενδοβρεγματικής περιοχής 7. Υποπεριοχές στο κοιλιακό τμήμα του ενδοβρεγματικού φλοιού (εκατέρωθεν του πυθμένα της ενδοβρεγματικής αύλακας) εμφανίστηκαν ενεργοποιημένες μόνο κατά την κίνηση του άνω άκρου στο φώς, συνθήκη κατά την οποία οπτική πληροφορία ήταν διαθέσιμη για την καθοδήγηση του κινούμενου άκρου. Αντίθετα υποπεριοχές στο ραχιαίο τμήμα της ενδοβρεγματικής φλοϊκής περιοχής 5 εμφανίστηκαν ενεργοποιημένες κατά την κίνηση του άνω άκρου τόσο στο φώς όσο και στο σκοτάδι, συνθήκες κατά τις οποίες μόνο σωματαισθητική πληροφορία ήταν διαθέσιμη από κοινού για την καθοδήγηση του άκρου. Η ενεργοποίηση στη ραχιαία ενδοβρεγματική περιοχή 5 ήταν αυξημένη κατά την κίνηση του άκρου στο σκοτάδι, δρώντας πιθανώς ως αντιστάθμισμα στην απουσία οπτικής πληροφορίας για την καθοδήγηση του άκρου. Τα παραπάνω μας οδηγούν στο συμπέρασμα ότι εντός της ενδοβρεγματικής αύλακας η οπτική καθοδήγηση της κίνησης σχετίζεται με τον κοιλιακό ενδοβρεγματικό φλοιό ενώ η

σωματαισθητική καθοδήγηση, που πραγματοποιείται βάση ιδιοδεκτικής πληροφορίας σχετικά με την τρέχουσα θέση του άκρου, συνδέεται με τη ραχιαία ενδοβρεγματική περιοχή 5.

Στον προκινητικό φλοιό η ραχιαία προκινητική περιοχή F2 εμφανίστηκε ενεργοποιημένη αντίπλευρα στο κινούμενο άκρο σε όλα τα ζώα που εκτελούσαν κίνηση του άνω άκρου. Η υποπεριοχή της F2 που εντοπίζεται ραχιαία και πίσω, κάτω από την άνω προκεντρική αύλακα, ήταν ενεργοποιημένη τόσο στα ζώα που εκτελούσαν κίνηση του άκρου στο φώς, όσο και σε αυτό που εκτελούσε κίνηση του άκρου στο σκοτάδι. Μια διαφορετική υποπεριοχή της F2, κοιλιακά και πρόσθια, πλησίον της τοξοειδούς αύλακας και εντός του δαπέδου της αύλακας, ήταν ενεργοποιημένη μόσο στα ζώα που εκτελούσαν κίνηση του άκρου στο φώς. Επομένως το τμήμα της F2 κάτω από την άνω προκεντρική αύλακα σχετίζεται με οπτικά καθοδηγούμενες κινήσεις. Στον κοιλιακό προκινητικό φλοιό η περιοχή F4 εμφανίστηκε ενεργοποιημένη σε όλα τα ζώα που δέχονταν οπτικό ερεθισμό ή πραγματοποιούσαν κίνηση του άνω άκρου. Αφαιρέσεις μεταξύ των χαρτών που αντιστοιχούσαν στις διαφορετικές συνθήκες έδειξαν ότι η περιοχή F4 σχετίζεται με την επεξεργασία οπτικής πληροφορίας και με τις σωματαισθητικά καθοδηγούμενες κινήσεις του άνω άκρου. Αντίθετα η περιοχή F5, η οποία εντοπίζεται πρόσθια της F4, δεν εμφανίσθηκε ενεργοποιημένη κατά την επεξεργασία οπτικής πληροφορίας όταν οι συνθήκες του πειράματος δεν απαιτούσαν κίνηση του άκρου. Ενεργοποιήσεις μέτριας έντασης εντοπίστηκαν στην περιοχή F5, εντός της πίσω όχθης της τοξοειδούς αύλακας στον πίθηκο που εκτελούσε κίνηση του άνω άκρου στο σκοτάδι. Σημαντικές ενεργοποιήσεις εντοπίστηκαν στα ζώα που πραγματοποιούσαν κίνηση του άκρου στο φώς, στην πίσω όχθη της τοξοειδούς αύλακας και στην πλάγια επιφάνεια του εγκεφάλου, πλησίον του πίσω χείλους της τοξοειδούς αύλακας. Επομένως στον κοιλιακό προκινητικό φλοιό η περιοχή F4 ελέγχει κυρίως σωματαισθητικά καθοδηγούμενες κινήσεις, ενώ η περιοχή F5 ελέγχει κυρίως οπτικά καθοδηγούμενες κινήσεις.

Στην πρόσθια όχθη της τοξοειδούς αύλακας, που αποτελεί τμήμα των μετωπιαίων οφθαλμικών πεδίων, τα οποία είναι το φλοιικό κέντρο ελέγχου των οφθαλμικών κινήσεων, η μεταβολική δραστηριότητα ήταν αυξημένη σε όλα τα ζώα που δέχονταν οπτικό ερεθισμό. Επιπρόσθετα, μια περιοχή εκατέρωθεν του πυθμένα της τοξοειδούς αύλακας εκτεινόμενη εντός των δύο όχθεων της αύλακας εμφανίστηκε ενεργοποιημένη σε όλα τα ημισφαίρια των πιθήκων που πραγματοποιούσαν εστίαση του βλέμματος και προτείνεται ότι σχετίζεται με την εστίαση του βλέμματος σε οπτικούς στόχους.

Εντός της κεντρικής αύλακας παρατηρήθηκε αμφοτερόπλευρη ενεργοποίηση στην περιοχή αντιπροσώπευσης του κορμού στον πρωτοταγή σωματαισθητικό και κινητικό φλοιό σε όλους τους πιθήκους που εκτελούσαν κίνηση του άκρου. Η ενεργοποίηση αυτή αποδίδεται στην προσαρμογή της θέσης του κορμού που υπαγορεύει η κίνηση του άκρου. Αμφοτερόπλευρη ενεργοποίηση της περιοχής αντιπροσώπευσης του στόματος στο κοιλιακό τμήμα της κεντρικής αύλακας σχετίστηκε με την εμπλοκή του στόματος κατά τη λήψη νερού ως ανταμοιβή στη διάρκεια του πειράματος. Η περιοχή αντιπροσώπευσης του άνω άκρου εμφανίστηκε συμμετρικά ενεργοποιημένη εντός της κεντρικής αύλακας στο αντίπλευρο από το κινούμενο άκρο ημισφαίριο, στα ζώα που εκτελούσαν κίνηση του άνω άκρου. Η ενεργοποίηση της αναπαράστασης του άνω άκρου στον πρωτοταγή σωματαισθητικό φλοιό ήταν αυξημένη στον πίθηκο που κινούσε το άκρο στο σκοτάδι συγκρινόμενη με την αντίστοιχη στους πιθήκους που κινούσαν το άκρο στο φώς. Η αυξημένη επεξεργασία σωματαισθητικής πληροφορίας όταν δεν υπάρχει διαθέσιμη οπτική πληροφορία για την καθοδήγηση του άκρου προτείνεται ότι δηλώνει την ύπαρξη ενός μηχανισμού που δρά αντισταθμιστικά στην απουσία οπτικής πληροφορίας.

Στην έσω επιφάνεια των ημισφαιρίων εμφανίστηκε ενεργοποιημένη η αναπαράσταση του άνω άκρου στην περιοχή F3 στο ημισφαίριο αντίπλευρα προς το κινούμενο άκρο σε όλα τα ζώα που εκτελούσαν κίνηση του άνω άκρου. Επιπρόσθετα η άνω όχθη της αύλακας του προσαγωγίου που αντιστοιχεί στην περιοχή 24 ήταν αμφοτερόπλευρα ενεργοποιημένη στα ζώα που κινούσαν το άνω άκρο και η μεταβολική δραστηριότητα ήταν σημαντικά αυξημένη σε σχέση με τα ζώα ελέγχου. Το γεγονός αυτό υποδεικνύει ότι η περιοχή σχετίζεται με την κίνηση του άνω άκρου.

Επίσης αποκαλύφθηκε μια εντοπισμένη ενεργοποίηση εντός της περιοχής 23, στην κοιλιακή όχθη της αύλακας του προσαγωγίου, προς τον πυθμένα της αύλακας, στο όριο με την περιοχή 24. Η ενεργοποίηση αυτή εμφανίστηκε μόνο στα ζώα που κινούσαν το άνω άκρο στο φώς.

Συνοψίζοντας, στην παρούσα εργασία αποκαλύπτονται οι βρεγματικές και μετωπιαίες περιοχές που σχετίζονται με τις οπτικά και σωματαισθητικά καθοδηγούμενες κινήσεις του άνω άκρου. Λειτουργικοί χάρτες υψηλής διακρισιμότητας ανέδειξαν την τοπογραφική οργάνωση των νευρωνικών πληθυσμών που εμπλέκονται στην εστίαση του βλέμματος, στην επεξεργασία οπτικής πληροφορίας, στην εκτέλεση σακκαδικών κινήσεων και στην εκτέλεση κινήσεων του άνω άκρου στο φώς και στο σκοτάδι. Τα αποτελέσματά μας υποδεικνύουν ότι διακριτά βρεγματο-μετωπιαία κυκλώματα ενεργοποιούνται κατά τις οπτικά και σωματαισθητικά καθοδηγούμενες κινήσεις.

REFERENCES

1   Alexander, G. E. and M. D. Crutcher (1990). "Preparation for movement: neural representations of intended direction in three motor areas of the monkey." J. Neurophysiol. **64**(1): 133-150.

2   Andersen, R. A., C. Asanuma and M. Cowan (1985). "Callosal and prefrontal associational projecting cell populations in area 7a of the macaque monkey: a study using retrogradely transported fluorescent dyes." J. Comp. Neurol. **232**(443-455).

3   Andersen, R. A., C. Asanuma, G. Essick and R. M. Siegel (1990). "Corticocortical connections of anatomically and physiologically defined subdivisions within the inferior parietal lobule." J. Comp. Neurol. **296**: 65-113.

4   Andersen, R. A., G. K. Essick and R. M. Siegel (1985). "Encoding of spatial location by posterior parietal neurons." Science **230**: 456-458.

5   Andersen, R. A., G. K. Essick and R. M. Siegel (1987). "Neurons of area 7 activated by both visual stimuli and oculomotor behavior." Exp. Brain Res. **67**: 316-322.

6   Ashe, J. and A. P. Georgopoulos (1994). "Movement parameters and neural activity in motor cortex and area 5." Cerebral Cortex **4**: 590-600.

7   Bachelard, H. S. (1971). "Specificity and kinetic properties of monosaccharide uptake into guinea pig cerebral cortex *in vitro.*" J. Neurochem. **18**: 213-222.

8   Balint, R. (1909). "Seelenhamung des Schauens, optische Ataxie, raumlische Storung des Aufmersamkeit." Monatschr.Psychiat. Neurol. **25**: 51-81.

9   Barash, S., R. M. Bracewell, L. Fogassi, J. W. Gnadt and R. A. Andersen (1991). "Saccade-related activity in the lateral intraparietal area. I. Temporal properties; comparison with area 7a." J. Neurophysiol. **66**(3): 1095-1108.

10   Barash, S., R. M. Bracewell, L. Fogassi, J. W. Gnadt and R. A. Andersen (1991). "Saccade-related activity in the lateral intraparietal area. II. Spatial properties." J. Neurophysiol. **66**(3): 1109-1124.

11   Barbas, H. and M. M. Mesulam (1981). "Organization of afferent input to subdivisions of area 8 in the rhesus monkey." J. Comp. Neurol. **200**: 407-431.

12   Barbas, H. and D. N. Pandya (1987). "Architecture and frontal cortical connections of the premotor cortex (area 6) in the rhesus monkey." J. Comp. Neurol. **256**: 211-228.

13   Ben Hamed, S., J. R. Duhamel, F. Bremmer and W. Graf (2001). "Representation of the visual field in the lateral intraparietal area of macaque monkeys: a quantitative receptive fields analysis." Exp. Brain Res. **140**(2): 127-144.

14   Bidder, T. G. (1968). "Hexose translocation across the blood-brain interface: configurational aspects." J. Neurochem. **15**: 867-874.

15   Blatt, G. J., R. A. Andersen and G. R. Stoner (1990). "Visual receptive field organization and cortico-cortical connections of the lateral intraparietal area (LIP) in the macaque." J. Comp. Neurol. **299**: 421-445.

16   Bonin, G. v. and P. Bailey (1947). The neocortex of *Macaca mulatta.* Urbana, Illinois, University of Illinois Press.

17   Boussaoud, D., T. M. Barth and S. P. Wise (1993). "Effects of gaze on apparent visual responses of frontal cortex neurons." Exp. Brain Res. **93**: 423-434.

18   Boussaoud, D., L. G. Ungerleider and R. Desimone (1990). "Pathways for motion analysis: Cortical connections of the medial superior temporal and fundus of the superior temporal visual areas in the macaque." J. Comp. Neurol. **296**: 462-495.

19   Brodmann, K. (1909). Vergleichende Lokalisationlehre der Grosshirnrinde. Leipzig, Barth.

20   Bruce, C. J. and M. E. Goldberg (1985). "Primate frontal eye fields. I. Single neurons discharging before saccades." J. Neurophysiol. **53**(3): 603-635.

21   Bruce, C. J., M. E. Goldberg, M. C. Bushnell and G. B. Stanton (1985). "Primate frontal eye fields. II. Physiological and anatomical correlates of electrically evoked eye movements." J. Neurophysiol. **54**(3): 714-734.

22   Burman, D. D. and C. J. Bruce (1997). "Suppression of task-related saccades by electrical stimulation in the primate's frontal eye fields." J. Neurophysiol. **77**: 2252-2267.

23   Caminiti, R., S. Ferraina and P. B. Johnson (1996). "The sources of visual information to the primate frontal lobe: a novel role for the superior parietal lobule." Cereb. Cortex **6**(3): 319-328.

24   Caminiti, R., P. B. Johnson, Y. Burnod, C. Galli and S. Ferraina (1990). "Shift of preferred directions of premotor cortical cells with arm movements performed across the workspace." Exp. Brain Res. **83**: 228-232.

25   Caminiti, R., P. B. Johnson, C. Galli, S. Ferraina and Y. Burnod (1991). "Making arm movements within different parts of space: The premotor and motor cortical representation of a coordinate system for reaching to visual targets." J. Neurosci. **11**(5): 1182-1197.

26   Caminiti, R., P. B. Johnson and A. Urbano (1990). "Making arm movements within different parts of space: Dynamic aspects in the primate motor cortex." J. Neurosci. **10**(7): 2039-2058.

27   Cavada, C. and P. S. Goldman-Rakic (1989). "Posterior parietal cortex in rhesus monkey: I. Parcellation of areas based on distinctive limbic and sensory corticocortical connections." J. Comp. Neurol. **287**: 393-421.

28   Cavada, C. and P. S. Goldman-Rakic (1989). "Posterior parietal cortex in rhesus monkey: II. Evidence for segregated corticocortical networks linking sensory and limbic areas with the frontal lobe." J. Comp. Neurol. **287**: 422-445.

29   Colby, C. L. and J.-R. Duhamel (1991). "Heterogeneity of extrastriate visual areas and multiple parietal areas in the macaque monkey." Neuropsychologia **23**: 517-537.

30   Colby, C. L., J.-R. Duhamel and M. E. Goldberg (1993). "Ventral intraparietal area of the macaque: Anatomic location and visual response properties." J. Neurophysiol. **69**(3): 902-914.

31   Colby, C. L., J.-R. Duhamel and M. E. Goldberg (1996). "Visual, presaccadic, and cognitive activation of single neurons in monkey lateral intraparietal area." J. Neurophysiol. **76**(5): 2841-2852.

32   Colby, C. L., R. Gattass, C. R. Olson and C. G. Gross (1988). "Topographical organization of cortical afferents to extrastriate visual area PO in the macaque: a dual tracer study." J. Comp. Neurol. **269**: 392-413.

33   Colby, C. L. and M. E. Goldberg (1999). "Space and attention in parietal cortex." Annu. Rev. Neurosci. **22**: 319-349.

34   Dalezios, Y., V. C. Raos and H. E. Savaki (1996). "Metabolic activity pattern in the motor and somatosensory cortex of monkeys performing a visually guided reaching task with one forelimb." Neuroscience **72**(2): 325-333.

35   di Pellegrino, G. and S. P. Wise (1991). "A neurophysiological comparison of three distinct regions of the primate frontal lobe." Brain **114**: 951-978.

36   Duffy, G. H. and J. L. Burchfiel (1971). "Somatosensory system: organizational hierarchy from single units in monkey area 5." Science **172**: 273-275.

37   Duhamel, J.-R., F. Bremmer, S. BenHamed and W. Graf (1997). "Spatial invariance of visual receptive fields in parietal cortex neurons." Nature **389**: 845-848.

38   Duhamel, J.-R. and M. Brouchon (1990). "Sensorimotor aspects of unilateral neglect: a single case analysis." Cog. Neyropsychol. **7**: 57-74.

39   Duhamel, J.-R., C. L. Colby and M. E. Goldberg (1998). "Ventral intraparietal area of the macaque: congruent visual and somatic response properties." J. Neurophysiol. **79**: 126-136.

40   Dum, R. P. and P. L. Strick (1991). "The origin of corticospinal projections from the premotor areas in the frontal lobe." J. Neurosci. **11**: 667-689.

41   Evarts, E. V. (1968). "Relation of pyramidal tract activity to force exerted during voluntary movement." J. Neurophysiol. **31**: 14-27.

42   Farah, M. J., J. L. Brunn, A. B. Wong, M. A. Wallace and P. A. Carpenter (1990). "Frames of reference for allocating attention to space." Cog. Neuropsychol. **28**: 335-347.

43   Fishman, R. S. and M. L. Karnovsky (1986). "Apparent absence of a translocase in the cerebral glucose-6-phosphatase system." J. Neurochem. **46**: 371-378.

44   Flanders, M., S. I. Helms Tillery and J. F. Soechting (1992). "Early stages in a sensorimotor transformation." Behav. Brain Sci. **15**(2): 309-320.

45   Fogassi, L., V. Gallese, G. Buccino, L. Craighero, L. Fadiga and G. Rizzolatti (2001). "Cortical mechanism for the visual guidance of hand grasping movements in the monkey. A reversible inactivation study." Brain **124**: 571-586.

46   Fogassi, L., V. Gallese, L. Fadiga, G. Luppino, M. Matelli and G. Rizzolatti (1996). "Coding of peripersonal space in inferior premotor cortex (area F4)." J. Neurophysiol. **76**(1): 141-157.

47   Fogassi, L., V. Gallese, L. Fadiga and G. Rizzolatti (1996). Space coding in inferior premotor cortex (area F4): facts and speculations. Neural Bases of Motor Behaviour. F. Lacquaniti and P. Viviani. Dordecht, Kluwer Academic Publishers**:** 99-120.

48   Fogassi, L., V. Raos, G. Franchi, V. Gallese, G. Luppino and M. Matelli (1999). "Visual responses in the dorsal premotor area F2 of the macaque monkey." Exp. Brain Res. **128**: 194-199.

49   Gallese, V., L. Fadiga, L. Fogassi and G. Rizzolatti (1996). "Action recognition in the premotor cortex." Brain **119**: 593-609.

50   Gallese, V., A. Murata, M. Kaseda and N. Niki (1994). "Deficit of hand preshaping after muscimol injection in monkey parietal cortex." Neuroreport **6**: 1525-1529.

51   Gentilucci, M., L. Fogassi, G. Luppino, M. Matelli, R. Camarda and G. Rizzolatti (1988). "Functional organization of inferior area 6 in the macaque monkey. I. Somatotopy and the control of proximal movements." Exp. Brain Res. **71**: 475-490.

52   Georgopoulos, A. P., R. Caminiti and J. F. Kalaska (1984). "Static spatial effects in motor cortex and area 5: Quantitative relations in a two-dimensional space." Exp. Brain Res. **54**: 446-454.

53   Georgopoulos, A. P., J. F. Kalaska, R. Caminiti and J. T. Massey (1982). "On the relation between the direction of two-dimensional arm movements and cell discharge in primate motor cortex." J. Neurosci. **2**: 1527-1537.

54   Georgopoulos, A. P., R. E. Kettner and A. B. Schwartz (1988). "Primate motor cortex and free arm movements to visual targets in three-dimensional space. II. Coding of the direction of movement by a neuronal population." J. Neurosci. **8**(8): 2928-2937.

55   Geyer, S., M. Matelli, G. Luppino, A. Schleicher, Y. Jansen, N. Palomero-Gallagher and K. Zilles (1998). "Receptor autoradiographic mapping of the mesial motor and premotor cortex of the macaque monkey." J. Comp. Neurol. **397**(231-250).

56   Geyer, S., M. Matelli, G. Luppino and K. Zilles (2000). "Functional neuroanatomy of the primate isocortical motor system." Anat. Embryol. **202**: 443-474.

57   Geyer, S., K. Zilles, G. Luppino and M. Matelli (2000). "Neurofilament protein distribution in the macaque monkey dorsolateral premotor cortex." Eur. J. Neurosci. **12**: 1554-1566.

58   Gnadt, J. W. and R. A. Andersen (1988). "Memory related motor planning activity in posterior parietal cortex of macaque." Exp. Brain Res. **70**: 216-220.

59   Godshalk, M., A. R. Mitz, B. Van Duin and H. Van der Burg (1995). "Somatotopy of monkey premotor cortex examined with microstimulation." Neurosci. Res. **23**: 269-279.

60   Goldberg, M. E. and M. C. Bushnel (1981). "Behavioral enhancement of visual responses in monkey cerebral cortex. Modulation in frontal eye fields specifically related to saccades." J. Neurophysiol. **46**: 773-787.

61   Goldberg, M. E., C. L. Colby and J.-R. Duhamel (1990). "Representation of visuomotor space in the parietal lobe of the monkey." Cold Spring Harbor Symp. on Quant. Biol. **55**: 729-739.

62   Gottlieb, J. P., M. Kusunoki and M. E. Goldberg (1998). "The representation of visual salience in monkey parietal cortex." Nature **391**: 481-484.

63   Graziano, M. S. A. (1999). "Where is my arm? The relative role of vision and proprioception in the neuronal representation of limb position." Proc. Natl. Acad. Sci. USA **96**: 10428-10421.

64   Graziano, M. S. A. and S. Gandhi (2000). "Location of the polysensory zone in the precentral gyrus of anesthetized monkeys." Exp. Brain Res. **135**: 259-266.

65   Graziano, M. S. A. and C. G. Gross (1998). "Visual responses with and without fixation: neurons in premotor cortex encode spatial locations independently of eye position." Exp. Brain Res. **118**: 373-380.

66   Graziano, M. S. A., X. T. Hu and C. G. Gross (1997). "Coding the locations of objects in the dark." Science **277**: 239-241.

67   Graziano, M. S. A., X. T. Hu and C. G. Gross (1997). "Visuospatial properties of ventral premotor cortex." J. Neurophysiol. **77**: 2268-2292.

68   Graziano, M. S. A., G. S. Yap and C. G. Gross (1994). "Coding of visual space by premotor neurons." Science **266**: 1054-1057.

69   Gregoriou, G. G. and H. E. Savaki (2001). "The intraparietal cortex: subregions involved in fixation, saccades and in the visual and somatosensory guidance of movement." J. Cereb. Blood Flow Metab **21**: 671-682.

70   Grunewald, A., J. F. Linden and R. A. Andersen (1999). "Responses to auditory stimuli in macaque lateral intraparietal area. I. Effects of training." J. Neurophysiol. **82**: 330-342.

71   Halsband, U. and R. Passingham (1982). "The role of premotor and parietal cortex in the direction of action." Brain Res. **240**: 368-372.

72   Hand, P. J. (1981). The 2-deoxyglucose method. Neuroanatomical Tracing Methods. L. Heimer and M. J. Robards. New York, Plenum**:** 511-538.

73   He, S. Q., R. P. Dum and P. L. Strick (1995). "Topographic organization of corticospinal projections from the frontal lobe: motor areas on the medial surface of the hemisphere." J. Neurosci. **15**: 3284-3306.

74   He, S.-Q., R. P. Dum and P. L. Strick (1993). "Topographic organization of corticospinal projections from the frontal lobe: Motor areas on the lateral surface of the hemisphere." J. Neurosci. **13**(3): 952-980.

75   Hers, H. G. (1957). Le metabolisme de fructose. Arscia. Bruxelles**:** 102.

76   Holmes, G. (1918). "Disturbances of visual orientation." <u>Br. J. Opthalm.</u> **2**: 449-506.

77   Hyvärinen, J. (1981). "Regional distribution of functions in parietal association area 7 of the monkey." <u>Brain Res.</u> **206**: 287-303.

78   Hyvärinen, J. (1982). <u>The parietal cortex of monkey and man. Studies of brain function.</u> Berlin, Heidelberg, New York, Springer-Verlag.

79   Hyvärinen, J. and A. Poranen (1974). "Function of the parietal associative area 7 as revealed from cellular discharges in alert monkeys." <u>Brain</u> **97**: 673-692.

80   Iriki, A., M. Tanaka and Y. Iwamura (1996). "Coding of modified body schema during tool use by macaque postcentral neurons." <u>Neuroreport</u> **7**: 2325-2330.

81   Jeannerod, M., M. A. Arbib, G. Rizzolatti and H. Sakata (1995). "Grasping objects: the cortical mechanisms of visuomotor transformation." <u>Trends Neurosci.</u> **18**(7): 314-320.

82   Johnson, P. B., S. Ferraina, L. Bianchi and R. Caminiti (1996). "Cortical networks for visual reaching: physiological and anatomical organization of frontal and parietal lobe arm regions." <u>Cereb. Cortex</u> **6**(2): 102-119.

83   Johnson, P. B., S. Ferraina and R. Caminiti (1993). "Cortical networks for visual reaching." <u>Exp. Brain Res.</u> **97**: 361-365.

84   Jones, E. G., J. D. Coulter and S. H. C. Hendry (1978). "Intracortical connectivity of architectonic fields in the somatic sensory, motor and parietal cortex of monkeys." <u>J. Comp. Neurol.</u> **181**: 291-348.

85   Jones, E. G. and T. P. S. Powell (1970). "An anatomical study of converging sensory pathways within the cerebral cortex of the monkey." <u>Brain</u> **93**: 793-820.

86   Judge, S. J., B. J. Richmond and F. C. Chu (1980). " Implantation of magnetic search coils for measurements of eye position: An improved method." <u>Vision Res.</u> **20**: 535-538.

87   Kadekaro, M., A. M. Crane and L. Sokoloff (1985). "Differential effects of electrical stimulation of sciatic nerve on metabolic activity in spinal cord and dorsal root ganglion in the rat." <u>Proc. Natl. Acad. Sci. USA</u> **82**: 6010-6013.

88   Kadish, A. H., R. L. Little and J. C. Sternberg (1968). "A new and rapid method for the determination of glucose by measurement of oxygen consumption." <u>Clin. Chem.</u> **14**: 116.

89   Kalaska, J. F. (1988). "The representation of arm movements in postcentral and parietal cortex." <u>Can. J. Physiol. Pharmacol.</u> **66**: 455-463.

90   Kalaska, J. F. (1996). "Parietal cortex area 5 and visuomotor behavior." <u>Can. J. Physiol. Pharmacol.</u> **74**: 483-498.

91   Kalaska, J. F., R. Caminiti and A. P. Georgopoulos (1983). "Cortical mechanisms related to the direction of two-dimensional arm movements: Relations in parietal area 5 and comparison with motor cortex." <u>Exp. Brain Res.</u> **51**: 247-260.

92   Kalaska, J. F., D. A. D. Cohen, M. Prud'homme and M. L. Hyde (1990). "Parietal area 5 neuronal activity encodes movement kinematics, not movement dynamics." <u>Exp. Brain Res.</u> **80**: 351-364.

93   Karnath, H. O., P. Schenkel and B. Fischer (1991). "Trunk orientation as the determining factor of the "contralateral" deficit in the neglect syndrome and as the physical anchor of the internal representation of body orientation in space." <u>Brain</u> **114**: 1997-2014.

94   Keizer, K. and H. G. J. M. Kuyepers (1989). "Distribution of corticospinal neurons with collaterals to the lower brainstem reticular formation in monkey (Macaca fascicularis)." Exp. Brain. Res. **74**: 311-318.

95   Kennedy, C., M. H. Des Rosiers, O. Sakurada, M. Shinohara, M. Reivich, J. W. Jehle and L. Sokoloff (1976). "Metabolic mapping of the primary visual system of the monkey by means of the autoradiographic [^{14}C]deoxyglucose technique." Proc. Natl. Acad. Sci. USA **73**: 4230-4234.

96   Kennedy, C., O. Sakurada, M. Shinohara, J. Jehle and L. Sokoloff (1978). "Local cerebral glucose utilization in the normal conscious macaque monkey." Ann. Neurol. **4**: 293-301.

97   Kurata, K. (1989). "Distribution of neurons with set- and movement-related activity before hand and foot movements in the premotor cortex of rhesus monkeys." Exp. Brain Res. **77**: 245-256.

98   Kurata, K. and D. S. Hoffman (1994). "Differential effects of muscimol microinjection into dorsal and ventral aspects of the premotor cortex of monkeys." J. Neurophysiol. **71**(3): 1151-1164.

99   Kurata, K. and J. Tanji (1986). "Premotor cortex neurons in macaques: activity before distal and proximal forelimb movements." J. Neurosci. **6**: 403-411.

100   Linden, J. F., A. Grunewald and R. A. Andersen (1999). "Responses to auditory stimuli in macaque lateral intraparietal area. I. Behavioral modulation." J. Neurophysiol. **82**: 343-358.

101   Luppino, G., M. Matelli, R. Camarda and G. Rizzolatti (1993). "Corticocortical connections of area F3 (SMA-proper) and area F6 (pre-SMA) in the macaque monkey." J. Comp. Neurol. **338**: 114-140.

102   Luppino, G., M. Matelli, R. Camarda and G. Rizzolatti (1994). "Corticospinal projections from mesial frontal and cingulate areas in the monkey." Neuroreport **5**: 2545-2548.

103   Luppino, G., M. Matelli, R. M. Camarda, V. Gallese and G. Rizzolatti (1991). "Multiple representations of body movements in mesial area 6 and the adjacent cingulate cortex: An intracortical microstimulation study in the macaque monkey." J. Comp. Neurol. **311**: 463-482.

104   Luppino, G., M. Matelli and G. Rizzolatti (1990). "Cortico-cortical connections of two electrophysiologically identified arm representations in the mesial agranular frontal cortex." Exp. Brain Res. **82**: 214-218.

105   Luppino, G., A. Murata, P. Govoni and M. Matelli (1999). "Largely segregated parietofrontal connections linking rostral intraparietal cortex (areas AIP and VIP) and the ventral premotor cortex (areas F5 and F4)." Exp. Brain Res. **128**: 181-187.

106   Lynch, J. C., A. M. Graybiel and L. J. Lobeck (1985). "The differential projections of two cytoarchitectonic subregions of the inferior parietal lobule of macaque upon the deep layers of the superior colliculus." J. Comp. Neurol. **235**: 241-254.

107   Lynch, J. C., V. B. Mountcastle, W. H. Talbot and T. C. T. Yin (1977). "Parietal lobe mechanisms for directed visual attention." J. Neurophysiol. **40**(2): 362-389.

108   Mata, M., D. J. Fink, H. Gainer, C. B. Smith, L. Davidsen, H. Savaki, W. J. Schwartz and L. Sokoloff (1980). "Activity-dependent energy metabolism in rat posterior pituitary primarily reflects sodium pump activity." J. Neurochem. **34**(1): 213-215.

109   Matelli, M., R. Camarda, M. Glickstein and G. Rizzolatti (1986). "Afferent and efferent projections of the inferior area 6 in the macaque monkey." J. Comp. Neurol. **251**: 281-298.

110   Matelli, M., P. Govoni, C. Galetti, G. F. Kutz and G. Luppino (1998). "Superior area 6 afferents from the superior parietal lobule in the macaque monkey." J. Comp. Neurol. **402**(3): 327-352.

111   Matelli, M., G. Luppino, P. Govoni and S. Geyer (1996). "Anatomical and functional subdivisions of inferior area 6 in macaque monkey." Soc. Neurosci. Abstr. **22**: 796.2.

112 Matelli, M., G. Luppino and G. Rizzolatti (1985). "Patterns of cytochrome oxidase activity in the frontal agranular cortex of the macaque monkey." Behav. Brain Res. **18**: 125-136.

113 Matelli, M., G. Luppino and G. Rizzolatti (1991). "Architecture of superior and mesial area 6 and the adjacent mesial cortex in the macaque monkey." J. Comp. Neurol. **311**: 445-462.

114 Matsuzaka, Y., H. Aizawa and J. Tanji (1992). "A motor area rostral to the supplementary motor area (presupplementary motor area) in the monkey: Neuronal activity during a learned motor task." J. Neurophysiol. **68**(3): 653-662.

115 Maunsell, J. H. R. and D. C. Van Essen (1983). "The connections of the middle temporal visual area (MT) and their relationship to a cortical hierarchy in the macaque monkey." J. Neurosci. **3**: 2563-2586.

116 Mays, L. E. and D. L. Sparks (1980). "Dissociation of visual and saccade-related responses in superior colliculus neurons." J. Neurophysiol. **43**: 207-232.

117 Mazzoni, P., R. M. Bracewell, S. Barash and R. Andersen (1996). "Spatially tuned auditory responses in area LIP of macaques performing delayed memory saccades to acoustic targets." J. Neurophysiol. **75**(3): 1233-1241.

118 Mitz, A. R. and S. P. Wise (1987). "The somatotopic organization of the supplementary motor area: intracortical microstimulation mapping." J. Neurosci. **7**: 1010-1021.

119 Moschovakis, A. K., A. B. Karabelas and S. M. Highstein (1988). "Structure-function relationships in the primate superior colliculus. II. Morphological identity of presaccadic neurons." J. Neurophysiol. **60**(1): 263-302.

120 Moscovitch, M. and M. Behrman (1994). "Coding of spatial information in the somatosensory system: evidence from patients with neglect following parietal lobe damage." J. Cog. Neurosci. **6**: 151-155.

121 Mountcastle, V. B. (1995). "The parietal system and some higher brain functions." Cereb. Cortex **5**(5): 377-390.

122 Mountcastle, V. B., J. C. Lynch, A. Georgopoulos, H. Sakata and C. Acuna (1975). "Posterior parietal association cortex of the monkey: Command functions for operations within extrapersonal space." J. Neurophysiol. **38**: 871-908.

123 Murata, A., L. Fadiga, L. Fogassi, V. Gallese, V. Raos and G. Rizzolatti (1997). "Object representation in the ventral premotor cortex (area F5) of the monkey." J. Neurophysiol. **78**: 2226-2230.

124 Murata, A., V. Gallese, G. Luppino, M. Kaseda and H. Sakata (2000). "Selectivity for the shape, size, and orientation of objects for grasping in neurons of monkey parietal area AIP." J. Neurophysiol. **83**: 2580-2601.

125 Mushiake, H., M. Inase and J. Tanji (1991). "Neuronal activity in the primate premotor, supplementary, and precentral motor cortex during visually guided and internally determined sequential movements." J. Neurophysiol. **66**(3): 705-718.

126 Nelson, T., E. E. Kaufman and L. Sokoloff (1984). "2-Deoxyglucose incorporation into rat brain glycogen during measurement of local cerebral glucose utilization by the 2-deoxyglucose method." J. Neurochem. **43**: 949-956.

127 Nordmann, J. J. (1977). "Ultrastructural morphometry of the rat neurohypophysis." J. Anat. **123**: 213-218.

128 Olson, C. R., S. Y. Musil and M. E. Goldberg (1996). "Single neurons in posterior cingulate cortex of behaving macaque: eye movement signals." J. Neurophysiol. **76**(5): 3285-3300.

129 Pandya, D. N. and B. Seltzer (1982). "Intrinsic connections and architectonics of posterior parietal cortex in the rhesus monkey." J. Comp. Neurol. **204**: 204-210.

130 Passingham, R. E. (1987). Two cortical systems for directing movement. Motor areas of the cerebral cortex., Wiley**:** 151-164.

131 Pearson, R. C. A. and T. P. S. Powell (1985). "The projection of the primary somatic sensory cortex upon area 5 in the monkey." Brain Res. Rev. **9**: 89-107.

132 Peele, T. L. (1942). "Cytoarchitecture of individual parietal areas in the monkey (*Macaca mulatta*) and the distribution of the efferent fibres." J. Comp. Neurol. **77**: 693-738.

133 Penfield, W. and T. Rasmussen (1952). The cerebral cortex of man. New York, Macmillan.

134 Penfield, W. and K. Welch (1951). "The supplementary motor area of the cerebral cortex." Arch. Neurol. Psychiatry **66**: 289-317.

135 Petrides, M. (1982). "Motor conditional associative-learning after selective prefrontal lesions in the monkey." Behav. Brain Res. **5**: 407-413.

136 Petrides, M. and D. N. Pandya (1984). "Projections to the frontal cortex from the posterior parietal region in the rhesus monkey." J. Comp. Neurol. **228**: 105-116.

137 Picard, N. and P. L. Strick (1997). "Activation on the medial wall during remembered sequences of reaching movements in monkeys." J. Neurophysiol. **77**: 2197-2201.

138 Ratcliff, G. and G. A. B. Davies-Jones (1972). "Defective visual localization in focal brain wounds." Brain **95**: 49-60.

139 Riddoch, G. (1935). "Visual disorientation in homonymous half-fields." Brain **58**: 376-382.

140 Rizzolatti, G., R. Camarda, L. Fogassi, M. Gentilucci and G. Luppino (1988). "Functional organization of inferior area 6 in the macaque monkey: II Area F5 and the control of distal movements." Exp. Brain Res. **71**: 491-507.

141 Rizzolatti, G., L. Fadiga, V. Gallese and L. Fogassi (1996). "Premotor cortex and the recognition of motor actions." Cogn. Brain Res. **3**: 131-141.

142 Rizzolatti, G., L. Fogassi and V. Gallese (1997). "Parietal cortex: from sight to action." Curr. Opin. Neurobiol. **7**: 562-567.

143 Rizzolatti, G., M. Gentilucci, R. M. Camarda, V. Gallese, G. Luppino, M. Matelli and L. Fogassi (1990). "Neurons related to reaching-grasping arm movements in the rostral part of area 6 (area 6a,)." Exp. Brain Res. **82**: 337-350.

144 Rizzolatti, G., M. Gentilucci, L. Fogassi, G. Luppino, M. Matelli and S. Ponzoni-Maggi (1987). "Neurons related to goal directed motor acts in inferior area 6 of the macaque monkey." Exp. Brain Res. **67**: 220-224.

145 Rizzolatti, G. and G. Luppino (2001). "The cortical motor system." Neuron **31**(6): 889-901.

146 Rizzolatti, G., G. Luppino and M. Matelli (1996). The classic supplementary motor area is formed by two independent areas. Advances in Neurology: Supplementary Sensorimotor Area. Lüders. Philadelphia, Lupincott-Raven Publishers. **70: 45-56.**

147 Rizzolatti, G., G. Luppino and M. Matelli (1998). "The organization of the cortical motor system: new concepts." Electroencephalogr. Clin Neurophysiol. **106**: 283-296.

148 Robinson, C. J. and H. Burton (1980). "Somatic submodality distribution within the second somatosensory (SII), 7b, retroinsular, postauditory, and granular insular cortex." J. Comp. Neurol. **192**: 93-108.

149 Robinson, D. A. (1963). "A method of measuring eye movement using a scleral search coil in a magnetic field." IEEE Trans. Bio-Med. Electron. **10**: 137-145.

150 Robinson, D. L., M. E. Goldberg and G. B. Stanton (1978). "Parietal association cortex in the primate: sensory mechanisms and behavioral modulations." J. Neurophysiol. **41**: 910-932.

151 Roland, P. E., B. Larsen, N. A. Lassen and E. Skinhoj (1980). "Supplementary motor area and other cortical areas in organization of voluntary movements in man." J. Neurophysiol. **43**(1): 118-136.

152 Rushworth, M. E. S., P. D. Nixon and R. E. Passingham (1997). "Parietal cortex and movement. I. Movement selection and reaching." Exp. Brain Res. **117**: 292-310.

153 Sakata, H., M. Taira, A. Murata and S. Mine (1995). "Neural mechanisms of visual guidance of hand action in the parietal cortex of the monkey." Cereb. Cortex **5**(5): 429-438.

154 Sakata, H., Y. Takaoka, A. Kawarasaki and H. Shibutani (1973). "Somatosensory properties of neurons in the superior parietal cortex (area 5) of the rhesus monkey." Brain Res. **64**: 85-102.

155 Savaki, H. E. and Y. Dalezios (1999). "^{14}C-Deoxyglucose mapping of the monkey brain during reaching to visual targets." Prog. Neurobiol. **58**: 473-540.

156 Savaki, H. E., C. Kennedy, L. Sokoloff and M. Mishkin (1993). "Visually guided reaching with the forelimb contralateral to a "blind" hemisphere: a metabolic mapping study in monkeys." J. Neurosci. **13**(7): 2772-2789.

157 Savaki, H. E., V. C. Raos and Y. Dalezios (1997). "Spatial cortical patterns of metabolic activity in monkeys performing a visually guided reaching task with one forelimb." Neuroscience **76**(4): 1007-1034.

158 Schieber, M. H. (2000). "Inactivation of the ventral premotor cortex biases the laterality of motoric choices." Exp. Brain Res. **130**: 497-507.

159 Schlag, J. and M. Schlag-Rey (1985). "Unit activity related to spontaneous saccades in frontal dorsomedial cortex of monkey." Exp. Brain Res. **58**: 208-211.

160 Schlag, J. and M. Schlag-Rey (1987). "Evidence for a supplementary eye field." J. Neurophysiol. **57**(1): 179-200.

161 Schuier, F., F. Orzi, S. Suda, C. Kennedy and L. Sokoloff (1981). "The lumped constant for the [^{14}C]deoxyglucose method in hyperglycemic rats." J. Cereb Blood Flow Metab. **1**(1): S63.

162 Schwartz, W. J., C. B. Smith, L. Davidsen, H. Savaki, L. Sokoloff, M. Mata, D. J. Fink and H. Gainer (1979). "Metabolic mapping of functional activity in the hypothalamo-neurohypophysial system of the rat." Science **205**: 723-725.

163 Shibutani, H., H. Sakata and J. Hyvärinen (1984). "Saccades and blinking evoked by microstimulation of the posterior parietal association cortex of the monkey." Exp. Brain Res. **55**: 1-8.

164 Sokoloff, L. (1982). The radioactive deoxyglucose method. Theory, procedure, and applications for the measurement of local glucose utilization in the central nervous system. Advances in Neurochemistry. B. W. a. A. Agranoff, M.H. New York, Plenum Press. **4:** 1-82.

165 Sokoloff, L., M. Reivich, C. Kennedy, M. H. D. Rosiers, C. S. Patlak, K. D. Pettigrew, O. Sakurada and M. Shinohara (1977). "The [^{14}C]deoxyglucose method for the measurement of local cerebral glucose utilization: theory, procedure, and normal values in the conscious and anesthetized albino rat." J. Neurochem. **28**: 897-916.

166 Sols, A. and R. K. Crane (1954). "Substrate specificity of brain hexokinase." J. Biol. Chem. **210**: 581-595.

167 Stanton, G. B., C. J. Bruce and M. E. Goldberg (1995). "Topography of projections to posterior cortical areas from the macaque frontal eye fields." J. Comp. Neurol. **353**: 291-305.

168 Suda, S., M. Shinohara, M. Miyaoka, C. Kennedy and L. Sokoloff (1981). "Local cerebral glucose utilization in hypoglycemia." J. Cereb. Blood Flow Metab. **1**(1): S62.

169 Tanji, J. and K. Shima (1994). "Role for supplementary motor area cells in planning several movements ahead." Nature **371**: 413-416.

170 Tanji, J., K. Shima and H. Mushiake (1996). "Multiple cortical motor areas and temporal sequencing of movements." Cogn. Brain Res. **5**: 117-122.

171 Tanji, K., K. Taniguchi and T. Saga (1980). "Supplementary motor area: Neuronal response to motor instructions." J. Neurophysiol. **43**: 60-68.

172 Thier, P. and R. A. Andersen (1996). "Electrical microstimulation suggests two different forms of representation of head-centered space in the intraparietal sulcus of rhesus monkeys." Proc. Natl. Acad. Sci. USA **93**: 4962-4967.

173 Ungerleider, L. G. and R. Desimone (1986). "Cortical connections of area MT in the macaque." J. Comp. Neurol. **248**: 190-222.

174 Vogt, C. and A. Vogt (1919). "Algemeinere Ergebnisse unserer Hirnforschung." J. Psychol. Neurol. **25**: 279-461.

175 Weinrich, M. and S. P. Wise (1982). "The premotor cortex of the monkey." J. Neurosci. **2**(9): 1329-1345.

176 Wise, S. P., D. Boussaoud, P. B. Johnson and R. Caminiti (1997). "Premotor and parietal cortex: corticocortical connectivity and combinatorial computations." Annu. Rev. Neurosci. **20**: 25-42.

177 Woolsey, C. N. (1958). Organization of somatic sensory and motor areas of the cerebral cortex. Biological and Biochemical bases of behavior. H. F. Harlow and C. N. Woolsey. Madison, Univ. Wisconsin Press**:** 63-81.

178 Woolsey, C. N., P. H. Settlage, D. R. Meyer, W. Sencer, T. Pinto Hamuy and A. M. Travis (1952). "Patterns of localization in precentral and 'supplementary' motor areas and their relation to the concept of a premotor area." Res. Publ. Assoc. Nerv. Ment. Dis. **30**: 238-264.

179 Wurtz, R. H. and C. W. Mohler (1976). "Enhancement of visual responses in monkey striate cortex and frontal eye fields." J. Neurophysiol. **39**(4): 766-772.

180 Zipser, D. and R. A. Andersen (1988). "A back propagation programmed network that simulated response properties of a subset of posterior parietal neurons." Nature **331**: 697-684.